TAMPERE UNIVERSITY OF TECHNOLOGY

NOORA KALEVO

MAGNETOELASTIC PROPERTIES OF HEAT TREATED STEELS

Master of Science Thesis

Examiners:
Professor Pekka Ruuskanen
Professor Tuomo Tiainen
Examiners and subject accepted in Automation, Mechanical and Materials Engineering faculty meeting on 9 May 2012

TIIVISTELMÄ

TAMPEREEN TEKNILLINEN YLIOPISTO
Materiaalitekniikan koulutusohjelma
KALEVO, NOORA: Lämpökäsiteltyjen terästen magneettiset ominaisuudet
Diplomityö, 91 sivua, 1 liitesivu
Toukokuu 2012
Pääaine: Metallimateriaalit
Tarkastajat: professori Tuomo Tiainen ja professori Pekka Ruuskanen
Avainsanat: magnetoelastisuus, magnetostriktio, magnetomekaaninen ilmiö, hiiletyskarkaisu, terästangot, iskukuormitus

Materiaalien mekaaniset ja magneettiset ominaisuudet liittyvät toisiinsa voimakkaasti, koska materiaalin rakenne määrittelee molemmat ominaisuudet. Magnetoelastisuus on ilmiö, joka kuvaa vuorovaikutusta materiaalin elastisten ja magneettisten ominaisuuksien välillä. Terästen magnetoelastisia ominaisuuksia voidaan hyödyntää rakenteellisten komponenttien kunnonvalvonnassa.

Tärkeimpiä magnetoelastisia ilmiöitä ovat magnetostriktio ja magnetomekaaninen ilmiö. Magnetostriktio tarkoittaa ulkoisen magneettikentän aiheuttamaa muutosta ferromagneettisen kappaleen dimensioissa. Magnetomekaaninen ilmiö taas kuvaa ulkoisen jännityksen aikaansaamaa muutosta ferromagneettisen materiaalin magnetisaatiossa. Molemmat ilmiöt esiintyvät samanaikaisesti.

Työn tavoitteena oli tutkia terästankojen magneettisia ja magnetoelastisia ominaisuuksia. Kirjallisuusselvityksestä havaittiin, että jännityksen ja magneettisten ominaisuuksien välinen vuorovaikutus teräksissä on monimutkainen, koska se on vahvasti epälineaarinen ja siinä esiintyy hystereesiä. Lisäksi havaittiin, että mikrorakenteelliset tekijät vaikuttavat terästen magneettiseen ja magnetoelastiseen käyttäytymiseen.

Työn kokeellinen osuus jakaantui kahteen osaan. Ensimmäisessä osassa mitattiin eri teräslaatujen hystereesikäyrät, joiden avulla tutkittiin näytteiden magneettisia ominaisuuksia. Havaittiin, että hiiletyskarkaisu ja kylmätyöstö pienentävät materiaalin permeabiliteettia. Materiaalin koostumuksen ja magneettisten ominaisuuksien välillä ei havaittu yksinkertaista riippuvuutta.

Kokeellisen osuuden toisen osan tavoitteena oli rakentaa testilaite, jossa näyte voidaan altistaa iskukuormitukselle. Testilaitteen avulla tutkittiin terästankojen magnetoelastista käyttäytymistä iskukuormituksessa. Työn päätavoite oli selvittää tankojen väliset erot. Tulokset osoittivat, että samasta teräslaadusta valmistettujen tankojen välillä on hajontaa. Työssä kartoitettiin magneettisiin mittauksiin liittyvät epävarmuustekijät. Magneettisten mittausten tulosten tulkinta on hankalaa, koska monet tekijät vaikuttavat mittaustuloksiin. Jatkossa tankojen mikrorakennetta täytyy tutkia tarkemmin, jotta tuloksia voitaisiin tulkita paremmin.

ABSTRACT

TAMPERE UNIVERSITY OF TECHNOLOGY
Master's Degree Programme in Materials Engineering
KALEVO, NOORA: Magnetoelastic properties of heat treated steels
Master of Science Thesis, 91 pages, 1 Appendix page
May 2012
Major: Metallic Materials
Examiners: Professor Tuomo Tiainen and Professor Pekka Ruuskanen
Keywords: magnetoelasticity, magnetostriction, magnetomechanical effect, gas carburizing, steel bars, impact loading

Mechanical and magnetic properties of materials are closely coupled, because both properties arise from the structure of the material. Magnetoelasticity describes the interaction between the elastic and magnetic properties of the material. The influence of stress on the magnetic properties of steels is of interest because magnetoelasticity can be exploited in the condition monitoring of structural components.

The most important phenomena related to magnetoelasticity are magnetostriction and magnetomechanical effect. Magnetostriction is a fractional change in length due to the applied magnetic field. Magnetomechanical effect describes the stress-induced change in the magnetization of ferromagnetic materials. Both phenomena occur simultaneously.

The aim of this work was to examine the magnetic and magnetoelastic properties of steel bars. The literature survey revealed that the interaction between stress and magnetic properties of steel is complicated because it is non-linear and exhibits hysteresis. It was found that the microstructural features influence the basic magnetic and magnetomechanical properties of steels.

The experimental part of this work consisted of two parts. In the first part the hysteresis curves of different steel grades were measured in order to investigate the basic magnetic properties of the samples. It was found that gas carburizing and prior cold working decrease the permeability of the material. No simple relationship was revealed between steel composition and magnetic properties.

The purpose of the second part of the experimental work was to build a test device in order to study the magnetoelastic properties and behaviour of the steel bars under impact loading. The main goal of this work was to find out the scatter of the measurement results between the samples. The impact tests revealed that there are differences in the results obtained on samples of the same material. The factors of uncertainty were identified and discussed. The main challenge in the magnetic measurements is the interpretation of the results because there are several factors influencing the results. Future work requires more detailed study of the microstructure of the samples in order to interpret the results with more accuracy.

PREFACE

The work for this thesis was carried out at the Department of Electronics in Tampere University of Technology. The work was performed during fall 2011 and spring 2012. The thesis was funded by TUT foundation.

I wish to thank my examiner Professor Pekka Ruuskanen for his guidance and the valuable work experience I gained during this project. I thank my examiner Professor Tuomo Tiainen for the comments and advices. I am grateful for M.Sc. Mika Inkinen for his help and assistance in the practical work, especially in the electrical measurements. I want to thank Hannu Niemi and Lasse Söderlund for helping me in constructing the measurement device. I thank also Sampo Tuominen for measurement results and advices.

I appreciate the support of my friends and family during my studies. Especially I want to thank Laura for her advice concerning electronics.

CONTENTS

ABBREVIATIONS AND NOTATIONS

A	Cross-sectional area of the bar
A_0	Original cross-sectional area of the specimen
AC	Alternating current
B	Magnetic flux density
B_{an}	Anhysteretic magnetic flux density
B_r	Remanence
B_s	Saturation flux density
ΔB	Change in the magnetic flux density
bcc	Body centered cubic crystal structure
c_1	Constant in Equation 6.1
c_2	Constant in Equation 6.1
d_f	Ferrite grain size
d_p	Pearlite colony size
d_{33}	Linear coupling coefficient at a constant stress
d_{33}^*	Magnetomechanical effect at a constant magnetic field strength
DC	Direct current
E	Elastic modulus
E^H	Elastic modulus at constant magnetic field strength
emf	Electromotive force
F	Force
fcc	Face centered cubic crystal structure
H	Magnetic field strength
H_c	Coercivity
H^*	Critical rotation field strength
H_m	Critical magnetic field strength
H_d	Demagnetizing field
I	Current
J	Intensity of magnetization
K	Strain gauge factor
K_0, K_1, K_2	Anisotropy constants
k	Boltzmann's constant
L	Initial length of the sample
ΔL	Change in length at some instant
$\Delta L(H)$	Change in the length as a function of magnetic field strength
l	Length of the solenoid
M	Magnetization
M_{an}	Anhysteretic magnetization
M_{irr}	Irreversible component of magnetization

M_s	Saturation magnetization
ΔM	Change in the magnetization
M_0	Complete magnetization
m	Magnetic moment
N	Number of turns of the search coil
n	Number of turns of the magnetizing coil
n	Sample size
R	Resistance
ΔR	Strain induced resistance change
T	Temperature
T_C	Curie temperature
t	Time
V	Voltage
V_{max}	Maximum of the tensile stress wave
V_{min}	Maximum of the compressive stress wave
V_f	Ferrite volume fraction
V_p	Pearlite volume fraction
V_{input}	Input voltage
V_{output}	Output voltage
v	Volume
W	Energy
W_H	Hysteresis loss
W_c	Magnetocrystalline anisotropy energy
W_{me}	Magnetoelastic anisotropy energy
wt%	Percentage of weight
x	Sample mean average
α	Mean field parameter representing the interdomain coupling
α_i	Direction cosines of domain magnetization with respect to the cube axis
γ_j	Direction cosines of stress with respect to the cube axis
ε	Strain, also a constant in Equation 5.7
λ	Magnetostriction constant
λ_{100}	Magnetostriction in the lattice directions <100>
λ_{111}	Magnetostriction in the lattice directions <111>
μ	Permeability
μ_r	Relative permeability
μ_0	Permeability of free space
μ^σ	Permeability at constant applied stress
σ	Stress
η	Constant in Equation 5.7
ϕ	Magnetic flux
<jkl>	Directions of crystal lattice

1 INTRODUCTION

The magnetic properties of a material are influenced by the mechanical state of the material. Mechanical and magnetic properties of the material are closely coupled, because both properties arise from the structure of the material. [1] The phenomenon, which describes the interaction between the mechanical and magnetic properties of a material, is called magnetoelasticity. [2] Magnetoelasticity strongly manifests itself in ferromagnetic materials such as iron, cobalt and nickel. They are typical ferromagnetic substances which exhibit strong magnetic properties. As steel is an iron-based metal alloy, it is a ferromagnetic material. [1, 3]

When a ferromagnetic material is subjected to magnetic field its dimensions change. This phenomenon is called magnetostriction. Magnetostriction was first discovered by Joule in 1842. [4] Nowadays the magnetostriction phenomenon is well known and it has important applications in measuring and electrical technology. [1, 3]

It has been known for many years that stress changes significantly the magnetic behavior of materials. The application of stress to a ferromagnetic material can cause changes in the magnetization under an applied magnetic field. The influence of stress on magnetization is called magnetomechanical effect. [1] Magnetostriction and magnetomechanical effect can be classified as magnetoelastic phenomena. [2]

Steels are widely used in different applications as constructional materials. The performance of structural components is influenced by mechanical stresses. Mechanical loading induces deformation and vibrations which eventually break the component. To save time and costs it is important to be able to evaluate the stress levels and the lifetime of the component.

Different magnetic methods can be used in nondestructive testing and materials characterization [3]. Recently the magnetoelastic phenomena have attracted interest [5, 6, 7, 8, 9, 10, 11, 12] because they can be exploited in different stress monitoring and sensing applications. However, some difficulties can be found. The magnetic response of steels is complex; the interaction between stress and magnetic behavior is non-linear and exhibits hysteresis. [1, 3] To enable the use of the magnetoelastic phenomena in condition monitoring applications, it is essential to understand the interaction between the magnetic and mechanical properties.

The aim of this work is to examine the magnetic and magnetoelastic properties of steel bars. In order to achieve the goal of the work the phenomena related to magnetism and magnetoelasticity of steels are studied by means of literature survey and experimentally.

At first the main basic mechanical and electromagnetic quantities related to this work are defined in chapter 2. In the literature survey, the basic magnetic properties are presented and magnetostriction and magnetomechanical effect are studied in detail in chapters 3, 4 and 5. The influences of the microstructural factors on magnetic properties are reviewed in chapter 6. The focus of the literature survey is in the interaction between the magnetic and mechanical properties in steels. The manufacturing process of steel bars is investigated. The composition, the heat treatment and the manufacturing process of the studied steel bar samples are characterized in chapter 7.

The experimental part of this work consists of two parts. In the first part different steel bars are studied in order to determine the influence of microstructural features on the basic magnetic properties. The objective of the second part of the experimental work and at the same time the primary goal of this work is to find out the differences in the magnetoelastic behavior between the steel bars. An impact test device is built in order to study the magnetoelastic properties and behavior of the steel bars under mechanical loading.

In order to evaluate the reliability of the measurement results, it is essential to know how a single parameter influences the measurement results. The identification of the factors of uncertainty related to the magnetic measurements is also an important goal of the work. The factors of uncertainty in the magnetic measurements are reviewed and discussed considering the literature survey and the measurements. The experimental details are presented in chapters 8, 9 and 10. In this work the basic terms and phenomena related to materials science are not explained, but they can be found in the book by Callister [13].

2 BASIC QUANTITIES

The basic mechanical and electromagnetic quantities are defined in this chapter in order to understand the phenomena research methods described later in the thesis.

2.1 Mechanical quantities

Stress can be defined according to Equation (2.1)

$$\sigma = \frac{F}{A_0}, \tag{2.1}$$

where F is the external load applied perpendicular to the specimen cross section and A_0 is the original cross sectional area before any load is applied. The units of stress are megapascals (MPa) which are equivalent to N/mm^2 (newton per unit area). Strain is defined according to Equation (2.2). [13]

$$\varepsilon = \frac{\Delta L}{L} \tag{2.2}$$

where ΔL is the change in length at some instant and L is the initial length of the specimen. Strain ε is unitless. Conventionally tensile strain (elongation) is referred as positive and compressive strain as negative (contraction). Stress and strain are related to each other by Hooke's law:

$$\sigma = E\varepsilon \tag{2.3}$$

where E is the elastic modulus. The unit for the elastic modulus is gigapascal (GPa). [26]

Hooke's law is valid in the elastic deformation region where the relationship between stress and strain is linear. Elastic deformation is reversible meaning that the sample returns its original shape when the load is removed. [13] Typical stress-strain curve for mild steel is shown in Fig. 1.1.

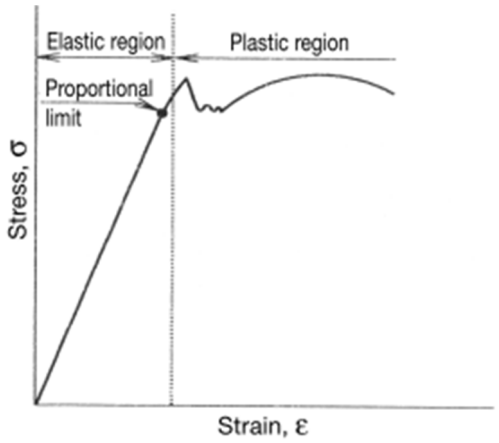

Figure 2.1 *Schematic stress-strain curve for mild steel showing linear elastic deformation region and plastic deformation region.* [48]

The point in the stress strain curve where plastic deformation starts, is called the yield strength. The units of yield strength are MPa. The maximum in the stress-strain curve is called tensile strength which is the stress required for the necking of the sample to initiate. If this stress is maintained, material fracture will occur. [13]

2.2 Electromagnetic quantities

There are three different systems of units used in magnetism: the CGS system, SI Sommerfield and SI Kennelly. Magnetic field strength can be defined in many ways but here it is defined according to the SI system which uses electrodynamic approach to magnetism. Magnetic field H arises from electric current loops. The magnetic field in the middle of the solenoid is:

$$H = \frac{nI}{l} \tag{2.4}$$

where n is the number of turns, I is the current flowing in the windings and l is the length of the solenoid. The unit of magnetic field is ampere per meter (A/m). [1]

Magnetic flux density B describes how a medium responds to a magnetic field. Magnetic flux density is also called magnetic induction and the unit in SI system is Tesla (T). The magnetic flux ϕ can be determined according to the Faraday's law of electromagnetic induction. The magnetic flux ϕ passing through a coil of N turns induces an emf signal (electromotive force) V:

$$V = N\frac{d\phi}{dt} \tag{2.5}$$

where $d\phi/dt$ is the rate of change of magnetic flux. Magnetic flux ϕ describes the total number of lines of electromotive force through a definite area A:

$$B = \frac{\phi}{A} \tag{2.6}$$

The magnetic flux is measured in units of weber. The ratio of B to H is called the permeability μ:

$$\mu = \frac{B}{H} \tag{2.7}$$

Permeability is measured in henries per meter (H/m). Henry is the unit of inductance.

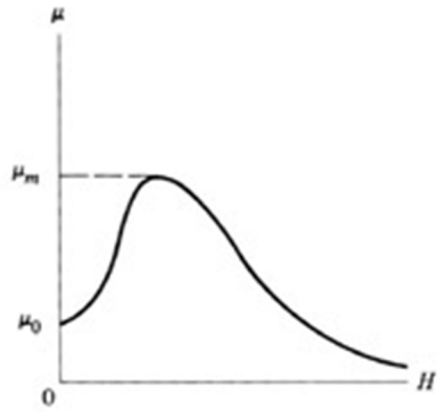

Figure 2.1 *Permeability μ as a function of magnetic field strength H. [1]*

Permeability is not constant and it varies as a function of applied magnetic field strength as shown in Fig. 2.1. The relative permeability μ_r, which is unitless, can be defined as:

$$\mu_r = \frac{\mu}{\mu_0} \tag{2.8}$$

where μ_0 is the permeability of empty space. Magnetization M, which has the same unit as H, is defined as the magnetic moment m per unit volume v of a solid:

$$M = \frac{m}{v} \tag{2.9}$$

Intensity of the magnetization J, which has a unit of Tesla, can be defined according to the equation (2.10).

$$J = \mu_0 M \tag{2.10}$$

The relationship between the magnetic field strength H, magnetization M and magnetic flux density B is [1]:

$$B = \mu_0 (H + M) \tag{2.11}$$

3 MAGNETISM IN STEELS

3.1 Ferromagnetism

Ferromagnetism is the most common type of magnetism. The most characteristic feature of the ferromagnetic materials is that they can be easily magnetized. When ferromagnetic materials are once exposed to the magnetic field, they retain their magnetization even when the field is removed. This retained magnetization, i.e. remanence B_r, distinguishes ferromagnetism and ferromagnetic materials from other types of magnetism and magnetic materials. Above the Curie temperature T_C ferromagnetic properties disappear. [1, 3]

The magnetization curve is the variation of magnetization M with the magnetic field strength H. The initial magnetization curve begins from the origin, where the material is in a demagnetic state. At high fields the change in the magnetization decreases and eventually reaches the saturation magnetization M_s. [1]

The magnetic properties depend on the crystallographic direction in which they are measured. This phenomenon is called magnetocrystalline anisotropy. Magnetic material tends to magnetize along certain crystallographic axes which are called easy directions of magnetization. Saturation magnetization M_s can be achieved with lower fields in the easy direction of magnetization than in the hard direction of magnetization. In iron, which has a body centered cubic (bcc) crystal structure, the easy direction of magnetization vectors are of <100> type as indicated in Fig 3.1. [1] In the bcc structure the atoms are located in the corners and one atom in the middle of the unit cell. [13]

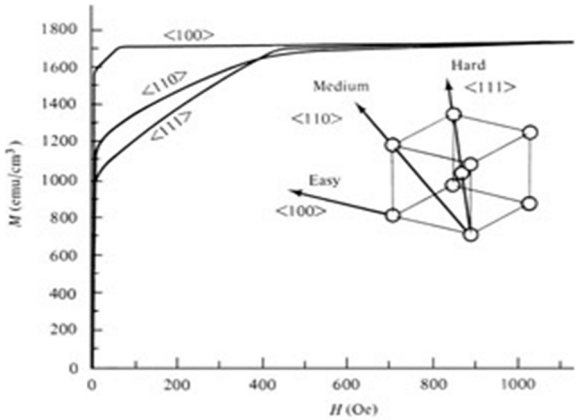

Figure 3.1 *Magnetocrystalline anisotropy. Magnetization curve of a single crystal of iron depends on the direction of the magnetization. Magnetization M to the easy directions of magnetization <100> requires lower magnetic field strength H than to the hard directions <111> of magnetization. [1] In this figure the unit of magnetic field strength H is Oe and the unit of magnetization is emu/cm^3 according to the CGS unit system.*

3.2 Domains and domain walls

Above Curie temperature ferromagnetic material consists of small regions called domains in which saturation magnetization vectors are oriented in the directions of easy magnetization. One grain in a metallic material consists of several thousands of domains as shown schematically in Fig. 3.2. [1, 15] Domains are usually between 0.01 and 0.1 cm wide. [14] In the demagnetic state, that is when the magnetic flux density B and magnetic field strength H are zero, each domain is spontaneously magnetized to the saturation value M_s, but the material as a whole has no net magnetization because the M_s vectors are not aligned in the same direction. The domain order in a material is formed due to the minimization of energy. [1]

Domains are separated from each other by domain walls, in which the direction of the magnetization vectors changes gradually as shown in Fig. 3.3. Domain walls are described by the angle between the saturation magnetization M_s vectors in the two domains on either side of the wall as indicated in Fig 3.4. Domain walls can be classified into 180˚ walls and non-180˚ walls. Usually all non-180˚ walls are called 90˚ walls although the actual angle can be 90°, 110°, or 71°. In iron and steels all the non-180˚ walls are 90˚ walls. Domain walls consist of magnetization vectors which are aligned in the non-easy direction of magnetization. [3]

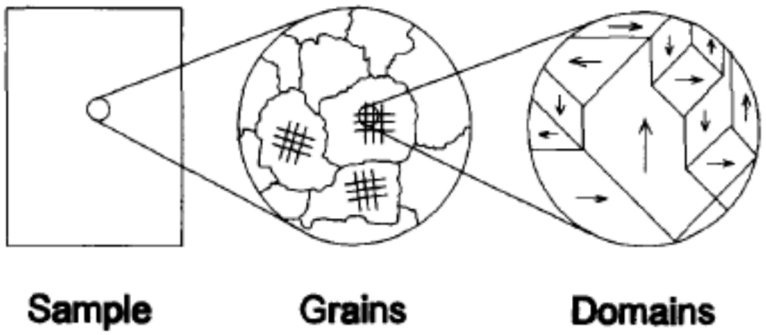

Figure 3.2 *Magnetic domains in polycrystalline steel. One grain consists of several thousands of domains. The arrows inside each domain indicate the M_s vectors. [15]*

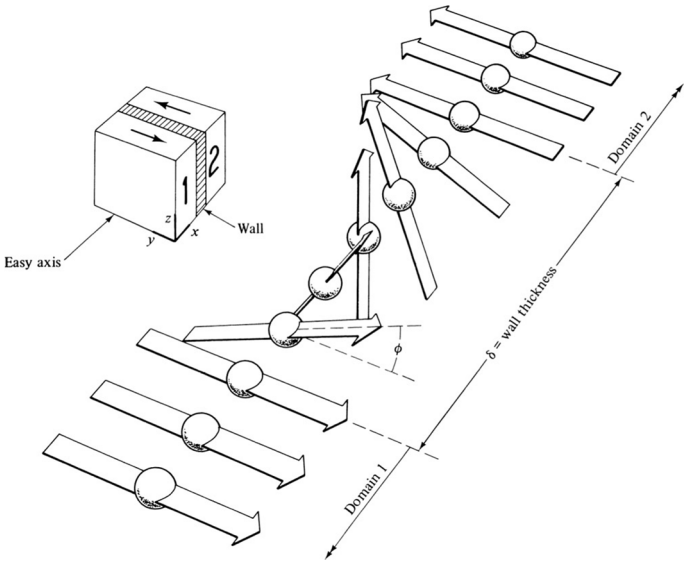

Figure 3.3 *Domain wall structure of an 180˚ wall. In the domain wall the direction of magnetization changes gradually from one easy crystallographic direction to another. [1]*

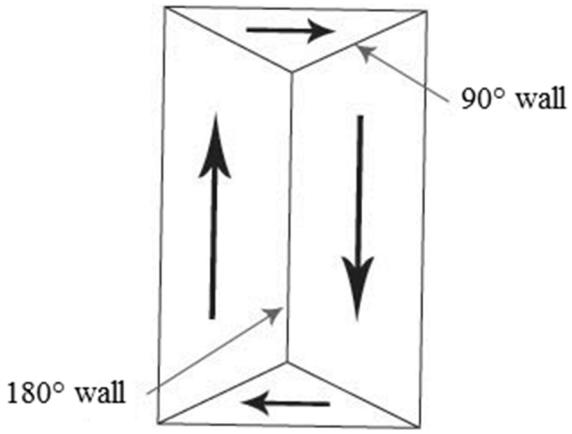

Figure 3.4 *Schematic presentation of the 180˚ and 90˚ domain walls. Black arrows describe the saturation magnetization vectors M_s. [3]*

3.3 Magnetization process

The magnetization process in ferromagnetic grain is described schematically in Fig. 3.5. In Fig. 3.5 a) the ferromagnetic material is in a demagnetic state and the grain consists of two domains in which saturation magnetization vectors are aligned in the direction of the easy magnetization because this is energetically favorable. In Fig. 3.5 b) the magnetic field strength H is applied and the domain in which the direction of the M_S vector is closest to the direction of the applied field, will grow by domain wall motion and eventually eliminate the unfavorably aligned domains until the grain consists only of one domain. This is due to the reduced magnetic potential energy of the crystal. [1] At low magnetic fields the changes in the magnetization are due to the 180˚ wall motion and at high fields due to the 90˚ wall motion [16].

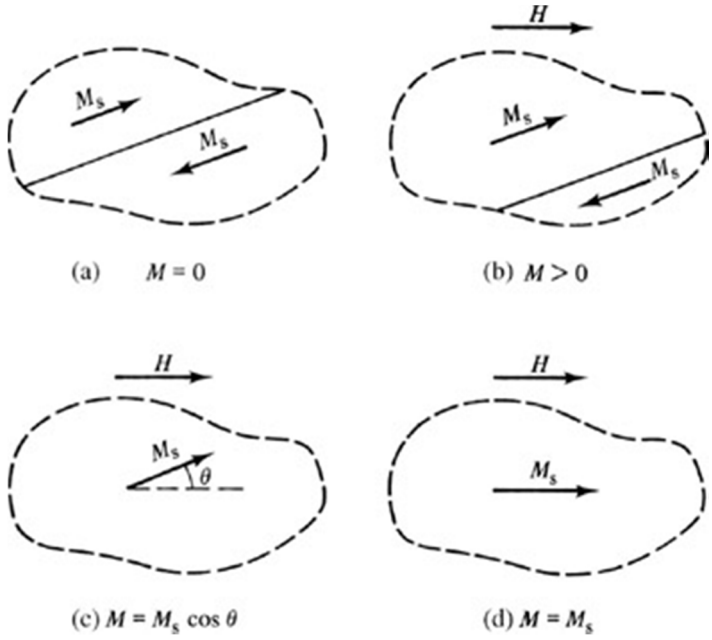

Figure 3.5 *The magnetization process in a ferromagnetic grain. The arrows indicate the saturation magnetization vectors. [1]*

When the magnetization process continues, finally no domain walls exist, as indicated in Fig. 3.5. c). In order to achieve the saturation magnetization, the M_s vectors in the material will rotate from the easy direction of magnetization to the direction of applied field H, as indicated in Fig. 3.5 d). [1]

The rotation of the saturation magnetization vectors requires energy. The work which the applied field does against the anisotropy force is called the magnetocrystalline anisotropy energy W_c. The magnetocrystalline anisotropy energy is the energy required to rotate the spin system of a domain away from the easy direction. Magnetocrystalline anisotropy energy takes the form of Equation (3.1).

$$W_c = K_0 + K_1(\alpha_1^2\alpha_2^2 + \alpha_2^2\alpha_3^2 + \alpha_3^2\alpha_1^2) + K_2(\alpha_1^2\alpha_2^2\alpha_3^2) + \cdots \qquad (3.1)$$

where K_0, K_1 and K_2 are the anisotropy constants and α_1, α_2, and α_3 are the direction cosines of the domain magnetization in relation to the three cube axis. The coefficients K_0 and K_2 can be neglected because K_0 is independent on angle and K_2 is usually small. Thus the easy direction of magnetization in the absence of external stress can be defined by the sign of K_1. Magnetocrystalline anisotropy energy W_c is at minimum when the saturation magnetization M_s is in the easy direction of magnetization. [1, 3]

Figure 3.6 shows the initial magnetization curve and the different stages of the magnetization process. The domain wall motion dominates the magnetization process from the demagnetic state to the knee point of the magnetization curve. At low fields the domain wall motion occurs as wall bowing, which is reversible process. When the magnetic field is removed, the domain wall returns its original position (a). The domain wall motion becomes irreversible when the magnetic field is increased (b). At moderate

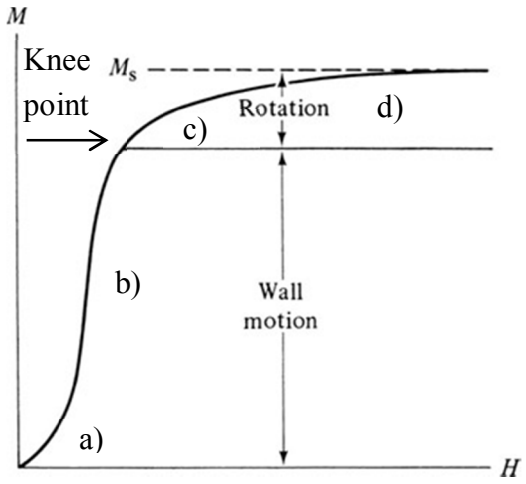

Figure 3.6 *Magnetization curve. Magnetization process occurs by two mechanisms: domain wall motion and rotation of magnetization vectors. The different stages of the magnetization process are indicated in the same way as in Fig. 3.5 [1]*

field strength values the mechanism of magnetization process changes to irreversible rotation of the magnetization vectors. The magnetic field is now strong enough to rotate the magnetization vectors from easy axis to another (c). When the field is further increased, the change in the magnetization is due to the reversible rotation of the magnetization vectors away from the easy direction towards the direction of applied field (d). [1, 3]

When a material consists of only one domain, it has reached technical saturation magnetization M_s. However, at high fields the magnetization continues to slowly increase beyond the technical saturation. This is called forced magnetization which is due to an increase in the spontaneous magnetization within the domain. When the magnetization no longer increases, material has reached its complete saturation M_0. [3]

3.4 Hysteresis curve

3.4.1 Characteristics of the hysteresis curve

Once the saturation magnetization state is reached and the magnetic field H is reduced to zero, the magnetic flux density B does not go to zero but lags behind. Consequently the hysteresis curve is formed. Figure 3.7 shows a typical hysteresis curve and the basic magnetic properties, such as coercivity H_c and remanence B_r, which can be used to characterize the magnetic material. Hysteresis loss W_H is the area of the hysteresis loop and describes the energy required to form the hysteresis. The hysteresis curve is also called BH-curve. [1]

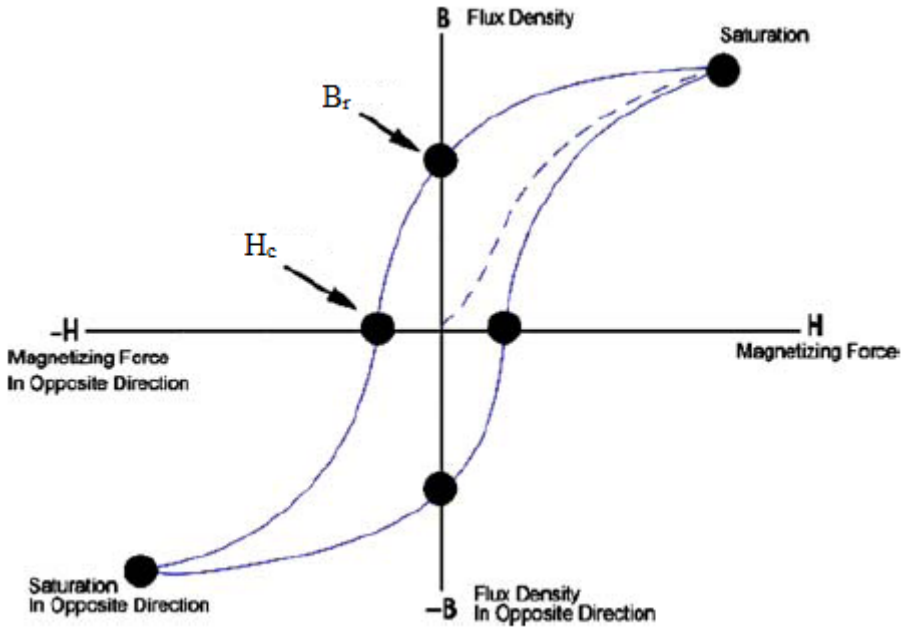

Figure 3.7 *Schematic illustration of a typical hysteresis curve or BH-curve and the basic magnetic properties. Coercivity H_c is the magnetic field strength H which is required to reduce the magnetization of the material to zero. Remanence B_r is the magnetic flux saturation which remains in the material after the external magnetic field is removed. The dashed line indicates the initial hysteresis curve. [17]*

Magnetic properties of materials can be classified into structure sensitive and structure insensitive properties. Structure insensitive properties, such as the Curie temperature T_c and saturation magnetization M_s, are not significantly influenced by materials processing, but they are dependent on the composition of the particular alloy. Permeability μ, coercivity H_c, hysteresis loss W_H, remanence B_r and the saturation value of magnetic flux density B_s are considered to be structure sensitive and they are radically influenced by mechanical and thermal treatments of material. [16]

The shape of the hysteresis curve reveals whether the material is magnetically soft or hard. Narrow hysteresis curve is typical for soft magnetic materials, which are easy to magnetize and demagnetize. Hard magnetic materials have wider hysteresis curves. Magnetocrystalline anisotropy is one factor influencing the shape of the magnetization and hysteresis curve. Ferromagnetic materials which have higher magnetocrystalline anisotropy have wider hysteresis. [3]

The magnetic properties of the material depend on the magnetic history, i.e., the magnetic fields to which the material has been exposed. The magnetic history of the material can be cancelled and the remanence of the material can be reduced or eliminated by demagnetizing process. After demagnetization the material is in the demagnetic state, where the domains are randomly oriented. Cyclic demagnetization process is described in Fig. 3.8. [1]

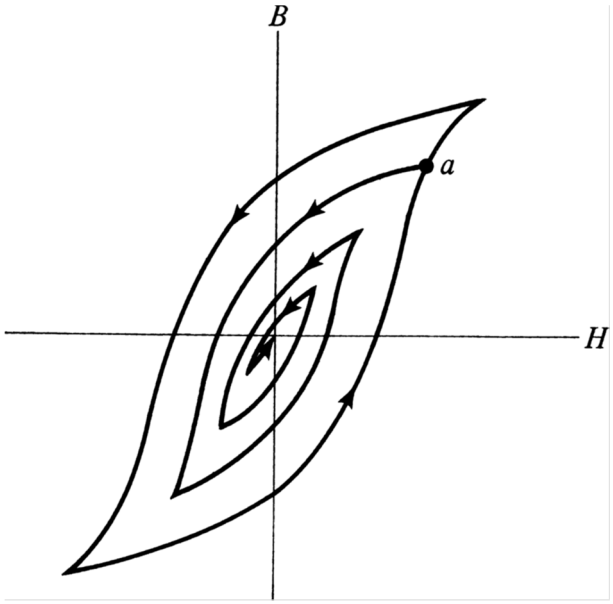

Figure 3.8 *Cyclic demagnetizing process. The material is subjected to a series of alternating fields of slowly decreasing amplitude. This process makes the hysteresis loop smaller and smaller until it reaches the origin and the material will be in the demagnetic state. [1]*

In reality, in a polycrystalline material, demagnetic state is difficult to achieve. This can be explained in terms of texture, which means that in a polycrystalline material grains or crystals are aligned in a specific direction. Texture induces preferred domain orientation and consequently influences the magnetic properties. [1]

3.4.2 Causes of hysteresis

Hysteresis phenomenon arises from the interaction between imperfections in the material and domain wall motion. When the material is subjected to the applied magnetic field, the domain wall motion is hindered due to the imperfections in the material such as nonmagnetic impurities, dislocations and grain boundaries. This leads to irreversible changes in the magnetization and therefore the magnetization process of ferromagnetic materials is hysteretic in nature. [1, 3] According to Jiles et al. [18] all the different types of obstacles to the domain wall motion are referred as pinning sites.

The microstructure of a material resulting from alloying, heat treatment and fabrication can contain various pinning sites, which restrict the domain wall motion. The pinning sites have the greatest influence on magnetic properties when they are nonmagnetic or when their sizes are similar to the domain wall width. Figure 3.9 shows schematically the interaction between the domain wall and a pinning site. [1]

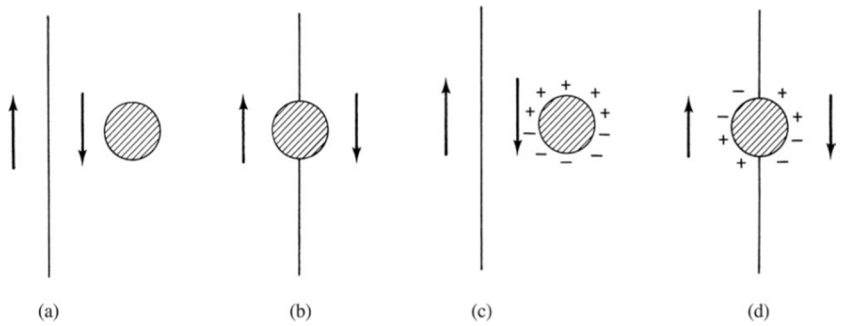

Figure 3.9 *Interaction of domain wall with a pinning site. [1]*

Domain walls tend to locate at pinning sites due to the reduction in energy. In Fig. 3.9 a) the energy of the wall is larger than in Fig. 3.9 b) in which there is no domain wall inside the inclusion and the area and thus the energy of the wall is smaller. The formation of free poles is also possible when domain wall and an inclusion interact, as shown in Fig. 3.9 c) and d). [1] The microstructural factors acting as pinning sites are discussed in detail in chapter 6.

3.5 Magnetoelasticity

The magnetic properties originate from the interaction between the magnetic moments of the domains. The distance between the magnetic moments is changed when the material is subjected to the applied stress which causes deformation in the material. [1] On the other hand the mechanical properties of the material, that is, how the material responses to the external stress σ, depend on the magnetic and electrical forces between the atoms in the material. Applied stress distorts the crystal lattice and will change the distance between the atoms. [26] Thus the magnetic and mechanical properties of the material are closely coupled. [1]

The mechanical response of metals to stress is not linear at all stress values. The response can be elastic or plastic and the material will fail at high stresses. Elastic deformation is reversible. Macroscopic elastic strain can be defined as small changes in the interatomic spacing and stretching of interatomic bonds. [13]

Magnetoelasticity means the connection between the elastic and the magnetic properties of the material. The most important phenomena related to magnetoelasticity are magnetostriction and magnetomechanical effect, which are explained in detail in the next chapters 4 and 5. Magnetostriction and the magnetomechanical effect are closely coupled because both phenomena occur simultaneously. [1]

4 MAGNETOSTRICTION

4.1 Mechanism of magnetostriction

The fractional change in length of a ferromagnetic material due to the applied magnetic field strength is described by the magnetostrictive constant λ. Magnetostriction forms mainly due to the spin-orbit coupling. In iron and iron alloys the coupling is weak and thus the magnetostriction constant λ is small, typically of the order of 10^{-5} to 10^{-6}. Magnetostriction is determined according to Equation (4.1):

$$\lambda = \frac{\Delta L(H)}{L} \tag{4.1}$$

where ΔL is the change in length and L is the initial length of the specimen. [1] In advanced materials such as Terfenol-D, which consist of terbium, dysprosium and iron, the magnetostriction can be as high as 10^{-3} [19].

Figure 4.1 shows schematic illustration of the mechanism of magnetostriction. Magnetostriction can be classified into spontaneous magnetostriction and field-induced magnetostriction. Above Curie temperature material is disordered and no domains exist. Below Curie temperature material becomes ferromagnetic and spontaneous change in length ΔL occurs. Spontaneous magnetostriction is due to the domain ordering, as shown in Fig 4.1 a).When an external magnetic field is applied, domains align themselves to the direction of applied field. Consequently field-induced change in length ΔL(H) occurs, as shown in Fig. 4.1 b). [3]

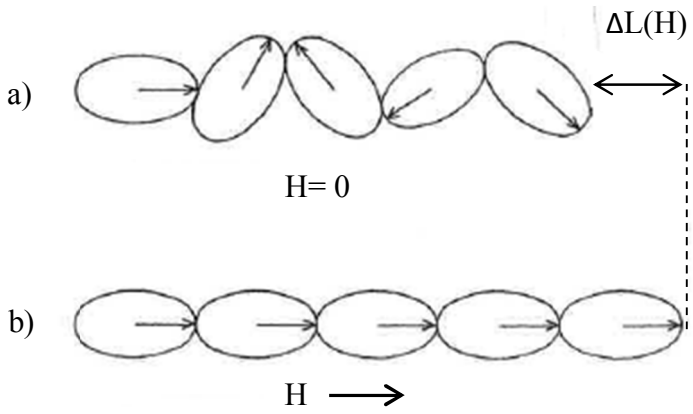

Figure 4.1 *Schematic illustration of the mechanism of magnetostriction. The arrows indicate the magnetization vectors and the oval lines are electron orbits. [3]*

Even though λ is called magnetostriction constant, in reality it is not constant. It can be positive, negative or zero depending on the material and it depends on the magnetic field strength H. Materials, such as nickel and cobalt, with negative magnetostriction, contract under the influence of a magnetic field. Materials with positive magnetostriction expand when exposed to the magnetic field. [1] In iron the magnetostriction constant changes its sign at a critical magnetic field value as indicated in Fig. 4.2. The magnetostrictive constant is positive when iron is subjected to low magnetic field and negative when exposed to high magnetic field. [20]

Magnetostriction is a consequence of the domain reorientation caused by an applied magnetic field. The process of magnetization as well as the magnetostriction occurs by two mechanisms: domain-wall motion and rotation of the magnetization vectors. At lower fields the change in the magnetization induced by the applied magnetic field occurs first through the domain wall motion as explained earlier. The magnetostrictive change in length occurs as a result of the movement of the 90° walls in the low field region. [1]

When the magnetic field increases, the magnetization vectors start to rotate and additional energy is required. This corresponds to the point where the λ vs. H-curve shows a maximum (Fig. 4.2). After the magnetostriction constant has reached the maximum value the length of the specimen starts to decrease. Now most of the magnetostrictive change in length is accomplished by the rotation of the magnetization vectors. Magnetostriction constant depends on the direction of the saturation magnetization vector M_s with respect to the crystal axes. [1]

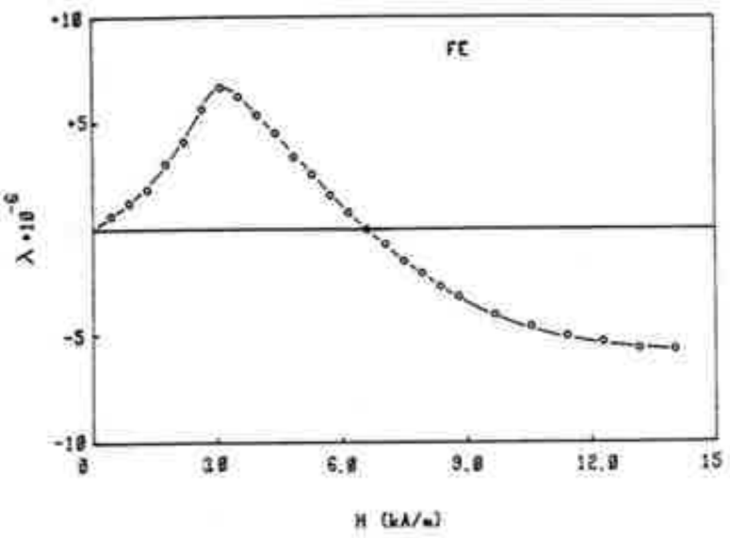

Figure 4.2 *The magnetostriction of polycrystalline iron as a function of magnetic field strength. At the critical magnetic field strength the magnetostriction constant changes its sign. In this case the critical magnetic field strength of iron is 6,5 kA/m. [20]*

At the critical magnetic field value the magnetostriction constant of iron becomes negative. At high magnetic field strength values beyond the magnetic saturation the volume of the iron specimen increases. This is called volume or forced magnetostriction. [1]

4.2 The stress dependence of magnetostriction

The magnetic behaviour of iron and steel is complicated because the sign of the magnetostriction constant is not only field-dependent but also stress-dependent [1]. The stress dependence of the magnetostriction constant of a polycrystalline iron is shown in Fig. 4.3. Applied stress changes the critical value of the magnetic field. Tension makes the magnetostriction more negative, whereas compression increases positive magnetostriction. [1, 20]

The stress response of the material can be seen from the sign of the product $\lambda\sigma$. It can be seen in Fig 4.3 that the sign of the $\lambda\sigma$ product is positive during tension and negative during compression when the magnetic field is below the critical value. At the magnetic field strength values above the critical value the situation is reverse. [1, 20]

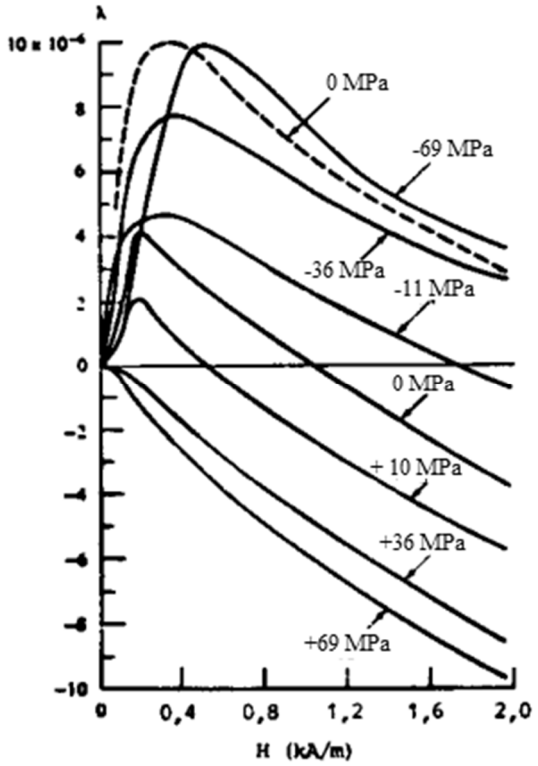

Figure 4.3 *Magnetostriction constant λ of polycrystalline iron as a function of the magnetic field strength H under tension (positive stress σ) and compression (negative stress σ). Each curve represents magnetostriction constant as a function of magnetic field at a definite stress level. [20]*

5 MAGNETOMECHANICAL EFFECT

It should be mentioned that concerning the definitions of the influence of stress on magnetization, confusion and inconsistency occur in the literature [21]. The term piezomagnetism is sometimes referred to as the change in the magnetization due to the external stress but it should be restricted only to materials which can get magnetized due to stress in the absence of magnetic field [1]. In this work the term magnetomechanical effect is used to describe the stress-induced change in the magnetization in a given magnetic field. This phenomenon is also called Villari effect [22] or inverse magnetostriction [1].

The influence of stress on magnetization can be divided into two phenomena: the influence of static stress on the magnetization under varying magnetic field and the influence of varying stress on magnetization under constant magnetic field. [3] The change in magnetization caused by varying stress is less understood than the effect of static stress. [20]

5.1 Magnetization under static stress

In the absence of stress the direction of saturation magnetization M_s is controlled by K_1 as described in Equation (3.1). When stress is applied, the easy direction of saturation magnetization is determined by both K_1, magnetostriction constant λ and stress σ. The relation of these three components can be presented as a sum of magnetocrystalline W_e and magnetoelastic W_{me} anisotropy energies according to Equation (5.1):

$$W = W_c + W_{me} \tag{5.1}$$

Magnetoelastic anisotropy energy W_{me} consists of magnetostrictive strain and stress and it is defined as follows:

$$W_{me} = -\frac{3}{2}\lambda_{100}\sigma(\alpha_1^2\gamma_1^2 + \alpha_2^2\gamma_2^2 + \alpha_3^2\gamma_3^2) - 3\lambda_{111}\sigma(\alpha_1\alpha_2\gamma_1\gamma_2 + \alpha_2\alpha_3\gamma_2\gamma_3 + \alpha_3\alpha_1\gamma_3\gamma_1) \tag{5.2}$$

where λ_{100} and λ_{111} are the magnetostrictive strains along the <100> and <111> directions, σ is stress, α_1, α_2 and α_3 are the direction cosines of domain magnetizations and γ_1, γ_2, γ_3 are the direction cosines of stress with respect to the cube axis. [1, 20]

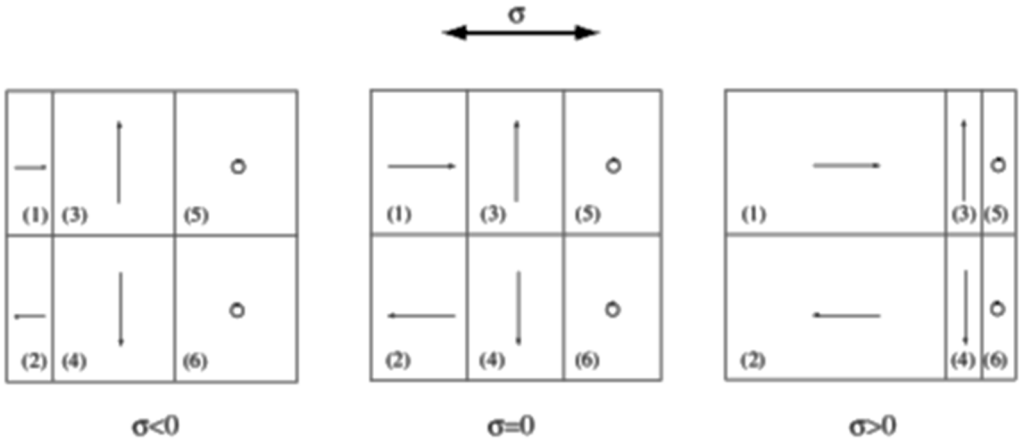

Figure 5.1 *Schematic illustration of the influence of applied static stress on the domain structure in a material with positive magnetostriction constant. The arrows indicate the magnetization vectors. [11]*

The influences of static stress on magnetization depend on the sign of the magnetostriction constant λ, on the sign of the applied stress and on the initial magnetic state. Consequently the stress response of the material can be seen from the sign of the product $\lambda\sigma$. In a material with positive magnetostrictive constant λ, magnetization vectors of the domain tends to align along the easy magnetization direction closest to the direction of the applied tension and the product $\lambda\sigma$ is then positive. In a material which has a negative magnetostriction constant λ, the magnetization vectors of the domain tends to align along the easy magnetization direction farthest from the applied tension, and the product $\lambda\sigma$ is then negative. [1, 23]

Figure 5.1 shows a schematic illustration of the domain structure in a material with positive magnetostriction constant. The single crystal is divided into six domains in which the magnetization vector is pointing to the direction of easy magnetization. When an external stress is applied to the material the domain configuration will change. This reorientation of the domains is due to the minimization of the total energy. Stress influences the domain structure through the magnetoelastic interaction according to Equation (5.2). The domains whose magnetization vectors are aligned parallel to the applied tension ($\sigma>0$) increase in size. Applied compression ($\sigma<0$) increases the size of the domains perpendicular to the stress. [11]

The direction of the magnetization vectors can be determined by comparing the values of K_1 and $\lambda\sigma$. If K_1 is larger than $\lambda\sigma$, the magnetocrystalline energy W_c is more important than magnetoelastic anisotropy energy W_{me}. If K_1 is smaller than $\lambda\sigma$, the stress and magnetoelastic anisotropy energy control the easy direction of magnetization. [20]

The influence of static stress on the magnetization curve depends on the applied magnetic field strength, on the sign of the stress and on the magnetostriction constant. In general in a material with negative magnetostrictive constant, compressive stress (negative stress) increases and tensile stress (positive stress) decreases magnetization. In a material which has positive magnetostriction the influence of applied stress is reverse. [1]

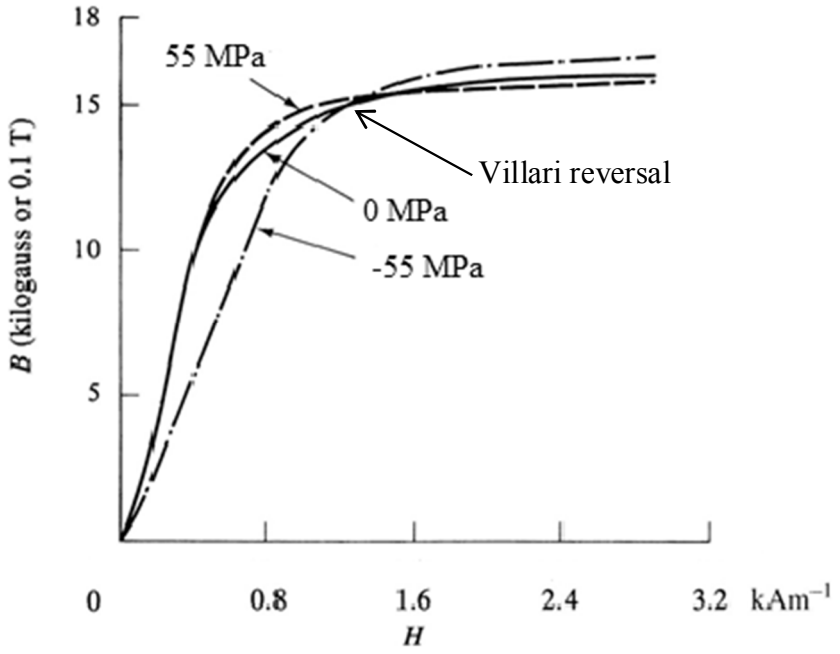

Figure 5.2 *The influence of static stress on the magnetization curve of iron. Negative stress is compression and positive is tension. [1]*

The magnetic behavior of iron and steel subjected to stress is complex. This is due to the magnetostriction constant of iron which assumes both positive and negative values depending on the magnetic field strength. [1]

Figure 5.2 shows the influence of static stress on the magnetization curve of iron. Compressive stress decreases magnetization with increasing magnetic field strength, except at very high fields. Tensile stress increases magnetization at low field strengths and decreases magnetization at high field strengths. At so called Villari reversal the sign of the change in the magnetization changes. It can be seen that the influence of compression is stronger than the influence of tension. [1] The Villari reversal represents the point where the rotation of the magnetization vectors begins. It is also the point where the sign of the magnetostriction constant changes due to the magnetic field. [11]

Recently Bulte et al. [10] measured several hysteresis curves of low carbon steel bars under a range of static stress values and placed the curves on top each other. They noticed that when analyzing groups of hysteresis curves in the same graph, changes which occur in the shapes of the loops at different stress values, can be seen. This method also shows the eventual intersection of the curves with each other.

The hysteresis curve measured in the absence of applied stress differs from the hysteresis measured under the influence of stress as indicated in Fig 5.3. It can be seen that in steel specimen compression decreases the magnetic flux density. In other words compression makes magnetization harder, whereas tension makes it easier. Tension tends to change the shape of the hysteresis curve towards square and narrow. [10]

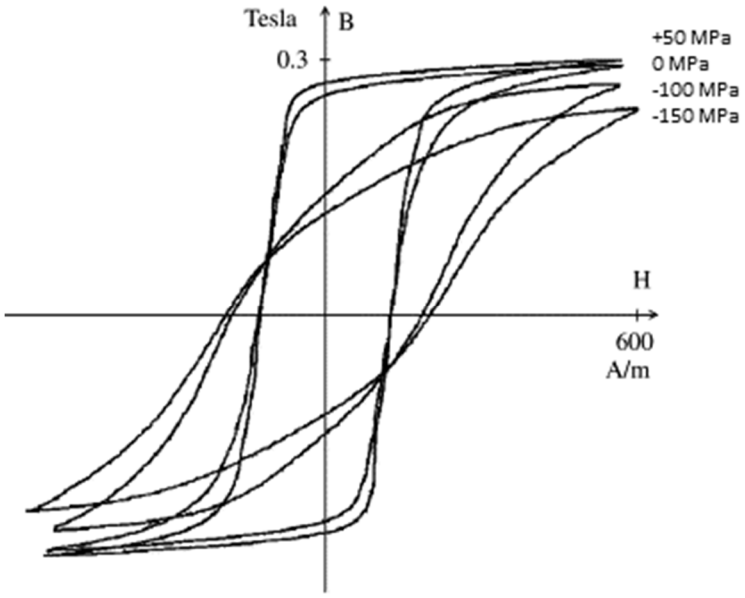

Figure 5.3 *The influence of static stress on the hysteresis curve of low carbon steel bar. In this sample the intersection point occurs at around 130 A/m. [10]*

Bulte et al. [10] also noticed that all hysteresis curves of steel specimen measured under different applied stresses intersect at two coincident points. At these points, located in the BH-plane, the applied stress does not influence the magnetization of the material. The magnetic field strength at which the curves intersect is called the critical rotation field H^*, which is for mild steel around 130 A/m.

When the critical rotational field is applied, 90° walls and the reversible rotations of magnetization vectors are absent at the intersection point. The magnetic behavior is independent on the applied stress, and it depends only on the history, temperature and magnetic field strength. Bulte et al. [10] suggest that the critical rotation field is required to produce an irreversible rotation of saturation magnetization vectors.

According to Bulte et al. [10] the intersection points can be explained by the nature of the domain walls. Applied stress will alter the structure of the crystal lattice and thus change the relative separations of the atoms. When the atoms move in relation to each other, the magnetocrystalline anisotropy energy, which is the energy required keeping the magnetization vectors pointing in any given direction, is changed. Any non-easy aligned spins are affected by the distortion in the lattice, but only 90° walls will move due to applied mechanical stress. [10]

Usually in the research papers the coincident points are ignored and only the basic magnetic properties are considered. In addition to Bulte et al. [10] also Perevertov [24] has found the coincident points when studying the influence of residual stress on the magnetization process in mild steel. According to Perevertov [24] there is no clear explanation why the hysteresis loops cross each other. Even though the recent study of the interception point in the hysteresis by Bulte et al. [10] does not give any accurate models, it provides an opportunity to understand the magnetomechanical effect in steel and gives a general trend which can be used in analyzing measurement results.

The most important factor determining how the magnetization and the mechanical stresses are related to each other is the domain structure of the material. The influence of the applied mechanical stress on the domain wall can be described as an effective pressure. The applied stress will not influence the 180˚ walls because the pressure is on both sides of the wall but in opposite directions. The 180˚ walls are not stress sensitive but 90˚ walls are. Consequently the change in the magnetization is caused by a displacement of 90˚ walls. [1, 10]

When the applied magnetic field strength is greater than the critical rotational field, magnetization of steel becomes again dependent on the applied stress. This is due to the reversible rotations of the magnetization vectors away from the easy directions. [10]

The linear relationship between the change in the magnetization and applied stress can be expressed as follows:

$$\varepsilon = \frac{1}{E^H}\sigma + d_{33}H \tag{5.3}$$

$$B = d_{33}^{*}\sigma + \mu^{\sigma}H \tag{5.4}$$

where ε is the strain, E^H is elastic modulus at constant magnetic field strength H, σ is stress, d_{33} is linear coupling coefficient at a constant stress and d_{33}^{*} is the magnetomechanical effect at a constant magnetic field, B is the magnetic flux density and μ^{σ} is the permeability at constant applied stress. These equations combine the Hooke's law of linear elasticity $\varepsilon=\sigma/E$ (Equation 2.3) and the basic magnetic equation $B=\mu H$ (Equation 2.7). The equation (5.3) defines the total strain in the material as a sum of mechanical stress-induced elastic strain and magnetic field-induced magnetostrictive strain. According to the equation (5.4) the magnetic flux density is the sum of the magnetic component $\mu^{\sigma}H$ and the term due to the magnetoelastic interactions $d_{33}^{*}\sigma$. [25]

These equations are valid only, if the behaviour of the material is assumed to be linear and elastic. In reality the magnetomechanical effect is nonlinear and hysteretic in nature, and consequently these linear equations are valid only in a very narrow region. However, the basic linear equations give the framework for modelling the magnetomechanical effect. [25]

5.2 Magnetization under varying stress

5.2.1 Anhysteretic curve

In an ideal case material would be defectless, and consequently the magnetization changes would be hysteresis-free and reversible. Anhysteretic or ideal magnetization curve is shown in Fig. 5.4. [3] Anhysteretic curve is located inside the main hysteresis loop and it approaches the initial hysteresis curve at high magnetic field strength values (see Fig. 5.5). [1]

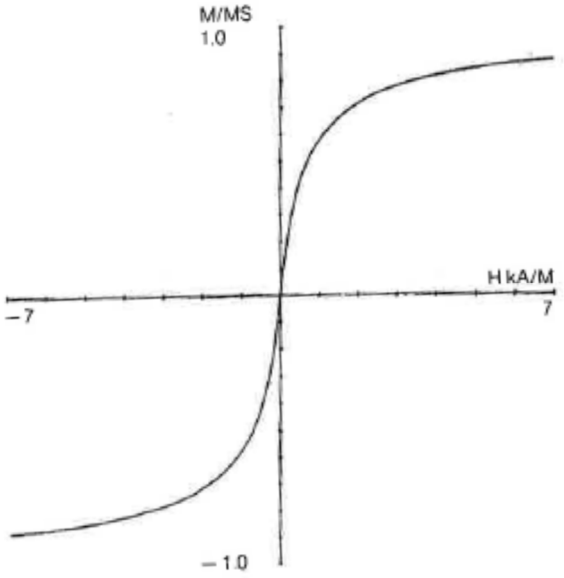

Figure 5.4 *Anhysteretic curve. Anhysteretic curve has no hysteresis and it is reversible [3]*

In the case of a real material, which contains defects, the anhysteretic curve can be reached by alternating magnetic field method described by Bozorth [16] or stress cycling described by Jiles et al. [18]. According to Jiles et al. [18] domain walls can overcome the pinning sites due to the applied stress. When a material is subjected to varying stress, at given constant magnetic field strength, domain walls will break away from the pinning sites and they will move until they reach the anhysteretic state. The anhysteretic state can be defined as the thermodynamic equilibrium of a ferromagnetic material. This state lies on the anhysteretic curve.

The influence of stress on magnetization can be theoretically treated by using the Langevin equation for bulk magnetization [26]:

$$M = M_s \coth\left[\frac{(H+\alpha M)}{a} - \frac{a}{(H+\alpha M)}\right] \tag{5.5}$$

where α is the mean field parameter representing the interdomain coupling and $a=kT/\mu_0 m$ in which k is Boltzmann's constant, T is the temperature, μ_0 is the permeability of free space and m is the magnetic moment. Parameters α and a depend on applied stress. Langevin equation (5.5) does not describe the behavior of a ferromagnetic material in the presence of pinning sites. Consequently this theory applies only to the anhysteretic curve and to the magnetization at high fields where the anhysteretic curve and the initial hysteresis curve approach each other. [26]

5.2.2 Law of approach

When a ferromagnetic material is subjected to stress the change in magnetization can be either positive or negative. The direction of the change in magnetization depends not only on the influence of stress and magnetic field strength but also on the initial magnetic state. The initial magnetic state means the magnetic history of the material [18] and it is also called as working point [20]. When interpreting the results of magnetic measurements, it has to be taken into account whether the initial magnetic state lies above or below the anhysteretic curve. [18, 20]

The factors influencing changes in the magnetization with stress depend on the magnetic field strength. In the low field region, when a ferromagnetic material is subjected to stress of either sign, the magnetization approaches the anhysteretic curve. This is sometimes referred as the law of approach. The sign of the change in magnetization is determined by the initial magnetic state and it is independent on the sign of the stress. However, it has been found that in steel the influence of compression on magnetization is greater than tension. [26]

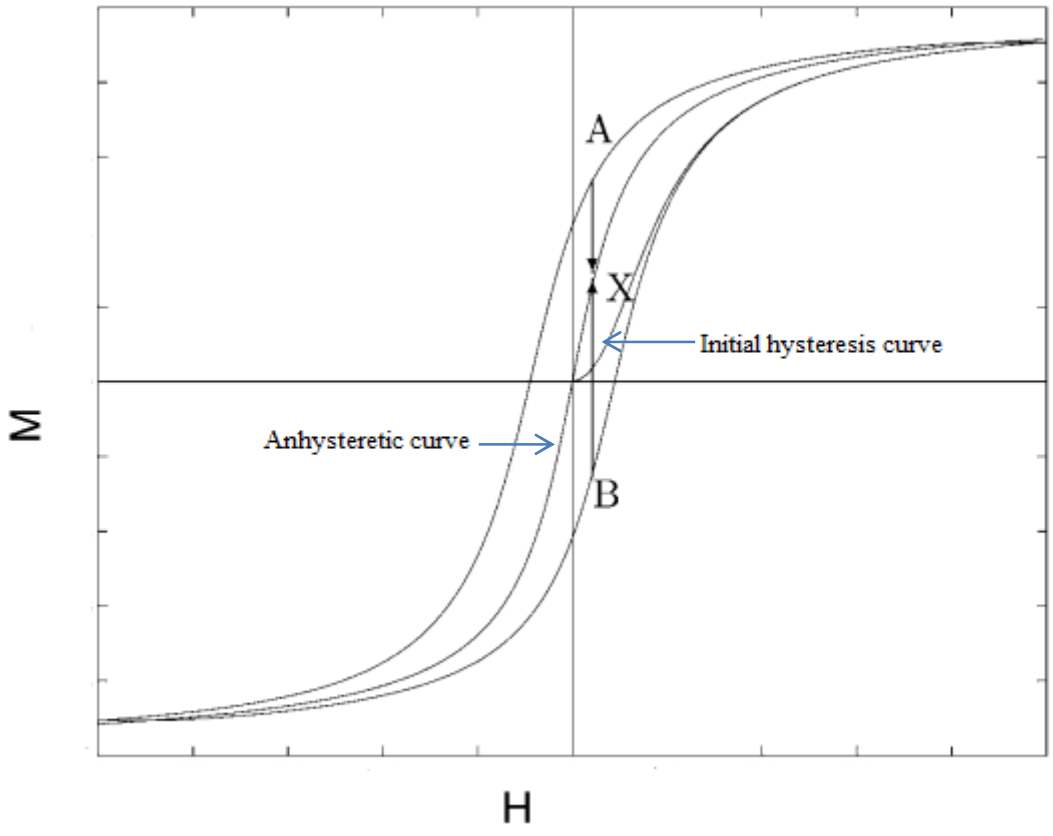

Figure 5.5 *Schematic illustration of law of approach in a ferromagnetic material, after Pitman [48] and Dapino et al [44]. Anhysteretic curve always lies above the initial hysteretic curve and it is located inside the main hysteresis loop. The arrows indicate the approach of the magnetization towards the anhysteretic curve from the position A (above the anhysteretic curve) and from the position B (below the anhysteretic curve).*

Figure 5.5 illustrates the law of approach. When the initial magnetic state lies above the anhysteretic curve (point A), the application of stress decreases the magnetization. When the initial magnetic state lies below the anhysteretic curve (point B), the applied stress will cause an increase in the magnetization. At low magnetic field strength values the sign of the change in the magnetization due to stress does not depend on the magnetostriction constant λ. [26, 18]

In the high field region where the initial hysteresis curve lies very close to the anhysteretic curve, the sign of the magnetostriction constant λ and the sign of stress define the direction of the change in magnetization. This is also true when the working point lies on the anhysteretic curve. [18]

The application of cyclic stress causes changes in the magnetization and also in the magnetic flux density B. Figure 5.6 shows the change in the flux density B as a function of stress σ at different magnetic field strength values when the working point lies on the initial hysteresis i.e. below the anhysteretic curve. It can be seen that the change in magnetization with increasing field strength is towards the anhysteretic curve. [26]

According to Jiles [26] the magnitude of the change in the magnetic flux density in iron is proportional to the difference between the anhysteretic and initial hysteresis states during one tension stress cycle. Figure 5.7 shows the maximum change in magnetic flux density ΔB with one stress cycle as a function of the magnetic field strength H. At first the change in the magnetic flux density ΔB increases as a function of magnetic field strength H. At a definite magnetic field strength value the change in the flux density

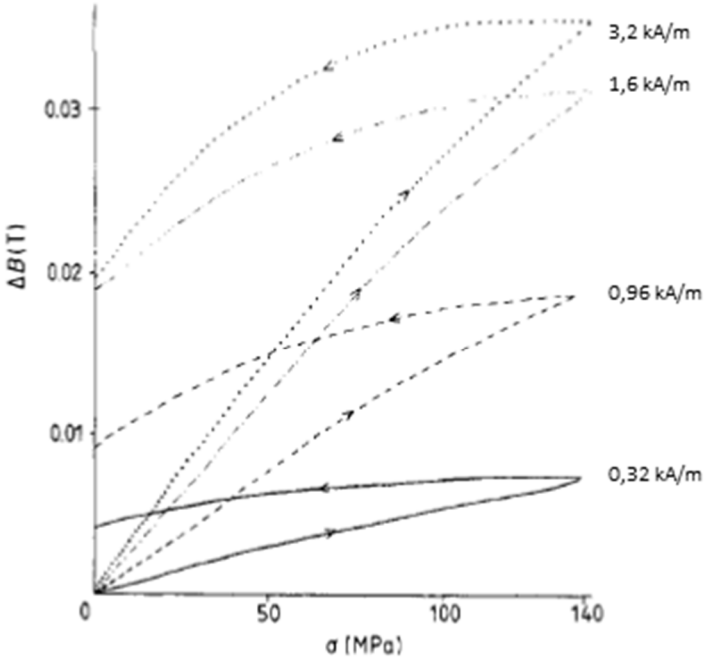

Figure 5.6 *Changes in the magnetic flux density ΔB with one tensile stress cycle of 140 MPa at different magnetic field strength H values in a steel sample. The working point lies on the initial hysteresis below the anhysteretic curve. [26]*

reaches a maximum and then reduces with increasing field strength. The maximum of the change in the magnetic flux density occurs above the field strength where the difference between initial and anhysteretic curves reaches its maximum. According to Ruuskanen [20] the changes in the magnetic flux density due to the cyclic stress also depend on the applied stress amplitude.

It has been found that the anhysteretic value of magnetization M_{an} itself is stress dependent. The anhysteretic value of magnetization of a material with positive magnetostriction constant λ increases under the influence of tension and decreases under compression. [26, 12] According to Jiles [28] the stress-dependence of the anhysteretic magnetization can be expressed with Equation (5.6).

$$M_{an}(H,\sigma) = M_{an}\left(H + \alpha M + \frac{3}{2}\frac{\sigma}{\mu_0}\left(\frac{d\lambda}{dM}\right)_{\sigma}, 0\right) \tag{5.6}$$

Equation (5.6) describes how the anhysteretic magnetization changes with static stress. The law of approach is based on the effective field theory, which states that both magnetic field and stress can be treated similarly.

The anhysteretic curve is reversible with respect to both magnetic field strength and stress. In Fig. 5.7 can be seen that when the initial magnetic state lies on the anhysteretic curve, the influence of cyclic stress on the net change in magnetic flux density ΔB is small. After one stress cycle the magnetization returns to its original anhysteretic value. [20, 26]

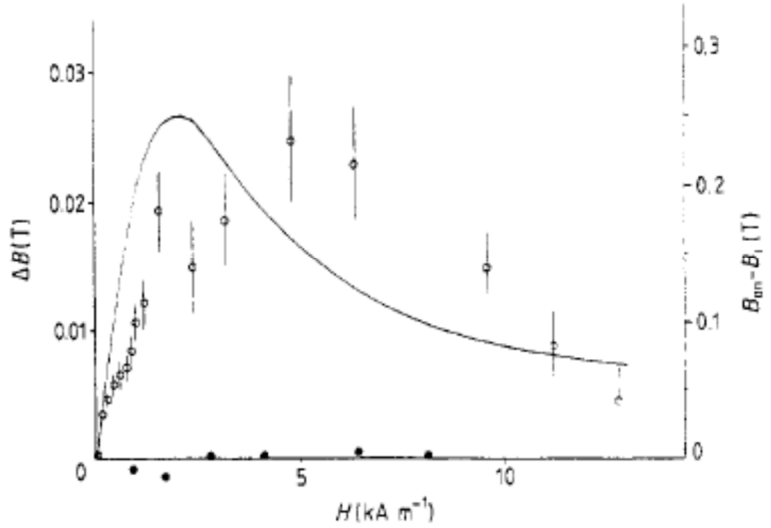

Figure 5.7 *Changes in the flux density* ΔB *with one tensile stress cycle of 140 MPa tension as a function of magnetic field strength H in a steel sample. Symbol (●): The initial magnetic state is on the anhysteretic curve. Symbol (○): The initial magnetic state is on the initial hysteresis curve. The solid curve describes the difference between the anhysteretic and the initial hysteresis value of magnetic flux density B. [26]*

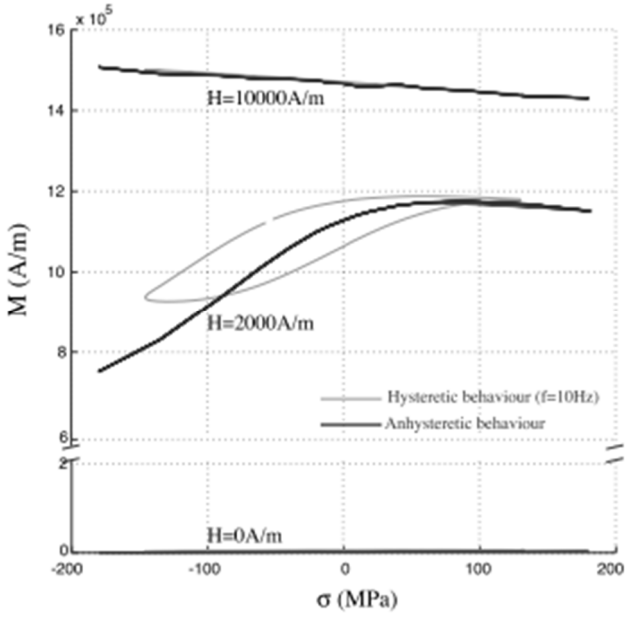

Figure 5.8 *Anhysteretic and hysteretic behavior of low carbon steel at three different magnetic field strength values. The black lines represent the anhysteretic behavior and gray lines the hysteretic behavior of the steel sample. The amplitude of stress varies from 0 to 180 MPa at the frequency of 10 Hz. When the magnetic field strength is zero, both anhysteretic and hysteretic curves lie close to the x axis. [11]*

Figure 5.8 by Rizzo et al. [11] describes the hysteretic behavior of low carbon steel as a function of stress amplitude and the stress dependence of anhysteretic curve. It can be seen that in the absence of applied magnetic field (H=0 A/m) the ferromagnetic material cannot be magnetized by mechanical stress only. When analysing the anhysteretic behaviour, Fig. 5.8 shows similar results as indicated in Fig. 5.2: tension increases magnetization and compression has the opposite effect. Compression has a greater influence on the anhysteretic curve than tension.

At very high magnetic field strength values (H=10 000 A/m) the hysteresis loop disappears and starts to follow the anhysteretic behaviour. The material has reached the saturation magnetization and consists only of one domain. There are no domain walls and thus no domain wall motion. The magnetization decreases linearly with increasing magnetic field strength. The measurements were carried out at frequencies from 5 to 50 Hz but in Fig. 5.8 only results at 10 Hz are presented. [11]

5.3 Modelling of the hysteresis and magnetomechanical effect

The study on the influence of stress on magnetization started in 1890 by Edwin and since then theories and mathematical models of the interaction between stress and magnetization have been developed. [18] The interaction between stress and magnetization is usually nonlinear and hysteretic, and thus difficult to model. The development of an accurate model of the magnetomechanical effect plays a major role in the application of magnetostrictive materials used in stress sensors and in magnetic measurements for

stress evaluation in materials. [9] A working mathematical model of hysteresis would ease the interpretation of the results, since a lot of factors influence the hysteresis and magnetoelastic properties. [3]

Jiles and Atherton [26, 18] and later Jiles et al. [30, 8, 28, 29, 9] have studied the magnetostriction and magnetomechanical effect from different points of view. The fundamental theory of the magnetomechanical effect is based on the law of approach, which states that changes in magnetization under applied stress are towards the anhysteretic curve and that the anhysteretic curve is itself stress-dependent. The law of approach is based on the effective field theory which states that the change in the magnetization due to stress is equal to the change caused by the effective field.

Recently Jiles and Li [8, 9] have generalized the theory of the magnetomechanical effect, which is based on the law of approach, by including linear and nonlinear factors to the theory. The change in the magnetization due to the varying stress can be described by the differential equation:

$$\frac{dM}{d\sigma} = \frac{1}{\varepsilon^2}(\sigma \pm \eta E)(1-c)(M_{an} - M_{irr}) + c\frac{dM_{an}}{d\sigma} \qquad (5.7)$$

where ε is a constant having the dimensions of stress, η is constant which represents the reversible change in the magnetization due to the stress, E is the elastic modulus, c is reversibility constant and M_{irr} is the irreversible component of the magnetization. Equation (5.7) describes the dependence of magnetization M on stress σ, anhysteretic magnetization M_{an} and the irreversible component of magnetization $M_{irr.}$

The new model was compared with the experimental results on a nickel sample. It was found that the results of the new model equation were in better agreement with experimental observations than the previous model. However, even the modified model is not yet accurate enough and further development is needed. [8]

Rizzo et al. [11] proposed a multiscale model for the magnetomechanical behavior based on the Jiles-Atherton model of hysteresis [18, 31]. The developed model and the experimental results are in good agreement and give at least reasonable guidelines for the future development.

In most electromagnetic applications, magnetic materials are subjected to multiaxial stress [16]. However, most models describing the influence of stress on the magnetic behavior are restricted to uniaxial, tensile or compressive stress [30]. Recent studies by Hubert and Daniel [6, 7] define equivalent stress criteria for the influence of stress on magnetic behavior, which gives more accurate prediction than the previous proposals. An equivalent stress is a fictive uniaxial stress that would change the magnetic behavior in a similar way than the multiaxial one.

6 MICROSTRUCTURAL FACTORS INFLUENCING THE MAGNETIC PROPERTIES

6.1 Different phases and microstructures

Alloys of iron and carbon containing carbon between 0,008 and 2,1 wt% (percentage of weight) are classified as steels. The mechanical behaviour of steel depends on the microstructure which is characterized by the number of existing phases and their volume fractions and distribution. The microstructure of steel specimen depends both on the carbon content and heat treatment. [13] In steels which require high ductility, high toughness and good weldability, carbon content is kept low. Carbon content is maintained at higher levels in steels that require high strength, high hardness, fatigue resistance, and wear resistance. [32]

Figure 6.1 shows a part of the iron-carbon phase diagram. Different areas describe phases or structures which are stable at different combinations of temperature and carbon content. Depending on carbon content and heat treatment, carbon can exist in martensite, ferrite, pearlite, carbide or graphite. When pure iron is heated it goes through a phase transformation twice before melting. Ferrite (α iron) is the stable form of iron at room temperature. Austenite (γ iron) exists at temperatures above 912 °C up to 1394 °C and δ ferrite at temperatures above 1394 °C. [13]

At temperatures below 727 °C (the vertical line on the phase diagram), only small amount of carbon is soluble in ferrite, the maximum solubility being 0,022 wt%. When the solubility limit of carbon in ferrite is exceeded, iron carbide Fe_3C, i.e., cementite inclusions are formed. Cementite is very hard and brittle and consequently the strength of steels can be improved by increasing the amount of cementite. [13]

In addition to iron and carbon, steels contain many other elements which move the boundaries between the phase fields, i.e., critical temperatures (A_1, A_3 and A_{cm}) of the iron-carbon phase diagram. Manganese and nickel are austenite stabilizers, which lower critical temperatures. Silicon, chromium, and molybdenum are ferrite stabilizers and carbide formers, which increase critical temperatures and shrink the austenite phase field. [33]

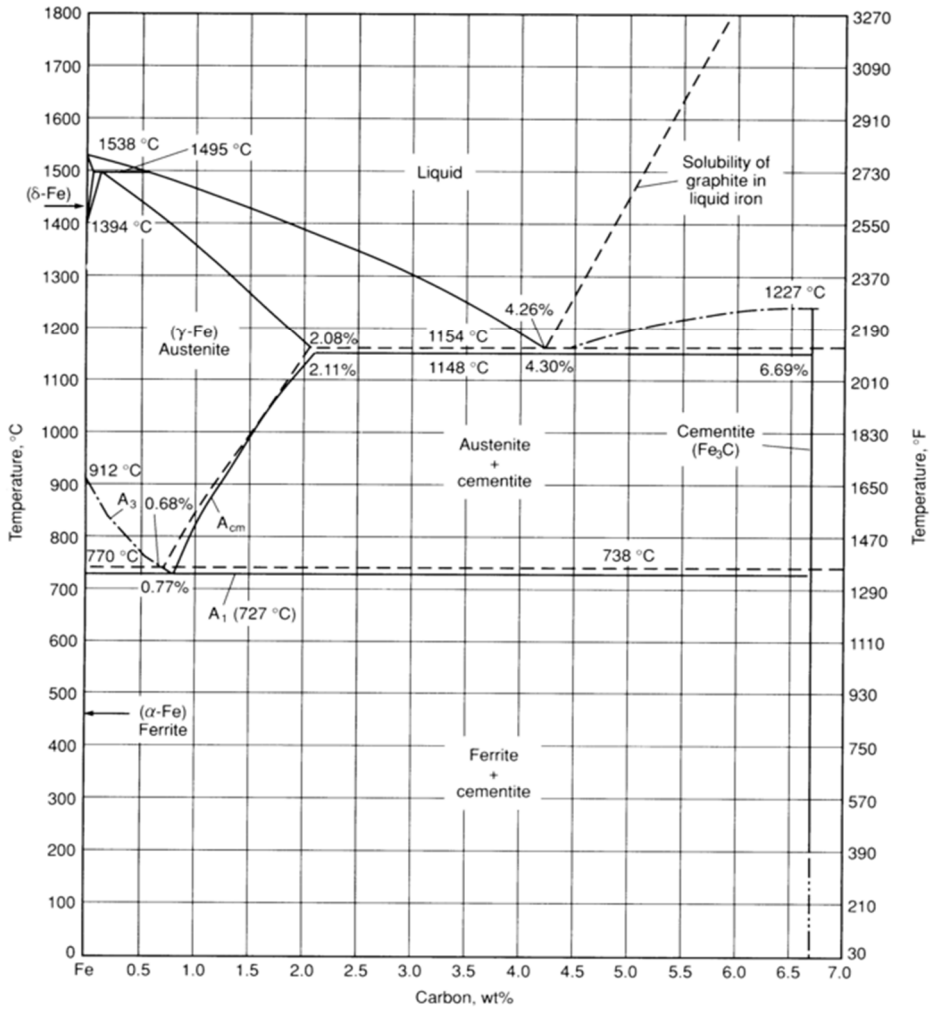

Figure 6.1 *The iron-carbon phase diagram. [32]*

Different phases have different magnetic properties. Ferrite, cementite and martensite are magnetic phases. Ferrite can be further defined as a magnetically soft material. Austenite is paramagnetic [13] which means that it has a net magnetic moment like ferromagnetic materials but it exhibits magnetic properties only when an external field is applied. [1]

Pearlite is a phase mixture which is formed when steel is heated to the austenite region and then slowly cooled down. Pearlite consists of alternating layers of α ferrite and cementite (Fe_3C). Pearlite exists as grains which are often called colonies. Within each colony the layers are mainly aligned in the same direction as indicated in Fig. 6.2. [13]

According to Devine et al. [34] the presence of different phases in steel influences its magnetic properties. Tanner et al. [35] correlated the coercivity H_c to the presence of pearlite and ferrite phases according to Equation (6.1):

$$H_c = c_1\left(\frac{V_p}{d_p}\right) + c_2\left(\frac{V_f}{d_f}\right) \tag{6.1}$$

where V_p and V_f are the pearlite and ferrite volume fractions, d_p is the average size of pearlite colonies, d_f is the grain size of ferrite and c_1 and c_2 are constants.

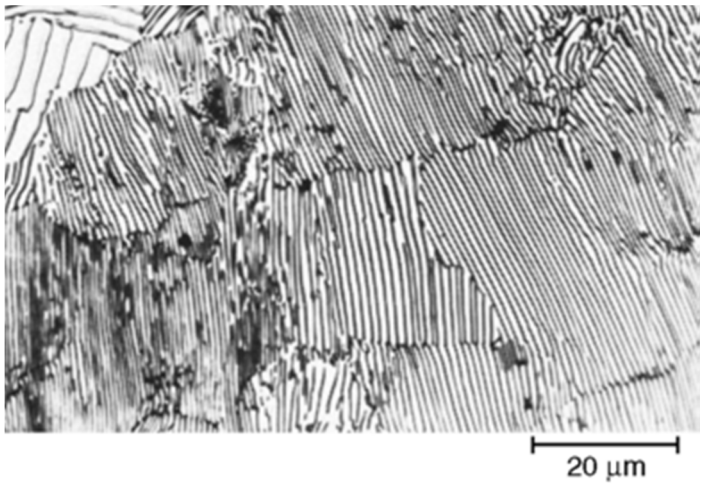

Figure 6.2 *The microstructure of pearlite in a eutectoid steel (~0.8% C) after slow cooling (2,5 °C/min) from austenite stability area. Pearlite consists of alternating layers of α ferrite (light phase) and cementite (dark phase). [36]*

6.2 Grain size

Steel consist of grains, where the structure of the crystal lattice may be relatively defectless. Grain size influences the mechanical properties [13] and also the magnetic properties of the material [37]. Anglada-Rivera et al. [37] studied the influence of grain size on the hysteresis curve in commercial AISI 1005 steel with different heat treatments. They found that the hysteresis and the saturation magnetic flux density B_{max} change with grain size. The results are shown in Fig. 6.3. Recent measurements on the magnetic properties of structural carbon steels by Rumiche et al. [17] show similar results; the increase in grain size decreases the saturation magnetic flux density and decreases the coercivity. Grain boundaries hinder the motion of the domain walls during magnetization process and thus make magnetization harder.

According to Ranjan et al. [38] grain size influences the magnetic properties in many ways. For instance, the grain boundaries provide obstacles to the domain wall motion during magnetization process. The smaller the grain size, the more grain boundaries can be found in the material. In addition, pinning sites tend to locate at grain boundaries.

Hardness is a mechanical property of materials which can be related to the grain size and phase distribution depending on the chemical composition and microstructure [13]. According to Rumiche et al. [17] the magnetic properties can be correlated with the hardness. The saturation magnetic flux density decreases with increasing hardness, while coercivity increases with increasing hardness.

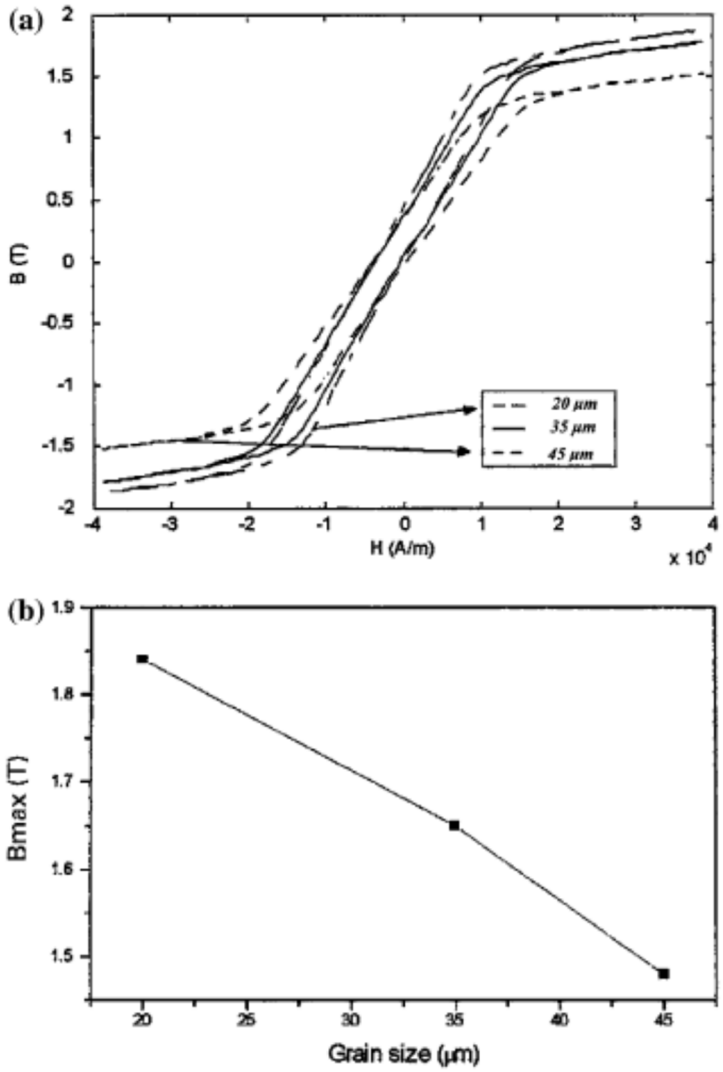

Figure 6.3 *The influence of grain size on a) the magnetic hysteresis curve b) the saturation flux density B_{max} of AISI 1005 steel (0,04 wt% C). [37]*

6.3 Carbon content

The alloying elements of steel have a significant influence on the mechanical properties but carbon is the most important compositional factor influencing the magnetic properties. [16] According to Buttle et al. [39] the carbon content is important because it determines whether the material is magnetically soft or hard. Carbon tends to cause domain wall pinning both in solution and in the form of precipitates.

Habermehl et al. [40] and Ranjan et al. [38] studied the relationship between the microstructural features and magnetic properties of steels. They found that when the carbon content of steel increases, the coercivity H_c, remanence B_r and hysteresis loss increase. According to Ranjan et al. [38] this can be explained in terms of an insoluble second phase of cementite (Fe_3C) which restricts the domain wall motion under the influence of magnetic field. According to Devine et al. [34] the formation of cementite

produces in the magnetoelastic energy localized variations which influence the domain wall motion and rotation of the magnetization vectors.

This type of behaviour has also been reported recently by Rumiche et al. [17]. When the carbon content increases, the amount of pearlite phase and consequently also the amount of cementite increases. This leads to a reduction in the magnetically soft ferrite phase. Cementite acts as an obstacle to the domain wall motion and the magnetization of the material becomes more difficult. When the carbon content is high, the reduction of the magnetization to zero is more difficult. In other words the coercivity increases with increasing carbon content. Rumiche et al. [17] did not find a correlation between remanence B_r and carbon content.

According to the studies of ferromagnetic steels by Habermehl et al. [40] the carbon content has also a secondary effect on the magnetic properties: high levels of carbon cause a reduction in the grain size which hinders the domain wall motion even more.

Habermehl et al. [40] also compared the hardened and annealed steel specimens in order to study the influence of heat treatment on magnetic properties. The hardened specimen containing mainly martensite was found to have significantly higher remanence and coercivity as compared with the annealed specimen having a fine pearlite structure.

6.4 The influence of carbon content on the magnetoelastic properties

Habermehl et al. [40] found that the anhysteretic magnetization also depends on the carbon content of the material. The anhysteretic magnetization decreases with increasing carbon content. This type of behaviour cannot be explained on the basis of increased number of pinning sites, as the anhysteretic magnetization is independent on the pinning sites. Habermehl et al. [40] suggest that the presence of pearlite reduces the interdomain magnetic coupling and this causes a reduction in the anhysteretic magnetization.

Devine et al. [34] studied the composition dependence of the magnetomechanical effect and magnetostriction on several plain carbon steels. The influence of carbon content on the magnetostriction is shown in Fig 6.4. It can be seen that the shape of the λ vs. B-curves for different steels is similar but the peak value of magnetostriction decreases with increasing carbon content.

Devine et al. [34] have also stated that the magnetomechanical effect is changed due to the differences in carbon content. Carbon was found to play a major role in determining the amplitude of the magnetomechanical effect. The working point in these measurements was the positive remanence point which lies above the anhysteretic curve.

Figure 6.5 shows the change in the magnetic flux density (induction) as a function of carbon content during one stress cycle. It can be seen that the carbon content dependence of magnetization is greater under compression than under tension. Tension alters the magnetization only little. The change in the magnetization due to compression decreases with increasing carbon content. [34]

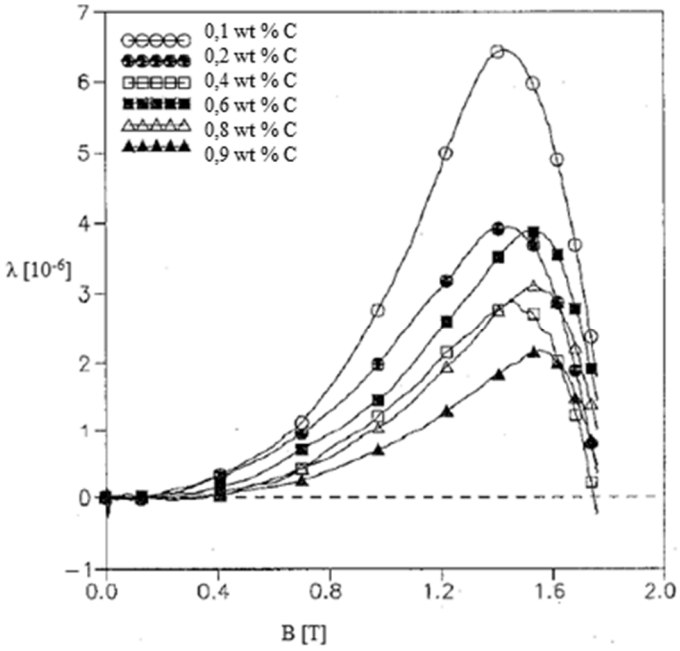

Figure 6.4 *Magnetostrictive curves for different annealed AISI plain carbon steels. The carbon content ranges from 0,1 to 0,9 wt %. [34]*

Figure 6.6 shows the influence of carbon content on the magnetomechanical effect for different steels. The magnetic flux density remaining after the removal of stress (remanence B_r) was found to change with carbon content. The change in the magnetic flux density increases with increasing carbon content, reaching a maximum at 0,6 wt %. After this critical carbon content the remanence decreases as shown in Fig. 6.7. [34]

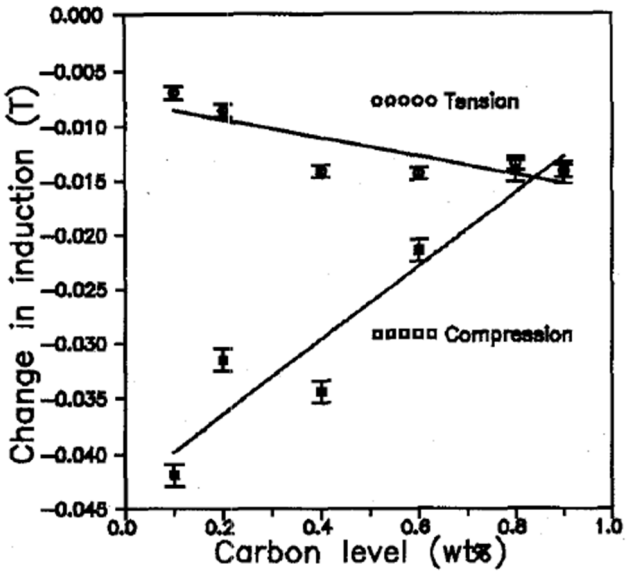

Figure 6.5 *The dependence of the magnetic flux density (induction) on carbon content during one stress cycle from 0 to 125 MPa. [34]*

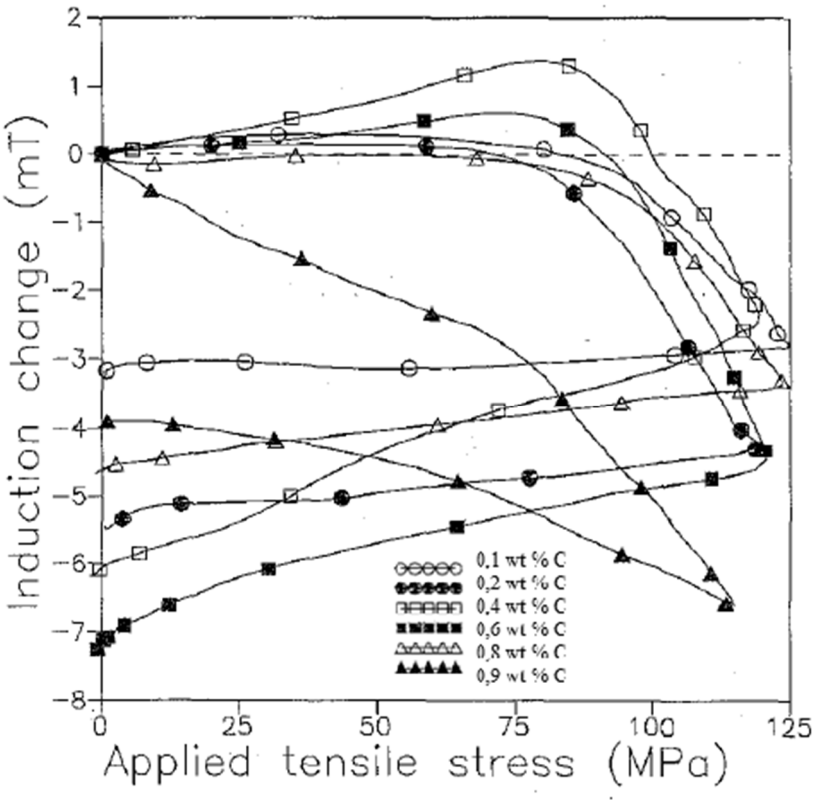

Figure 6.6 *The dependence of the magnetic flux density on tensile stress cycle for six different plain carbon steels. The carbon content ranges from 0,1 to 0,9 wt %. [34]*

The domain wall motion is reversible at low carbon levels. When the stress is removed, there are not enough pinning sites to hold the domain walls in their new positions. When the carbon content increases, also the number of pinning sites increases. This is due to the formation of cementite which restricts the reversible behaviour. [34]

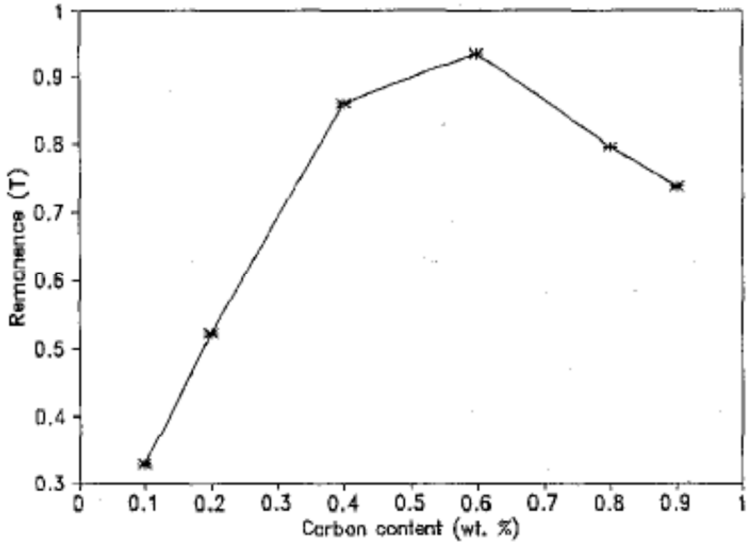

Figure 6.7 *The change in the remanence B_r as a function of carbon content for six different plain carbon steels. [34]*

6.5 Other alloying elements

The magnetic properties can be changed by alloying [16]. The alloying elements of the steel samples considered this work (in addition to carbon) are nickel, silicon, chromium, molybdenum and manganese. In addition phosphorus and sulphur could be found in small amounts.

In addition to iron and cobalt, nickel is one of the most common ferromagnetic materials. It has negative magnetostriction constant. Nickel is used in transducers (magnetostrictive oscillators) because it has a relatively high magnetostriction constant. [41] Wun-Fogle et al. [42] studied the magnetostriction and magnetization of common high strength steels. They compared the magnetostriction values of binary Fe-Ni systems with steels with same nickel content and found that the values of the magnetostriction of the steel and the binary alloys are similar. Wun-Fogle et al. [42] suggested that the nickel content is the principal factor determining the magnetostriction in the measured steels.

Silicon changes several magnetic quantities when added to iron. Silicon increases the electrical resistivity and permeability of the alloy. It also decreases eddy current losses. Iron-silicon alloys are the most important ones of the soft magnetic alloys and consequently they are widely used in power applications such as generators, transformers and motors. These alloys are usually referred as electrical steel. [41] Manganese and chromium are antiferromagnetic. Molybdenum is a paramagnetic substance. [1]

In the manufacturing process the magnetic properties of steel bars are of secondary importance to mechanical properties. The elements and their amounts are selected to achieve ideal mechanical properties of the steel components. For many low-alloy steels, the primary function of the alloying elements is to increase hardenability in order to optimize mechanical properties and toughness after heat treatment [32].

There is no known complete theoretical model available to predict the influence of different alloying elements on the magnetic behavior of steel. [1] Hence it is impossible to predict the magnetic properties of alloyed steel directly from the chemical analysis. In general, the alloying elements in small amounts have only little influence on the magnetic properties of steel. However, the non-ferromagnetic alloying elements (manganese, chromium and molybdenum) may reduce the magnetic properties of steel.

6.6 Service loading

If the service loading of a component exceeds the plastic deformation limit, the consequent deformation causes strain hardening in the metals. This deformation is also called cold working. When a metal is subjected to cold working, its dislocation density increases, and consequently the dislocation motion is hindered to by the presence of other dislocations. Strain hardening increases the strength and makes material harder. [13]

It is well known that plastic deformation causes reduction in magnetic properties due to the creation of new dislocations and dislocation tangles which impede the domain wall motion [16]. Cold working increases the number of pinning sites, and thus increases the hysteresis loss and coercivity as shown in Fig. 6.8 [3].

Figure 6.8 by Jiles [3] misrepresents the influence of strain hardening on the saturation magnetization M_s. In reality M_s value is not influenced by strain hardening so drastically. The hysteresis curve of hardened steel is wider than the hysteresis curve of magnetically soft iron as shown in Fig. 6.8 but the M_s value of hardened steel should approach the M_s value of soft iron at high magnetic field strength values.

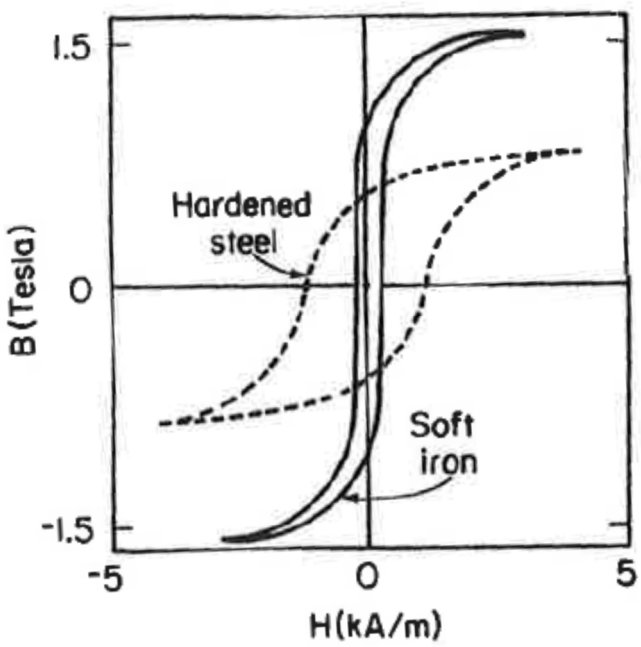

Figure 6.8 *The influence of strain hardening on the hysteresis curve of iron. Hysteresis curves of strain hardened steel is wider than the hysteresis curve of magnetically soft iron. The number of pinning sites is increased by hardening. [3]*

7 STEEL BAR SAMPLES

7.1 Manufacturing process

Steel bars are manufactured by using the continuous casting method. In continuous casting process two manufacturing steps are combined: casting and rolling. The manufacturing process begins by selecting the raw material which is melted in the electric arc furnace. The molten metal is cast into a water-cooled mold. The molten metal freezes against the mold walls. The molten metal is cast directly into a continuous strand by withdrawing the casting from the bottom of the mold. The steel strand is mechanically supported by rolls below the mold. The surface of the strand starts to solidify in the mold and forms finally a steel bar billet, which is rolled in a billet mill. Continuous casting method gives uniform mechanical properties to the blank. [43]

Next the billet is heated and hot rolled in a steel mill. Hot rolling is the process which gives the form to the steel product. Hot rolling takes place in the austenite region where steel is very malleable and the thickness of the billet can be reduced with relative small force. The final stage is the carefully controlled cooling process in which the microstructure of steel transforms from austenite to a mixture of ferrite and cementite. The characteristics of the formed microstructure depend on the cooling rate and carbon content. Hot rolling gives uniform mechanical properties throughout the bar. [44]

7.2 Gas carburizing

Steels are heat treated in order to achieve the hardness and microstructure suited best for the final product. The heat treatment of the steel bar depends on the steel grade and the application. Three different steel grades were studied in this work (see Table 7.1). Steel grade 3 differs from the other steel grades because it is gas carburized. In gas carburizing the carbon content of the surface is increased so that the surface can be hardened. Carburizing and consequent hardening produce a high-carbon martensitic surface layer with good wear and fatigue resistance on the top of a tough, low-carbon steel core. Gas carburizing is also called as case hardening. [45]

Steel bar is annealed (steel is heated and kept in the austenite region) in a carbon-rich environment and held there for some period of time depending on the dimensions of the bar and the desired thickness of the carbon-rich layer. At this temperature also the carbon in the carbides dissolves. Hardening is accomplished when the high-carbon surface layer is quenched. Upon rapid cooling the face-centered cubic austenite transforms to the crystal structure of body-centred cubic martensite. In the martensitic structure the carbon atoms are located in the interstitial sites, creating lattice distortion. The marten-

sitic structure is hard and brittle due to the lattice strains and residual stresses from the quench. [27]

To increase the ductility of the surface the bar is tempered, which means that the bar is heated to a temperature below the A_1 temperature, see Fig. 6.1. This enables the precipitation of small cementite inclusions, which reduces the carbon content of the matrix and consequent lattice distortions. Tempering makes the steel more ductile, but at the same time the strength is decreased. [45]

The steel grades 1 and 2 are heat treated after the manufacturing process. The steel grades are quenched (annealed and rapidly cooled) and tempered which gives to steel tough and ductile structure. The carburizing changes the microstructure of the surface of the sample but quenching and tempering changes the microstructure of the whole sample.

7.3 Chemical compositions

The compositions of the steel grades studied in this work are presented in Table 7.1. When comparing the compositions it can be seen, that the carbon content ranges from 0,22 %C to 0,97 %C. All the grades can be classified as low alloy steels because they contain alloying elements less than 8 %. Grade 1 has the highest carbon content of the three steel grades. Grade 2 has high silicon content (1,5 wt%) and grade 3 has high nickel content (2,9 wt%). The alloy compositions of these steels provide high fatigue strength, toughness and wear resistance. The yield strength values of the steel grades range from 820 to 1000 MPa.

Table 7.1 *Carbon contents of the studied steel grades.*

Steel grade	Grade 1	Grade 2	Grade 3
wt% C	0,97	0,41	0,22

8 HYSTERESIS CURVE MEASUREMENTS

The hysteresis curves are measured in order to characterize the basic magnetic properties of the samples without the influence of an applied mechanical load. The influence of carburizing, prior cold work and composition on the magnetic properties of the samples is studied. The magnetic field strength required to achieve the saturation magnetization state can be obtained from the hysteresis curve. This information is needed in the impact tests in order to reveal the ideal magnetization for the measurements.

8.1 Measurement procedure

The hysteresis curves were measured in the Magnet Technology Center Prizztech in Pori. The samples were measured using an AMH1050-50 hysteresisgraph (Walker Scientific) in order to obtain the materials response to an external magnetic field in a closed magnetic circuit. Hysteresisgraph is a measurements system used for testing and analysing the hysteresis properties of magnetic materials [1]. A search coil was wound around the sample. The number of turns in the search coils was 29 to 31 depending on the sample. The output of the search coil was connected to the fluxmeter in order to determine the magnetic flux density B. The intensity of the magnetization J was calculated according to Equations (2.10) and (2.11).

The sample was placed between two iron-cobalt pole pieces of an electromagnet so that the ends of the sample were in direct contact with the pole pieces. The magnetic field strength H was controlled by a bipolar current source and detected with a gaussmeter using a Hall probe.

8.2 Samples

The samples for the hysteresis curve measurements were cut from the steel bars. The length of the samples was 50 mm. There are two sample groups and their characteristics are described in Table 8.1. The samples from TP 4.1 to TP 6.3 in the sample group 2 are cut from the parent material by wire cutting. The steel grades 1 and 2 are quenched and tempered. The steel grade 3 in the sample group 1 is gas carburized and in the sample group 2 it is not heat treated. The material of the sample TP 3.1 is unknown, but it was cut from the bar which had been exposed to prior cold working (service loading). The samples are numbered so that the first number indicates the bar and the second number is the number of the specimen. For example, TP 3.1 is the sample number one cut from the bar number three.

Table 8.1 *Characteristics of the samples studied in the hysteresis curve measurements. There are two sample groups. The samples in the group 2 are cut by wire cutting method from the parent material.*

Steel grade	Sample	Heat treatment	Comments	
Grade 3	TP 1.1	Gas carburized		**Sample group 1**
	TP 1.2			
	TP 1.3			
	TP 2.1			
	TP 2.2		Sectional area is not planar	
Unknown	TP 3.1	Unknown	Cold worked	
Grade 1	TP 4.1	Quenched and tempered		**Sample group 2**
	TP 4.2			
	TP 4.3			
Grade 3	TP 5.1	Non-heat treated		
	TP 5.2			
	TP 5.3			
Grade 2	TP 6.1	Quenched and tempered		
	TP 6.2			
	TP 6.3			

8.3 Results and discussion

8.3.1 The basic magnetic properties

Figure 8.1 shows typical hysteresis curve drawn from the measurement data of the samples. Both the intensity of magnetization J and the magnetic flux density B are presented as a function of the magnetic field strength H. Only one curve of the samples is presented here because the curves are very similar and the differences between the hysteresis of different samples are difficult to notice. More detailed hysteresis curves can be obtained when the H scale is expanded to reveal more information at low field strength values (see Fig 8.2).

It can be seen in Fig. 8.1 that after the magnetization has reached its technical saturation the magnetization continues to slowly increase with increasing magnetic field strength. The saturation values of the intensity of magnetization J_s were obtained from the hysteresis curve and converted to M_s values. The sample TP 1.1 reaches its technical saturation value approximately at magnetic the field strength value of 33 kA/m.

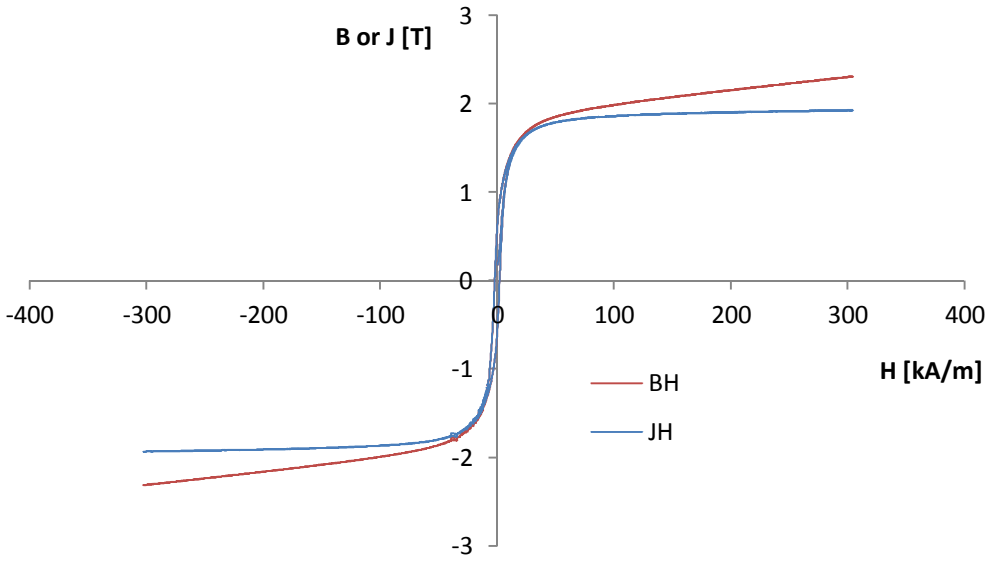

Figure 8.1 *The BH curve (or JH curve) of the sample TP 1.1. J is the intensity of magnetization (see Equation 2.10).*

The basic magnetic properties of the steel samples were obtained from the measurement data. The coercivity H_c and remanence B_r values were measured by linear interpolation from the measurement data. For coercivity the interpolation was made between the points where the magnetic flux density B changes its sign and respectively for remanence between the points where magnetic field changes its sign. Coercivity and remanence were defined both from the negative side and positive side of the hysteresis curve. The average value of these two measured values was calculated in order to get more accurate result. The maximum relative permeability μ_r was calculated from the measurement data. The results in Table 8.2 show the variation of the magnetic parameters from sample to sample.

The saturation value of magnetization M_s is not significantly influenced by the mechanical or the thermal treatment of the material. The results in Table 8.2 show that the saturation value does not vary much between the samples and different materials. The coercivity and remanence are influenced by the manufacturing process and the chemical composition of the material. Permeability is the most structure sensitive property. Differences in relative permeability, coercivity and remanence between the materials can be found.

The results of the sample TP 2.2 can be ignored because the sectional area of the surface is not planar and perpendicular to the sample axis and the ends of the sample were not in direct contact with the pole pieces of the electromagnet. The sample TP 2.2. was defective because the cutting of the sample from the parent material was inadequate. The planarity and perpendicularity of the sectional area of the sample are essential in order to achieve accurate results.

In Table 8.2 it can be seen that there is more variation in the results of the same steel grade in the sample group 1 than in the sample group 2. This may be explained in terms of the cutting method. Wire cutting produces better planarity for the sectional area of the sample than the conventional sawing. In the sample group 2, three samples were cut from each material to ensure the repeatability of the results. The hysteresis curves of the samples are presented in Fig. 1 of Appendix 1. Variations in the shape of the hysteresis curves cannot be revealed within the same steel grade. Very small scatter of the coercivity and remanence values was obtained within the same material in the sample group 2.

Table 8.2 *The basic magnetic properties of the samples.*

Steel grade	**Sample**	**B_r [T]**	**H_c [kA/m]**	**M_s [kA/m]**	**μ_r**
Grade 3	TP 1.1	0,60	2,02	1536	258870
	TP 1.2	0,50	1,98	1536	204773
	TP 1.3	0,44	2,10	1528	171201
	TP 2.1	0,61	2,18	1536	233413
	TP 2.2	0,48	2,18	1552	181941
Unknown	TP 3.1	0,43	1,89	1512	187987
Grade 1	TP 4.1	0,75	1,61	1528	397930
	TP 4.2	0,81	1,71	1520	389331
	TP 4.3	0,82	1,62	1520	397293
Grade 3	TP 5.1	0,78	1,35	1592	439809
	TP 5.2	0,88	1,42	1592	531449
	TP 5.3	0,88	1,32	1592	546656
Grade 2	TP 6.1	0,99	1,25	1568	731290
	TP 6.2	0,89	1,15	1560	551707
	TP 6.3	1,00	1,22	1560	655255

In Figure 8.2 the hysteresis curves of the samples in the steel grade 3 are plotted in the same graph in order to compare the curves and the variation of the results within the same material. Samples were cut from two different bars of the same material. The hysteresis curve of the sample TP 1.3 differs from the other hysteresis curves; the position of the curve is tilted. There is some variation in the remanence B_r and relative permeability μ_r values of the samples but the coercivity H_c values vary only little within the sample range.

It can be seen in Fig 8.2 that the initial hysteresis curve does not begin from the origin where both the magnetic field strength H and the magnetic flux density are zero. This is due to the retained magnetization of the magnetic poles of the electromagnet. In the beginning of the measurement the integrator is drifted to zero, in which case the magnetic flux density B values start erroneously from zero. This aberration is taken off from each measurement point.

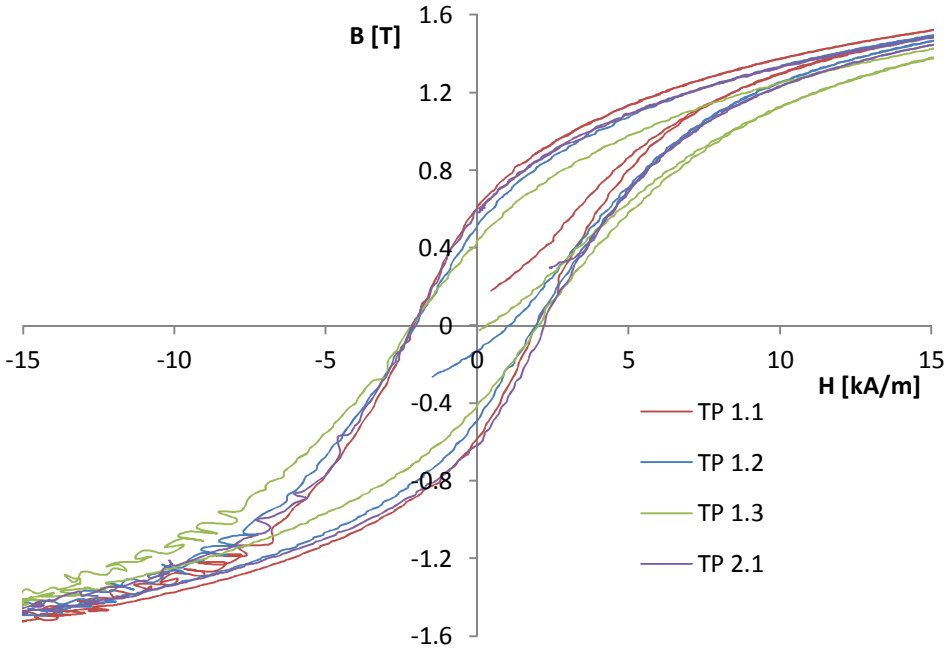

Figure 8.2 *The differences between the hysteresis curves between the samples of the steel grade 3.*

In the negative side of the hysteresis curves in Fig 8.2 the changes in the magnetization as a function of magnetic field strength are not smooth, but the curve is fluctuating. This arises from the measurement technique, not from the magnetic properties of the samples. The power source, by which the magnetizing coil is magnetized, does not exactly follow the controlling voltage at specific points in the hysteresis curve. This manifests as disturbances in the output signal.

Table 8.3 *The average values of the basic magnetic properties of the samples from TP 1 to TP 6.*

Steel grade	**Average over the samples**	**B_r [T]**	**H_c [kA/m]**	**M_s [kA/m]**	**μ_r**	**Heat treatment**
Grade 3	TP 1.1-TP 1.3	0,51	2,04	1533	211615	Gas carburized
	TP 2.2	0,61	2,18	1552	233143	
Unknown	TP 3.1	0,43	1,89	1512	187987	Unknown
Grade 1	TP 4.1-TP 4.3	0,79	1,65	1523	408811	Quenched and tempered
Grade 3	TP 5.1-TP 5.3	0,85	1,36	1592	505971	Non-heat treated
Grade 2	TP 6.1-TP 6.3	0,96	1,21	1562	646417	Quenched and tempered

The average values of the basic magnetic properties of the samples cut from the same bar were calculated. Results are presented in Table 8.3 and the differences between the steel grades can be compared. The differences in the basic magnetic properties between the steel grades are discussed in chapters 8.3.2, 8.3.3, and 8.3.4.

8.3.2 The influence of carburizing on magnetic properties

The influence of carburizing on magnetic properties of the material was studied on steel grade 3. Figure 8.3 shows the hysteresis curves of the carburized and the non-heat treated material. The material, which has not been heat treated, is in the as-hot rolled condition. When comparing the curves of carburized and non-carburized samples it can be seen that the carburizing has enlarged the hysteresis curve of the material. Wider hysteresis means that the carburized sample is more difficult to magnetize than the sample in the hot rolled condition. This result was expected, because the previous studies [28, 30, 31] have shown that the magnetic properties of steels depend on the carbon content, mechanical properties and microstructure of the material.

Enlarged hysteresis means also larger coercivity and reduced permeability. Carburizing produces hard martensitic structure to the material. The internal strains in the martensitic structure of the carburized sample impede the domain wall motion in the magnetization process, consequently increasing coercivity. The microstructure of the sample in the as-hot rolled condition consists of magnetically soft ferrite and small amount of pearlite. Domain walls can move more freely and the magnetization is easier in this sample.

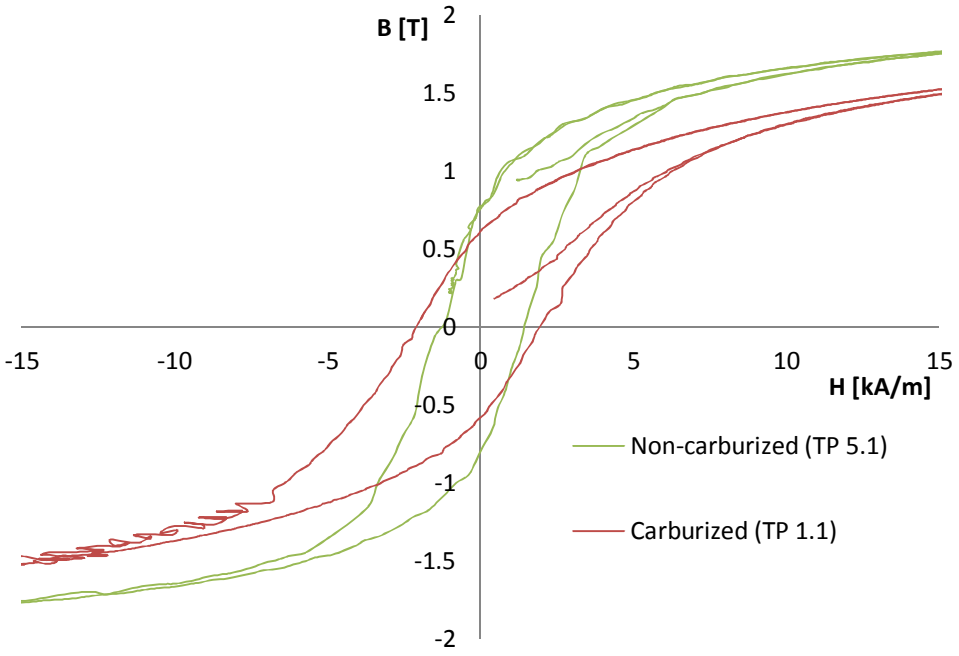

Figure 8.3 *The influence of carburizing on the hysteresis curve of steel grade 3. The samples TP 5.1 and TP 1.1 are from the same material, but different bars.*

8.3.3 The influence of strain hardening on magnetic properties

The composition of the sample TP 3.1 was unknown, but the sample had been exposed to prior service loading. The composition was analyzed with optical emission spectrometry. The assumption is that the sample TP 3.1 is one of the three steel grades. According to the elementary analysis the carbon content of the sample TP 3.1 is 0,84 %C, which is closest to the carbon content of the steel grade 1, 0,97 %C. The contents of the other alloying elements in the sample TP 3.1 are very close to the content of alloying elements in steel grade 1. The differences in carbon contents between these two samples might result from the production tolerances of the bars.

The influence of prior service loading on the magnetic properties was studied on sample TP 3.1. The hysteresis curves of the grade 1 (sample TP 4.3) and the sample TP 3.1 are presented in Fig. 8.4. The service loading has strain hardened the material and consequently changed the magnetic properties.

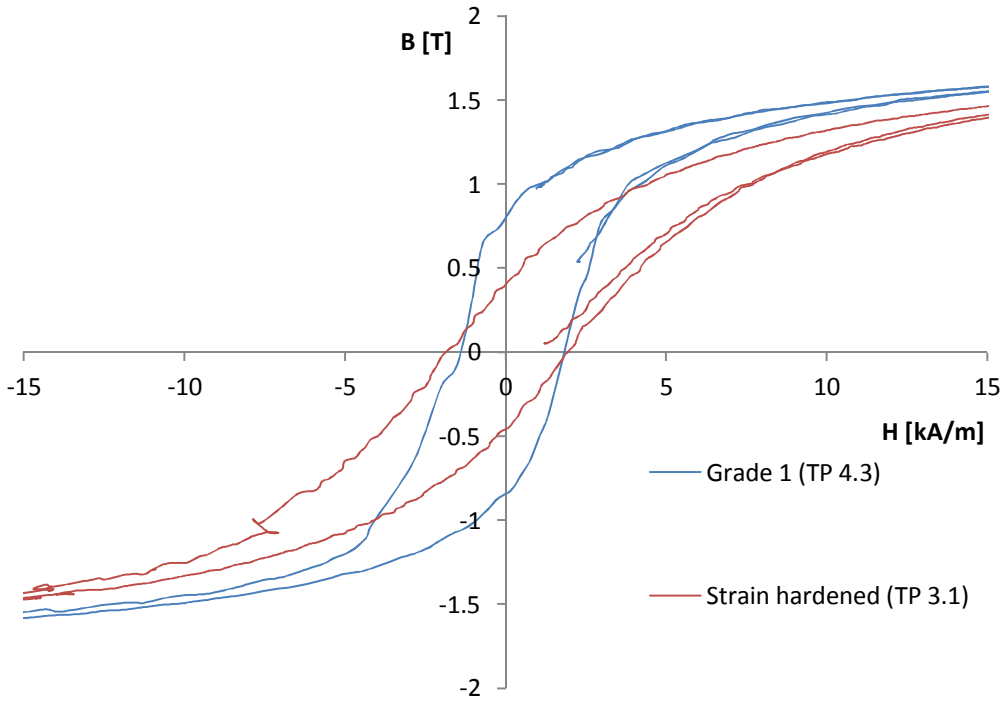

Figure 8.4 *The influence of strain hardening on the hysteresis curve. The figure shows hysteresis curves of the steel grade 1 and of the sample TP 3.1, which has been exposed to prior service loading.*

The influence of strain hardening on hysteresis curve cannot be seen directly by comparing the samples because the carbon content of the samples is not the same. The permeability of the strain hardened material is smaller than that of the grade 1, as expected, because strain hardening makes the magnetization harder due to the formation of dislocations. However, the carbon content of the strain hardened sample is smaller than that of the grade 1, which should result in larger permeability. The influences of carbon content and strain hardening on the magnetic properties of the material are over-

lapping, which makes the interpretation of the results difficult. In this case, the dislocations in the strain hardened material have hindered the motion of the domain walls more than the larger number of pinning sites due to the higher carbon content in the non-strain hardened material. It can be suggested, that in this case dislocations have greater influence on the magnetic properties than carbon content.

8.3.4 The influence of carbon content on magnetic properties

The influence of the carbon content of steel on magnetic properties was studied. The hysteresis curves of three different steel grades are plotted in the same graph in Fig. 8.6. The samples have a carbon content ranging from 0,97 wt% C (grade 1) down to 0,22 wt% (grade 3). From this figure it becomes clear that differences exist between the materials. The coercivity, remanence and relative permeability values of the steel grades are correlated with carbon content in Fig 8.7, Fig 8.8 and Fig 8.9. The sample of steel grade 1 with highest carbon content has higher coercivity as compared with the other two materials. This result is in agreement with the earlier studies by Rumiche et al. [17] and Ranjan et al. [38] which imply that increasing carbon content increases the amount of cementite which acts as pinning sites to the domain wall motion.

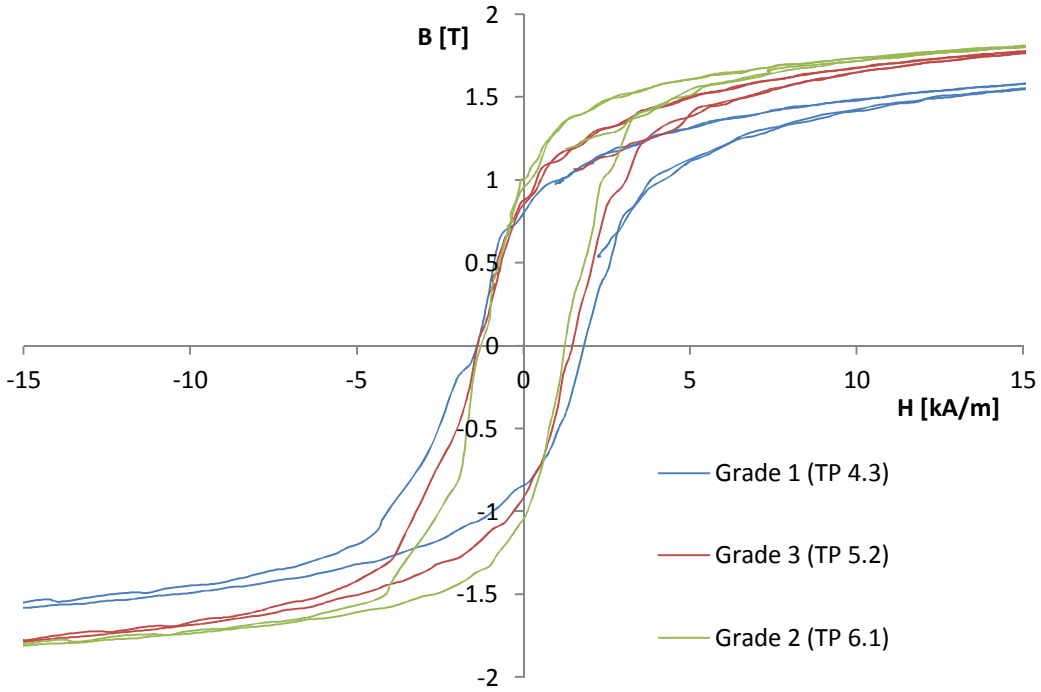

Figure 8.6 *The influence of carbon content of steel on the hysteresis curve. The carbon content of the steel grades ranges from 0,97 wt% (grade 1) down to 0,22 wt% (grade 3).*

The samples with carbon content of 0,22 wt% C and 0,44 wt% C do not follow this hypothetical trend. The sample with carbon content of 0,44 wt% C has smaller coercivity than the sample with carbon content of 0,22 wt% C. It can be suggested that the high silicon content in the sample with the carbon content of 0,44 wt% C lowers the coercivity of the material. Consequently in this case the silicon has a stronger influence on the magnetic properties than carbon. Because there is no simple relationship between the composition and the magnetic properties of steel, the interpretation how a specific alloying element is influencing the magnetic properties is difficult.

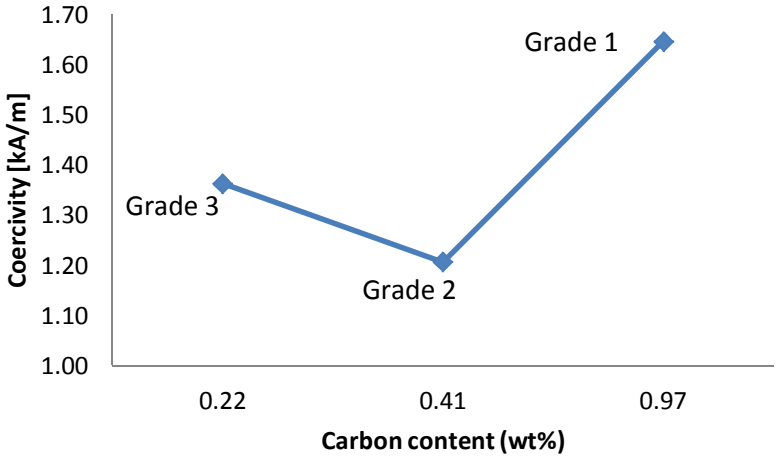

Figure 8.7 *Coercivity as a function of carbon content for the three studied steel grades.*

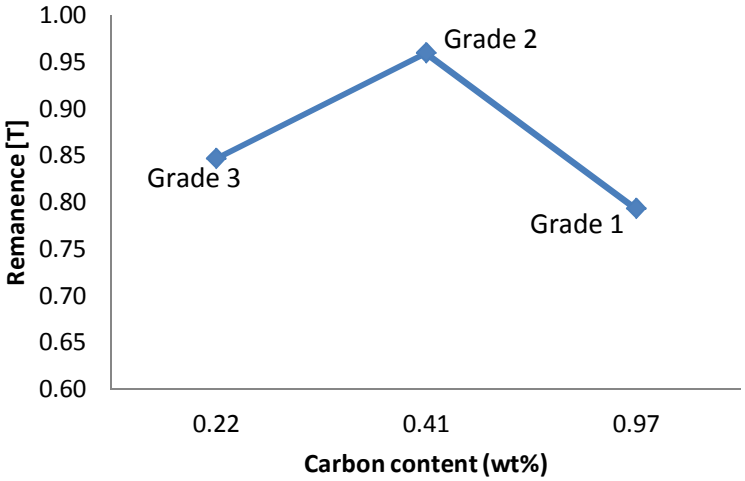

Figure 8.8 *Remanence as a function of carbon content for the three studied steel grades.*

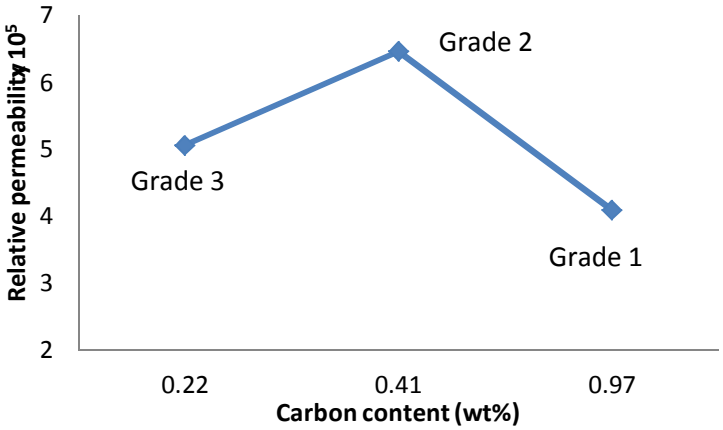

Figure 8.9 *Relative permeability as a function of carbon content for the three studied steel grades.*

8.4 Conclusions

The hysteresis curves of the studied steels were measured and analysed. Slight differences occur in the magnetic properties in different samples of the same material. It was observed that the magnetic properties and the shape of the hysteresis curve of the carburized sample and the non-carburized sample in the as-hot rolled condition differ from each other. Carburizing has changed the microstructure of the sample and consequently has also altered the magnetic properties. Carburizing makes the hysteresis curve wider and thereby makes the magnetization harder.

The influence of strain hardening on magnetic properties was also studied. Due to the differences between the compositions of the samples the hysteresis curves cannot be directly compared. In general, cold working strain hardens the steel. Consequently it provides obstacles to the domain wall motion and increases hysteresis losses. In order to compare the materials successfully, the influence of one variable on the magnetic properties should be studied at a time. The influences of different parameters are overlapping, which makes the interpretation of the results difficult.

According to the earlier studies the carbon content is the most important compositional factor influencing the magnetic properties of steel. This was not the case in the results presented in this work and no simple relationship emerged between the steel composition and magnetic properties such as coercivity, remanence and permeability.

9 IMPACT LOAD MEASUREMENTS

9.1 Background of the measurements

Structural steel components in mechanical engineering applications are exposed to mechanical loadings which create stress waves to the components. In general, the efficiency and the safe usage of the components depend on the stress waves. Stress evaluation is essential in order to enable reveal the remaining lifetime of the component.

There are various types of stress wave measurement methods, which are based on the mechanical deformation of the material. A common method used for stress measurement is based on the resistance change. Measurements are performed by using strain gauges (gages). Strain gauges are sensing elements to measure the mechanical loading inducing surface strain in the material. The operating principle of the strain gauges is based on the change in the electrical resistance. Strain gauge is bonded to the surface of the sample to make it to elongate or contract together with to the sample. When a load is applied to the sample, the strain gauge changes its shape and undergoes a change in the resistance. [48]

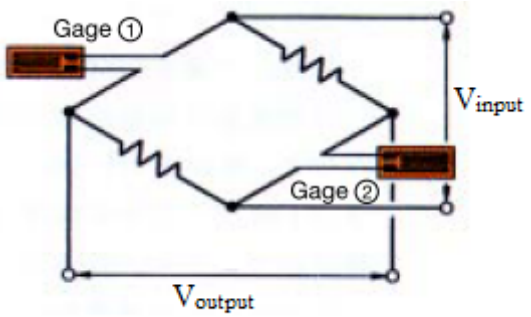

Figure 9.1 *Wheatstone bridge circuit in a 2-gauge system. Strain gauges 1 and 2 are connected to the opposite sides of the bridge. This type of bridge configuration cancels the bending strain and only compressive and tensile stresses are obtained. [46]*

The strain gauge measurement system consists of the bridge circuit and an amplifier. The input voltage V_{input} is fed to the strain gauge through a measuring bridge shown in Fig. 9.1. Wheatstone bridge is an electric circuit used in the strain gauge measurements because it can detect small changes in the resistance. [46]

The output voltage V_{output} is proportional to the resistance change of the strain gauge which can be further converted to the strain of the specimen. The output voltage is am-

plified. The rate of the resistance change is proportional to the strain according to Equation (9.1):

$$\frac{\Delta R}{R} = K\varepsilon \tag{9.1}$$

where ΔR is the strain induced resistance change, R is the original resistance of the strain gauge, K is the gauge factor and ε is strain. The 2-gauge system provides the following output voltage [46]:

$$V_{output} = \frac{1}{4}\left(\frac{\Delta R_1}{R_1} + \frac{\Delta R_2}{R_2}\right)E \tag{9.2}$$

or $$V_{output} = \frac{1}{4}K(\varepsilon_1 + \varepsilon_2)E. \tag{9.3}$$

where E is the Elastic modulus (Equation 2.3) Since strain gauge measurement system consists of wiring, voltage source and an amplifier, it is best usable in the static applications. However, there are applications in which the requirements for a successful strain gauge measurement cannot be reached. For example, rotating components are difficult in terms of wiring.

Another method for measuring stresses, which is used in the impact load measurements in this work, is based on the electromagnetic induction and magnetomechanical effect. When passing through the search coil located around a magnetostrictive material, stress wave changes the magnetic flux and induces a voltage signal V according to the Faraday's law of electromagnetic induction. This signal describes the changes in the magnetic flux density B under varying stress σ according to Equation (9.4) [47]:

$$V = NA\frac{dB}{dt} = NA\frac{d\sigma}{dt}\left(d_{33} - \frac{\mu^{\sigma}}{d_{33}E^{H}}\right) + NA\frac{d\varepsilon}{dt}\frac{\mu^{\sigma}}{d_{33}} \tag{9.4}$$

where A is the cross-sectional area of the bar, N is the number of turns in the search coil, d_{33} is the linear coupling coefficient at a constant stress, μ^{σ} is the permeability at constant applied stress and E^{H} is the elastic modulus at constant magnetic field strength. The magnetic flux density B is the time integral of the induced voltage in the search coil:

$$B = -\frac{1}{NA}\int V dt \tag{9.5}$$

where A is the cross-sectional area of the studied bar and N is the number of turns in the search coil. [3]

When the magnetic flux changes rapidly in the bar-shaped specimen, it induces an electromotive force (emf) which causes eddy currents. Eddy currents in the bar are called macro eddy currents which influence the magnetic measurements by decreasing

the change in the magnetic flux. Magnetization occurs by domain wall motion or rotation of the magnetization vectors. Micro eddy currents form around the moving wall causing domain wall damping. [1] Macro and micro eddy currents have to be taken into account when interpreting the results of magnetic measurements.

Unlike the hysteresis curve measurement, impact load measurements are carried out in an open magnetic circuit. In the open magnetic circuit measurements the magnetic path of the magnetic flux lines is not closed, which causes a demagnetizing field H_d. When a bar-shaped sample is magnetized, a demagnetizing field H_d is generated inside the material. The demagnetizing field is of opposite sign with the applied field and consequently decreases it. When the applied field is removed, the demagnetizing field remains. Demagnetizing field depends mainly on the shape of the specimen. The shorter the bar is the stronger is the influence of the demagnetizing field. The demagnetizing field is not uniform inside the bar: H_d is stronger at the ends and weaker in the middle of the bar. Hence, the magnetic flux density is reduced at the ends of the bar due to the demagnetizing field. Demagnetizing field influences the magnetic measurement results and has to be taken into account. [1]

Figure 9.2 shows the basic properties of the electrical signal. The root mean square (RMS) values are used when dealing with alternating currents and voltages. The value of an alternating voltage is continually changing from zero up to the positive peak, through zero to the negative peak and back to zero again. V_{rms} is the effective value of the voltage an can be defined according to Equation (9.6)

$$V_{rms} = \frac{V_p}{\sqrt{2}} \tag{9.6}$$

Most of the time, the value of the signal is smaller than the peak voltage V_p. Peak to peak voltage $V_{p\text{-}p}$ is useful when the wave form is not symmetrical.

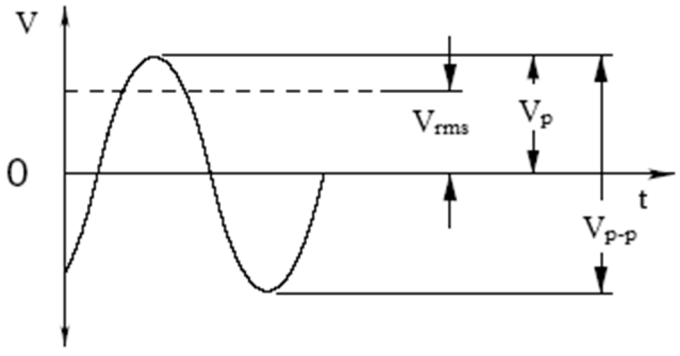

Figure 9.2 *The basic properties of the electrical signal. V_{rms}, V_p and $V_{p\text{-}p}$ are used in characterizing the output signal of the measurement device.*

9.2 Measurement set-up

The impact test device was designed and built in order to create a stress generated by an impact piston. In the impact test the piston produces a stress wave of around 8 MPa. Figure 9.3 shows a photograph of the measurement device and Fig 9.4 shows the schematic view of the measurement set-up. Steel bar samples were magnetized with magnetic field generated by an electromagnet. The magnetic field was parallel to the sample axis. The magnetizing coil consisted of 4700 turns copper wire in 100 mm length. Its outer diameter was 147,3 mm and inner diameter 39,5 mm. Demagnetization of the sample was carried out with an AC source with voltage alternating from 0 V to 230 V.

Figure 9.3 *A photograph of the measurement device set-up with the solenoid controlled impact piston.*

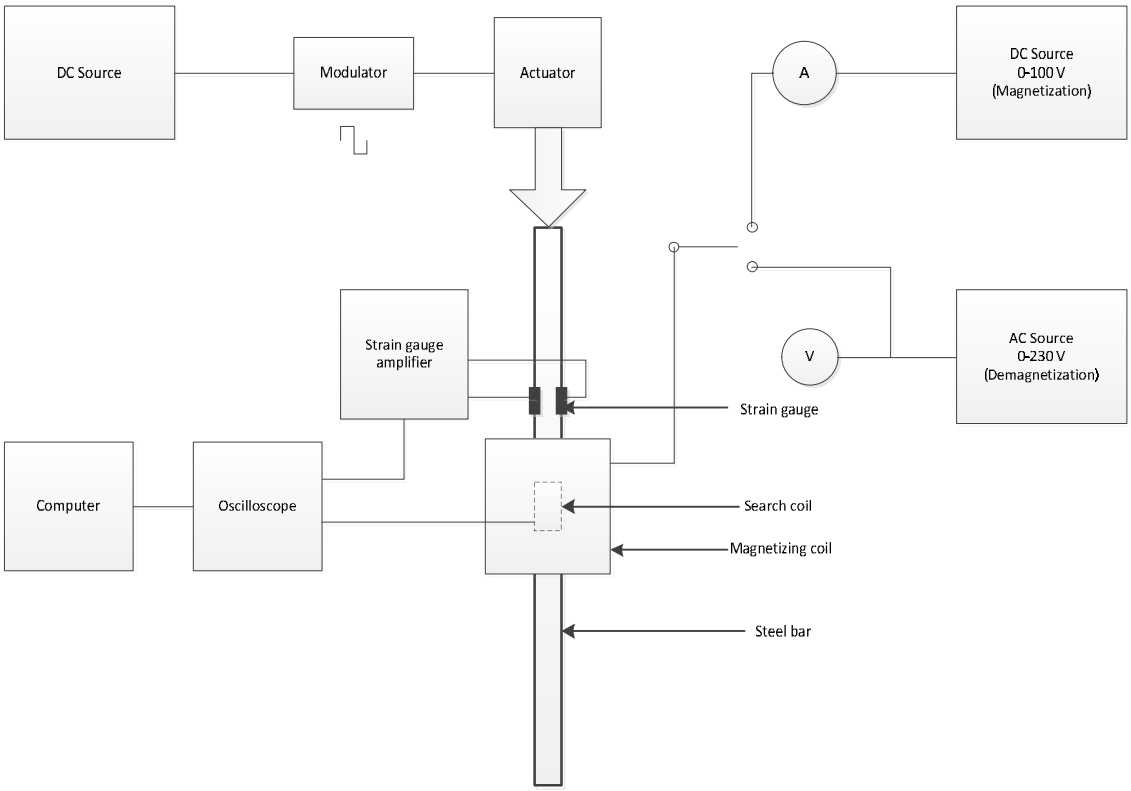

Figure 9.4 *Block diagram of the measurement set-up with the solenoid controlled impact piston (actuator).*

The detection of the stress-induced changes in the voltage was carried out with a search coil. Figure 9.5 shows the photograph of the search coil. The search coil of 200 turns was wound on top of the plastic body which was placed between the sample and the magnetizing coil to ensure that the search coil is in the same position when changing samples. The search coil was directly connected to the computer controlled USB oscilloscope (Handyscope). The computer was used for data collection.

Figure 9.5 *A photograph of the search coil of 200 turns. The search coil was wound on top of a plastic body. The blue wire is the wire of the thermoelement. In the first measurements a search coil of 50 mm in length was used. Later the measurements were carried out with a 20 mm search coil which is presented in this figure.*

In the final state the measurement device included also strain gauges for direct strain measurement. 120 ohm strain gauges were adhesively bonded to the surface of the bar samples. One gauge was bonded to the same position at both sides of the bar as shown in Fig. 9.6. Both gauges were at the same distance (53,5 cm) from the lower end of the bar. Two strain gauges were used in order to compensate the bending stress in the sample.

Two types of signals were obtained from the loading impact: the search coil signal and the strain gauge signal. Strain gauge signal was used as reference. The output of the strain gauges was connected to the same oscilloscope as the search coil signal.

The impact was applied in the axial direction. The piston had a cylindrical form with the diameter of 75 mm and height of 50 mm. The piston hits the bar sample at the upper end. The lower end is fixed to the concrete base. In order to get the reflected tensile stress wave a rubber mat was placed between the bar and the concrete base. The impact piston was controlled by a solenoid by which the impact could be generated with a specific frequency. DC power source fed current to the modulator which generated a rectangular wave form which was fed further to the actuator.

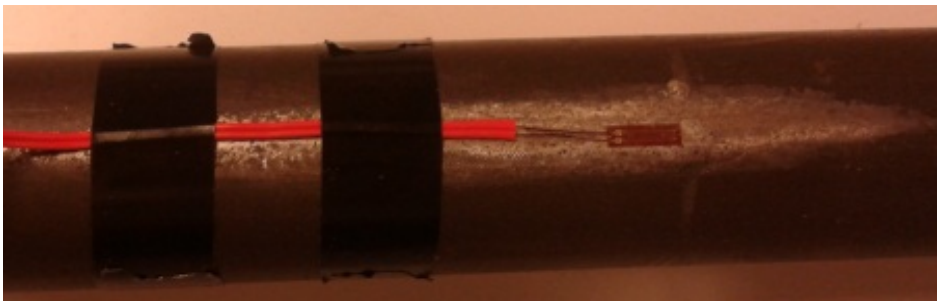

Figure 9.6 *Strain gauge bonded adhesively on the surface of the bar sample. The distance of the strain gauge from the lower end of the bar is 53,5 cm.*

9.3 Samples

The physical parameters of the bar samples are described in Table 9.1. The samples T1-T9 are of steel grade 3, but the manufacturing date varies. The samples T1-T4 and the samples T5-T9 are manufactured on a different day.

Table 9.1 *Steel bar samples. Samples T1-T9 are of steel grade 3. The cross-sectional shape of the samples T1-T9 is round and they are in the as-received condition, which means that the samples have not been subjected to external loads.*

Steel grade	Sample	Length [mm]	Diameter [mm]
Grade 3	T1	907	32,3
	T2	909	32,1
	T3	907	32,0
	T4	915	32,1
	T5	915	32,0
	T6	915	32,2
	T7	915	32,0
	T8	915	32,1
	T9	915	32,0

9.4 Objective of the measurements

The objective of the measurements under mechanical stresses is to study the magnetoelastic behavior of the steel bars and to reveal the eventual scatter of the results between the samples. One of the goals of this work is also to identify the parameters which influence the magnetic properties and have to be taken into account when interpreting the results. Measurements of the magnetoelastic properties are carried out on nine samples of steel grade 3 under impact loading.

The first measurements are carried out in order to adjust and optimize the measurement parameters as well as in order to study the magnetoelastic behavior of the sample T1. A search coil of 200 turns in 50 mm length is used. The sample T1 is magnetized to different points at the hysteresis curve and the influence of the impact on the magnetic behavior is studied. At the final state, after the optimal measurement parameters are found, the samples T1-T9 are tested and the results are compared.

10 RESULTS OF THE IMPACT LOAD MEASUREMENTS AND DISCUSSION

10.1 Measurements for characterizing the magnetoelastic behavior

Typical measurement result obtained from the impact tests is shown in Fig. 10.1 where the induced voltage is plotted as a function of time. The impact creates compressive stress wave and reflective stress tensile wave to the bar. In this work the compressive stress wave is negative and tensile stress wave is positive.

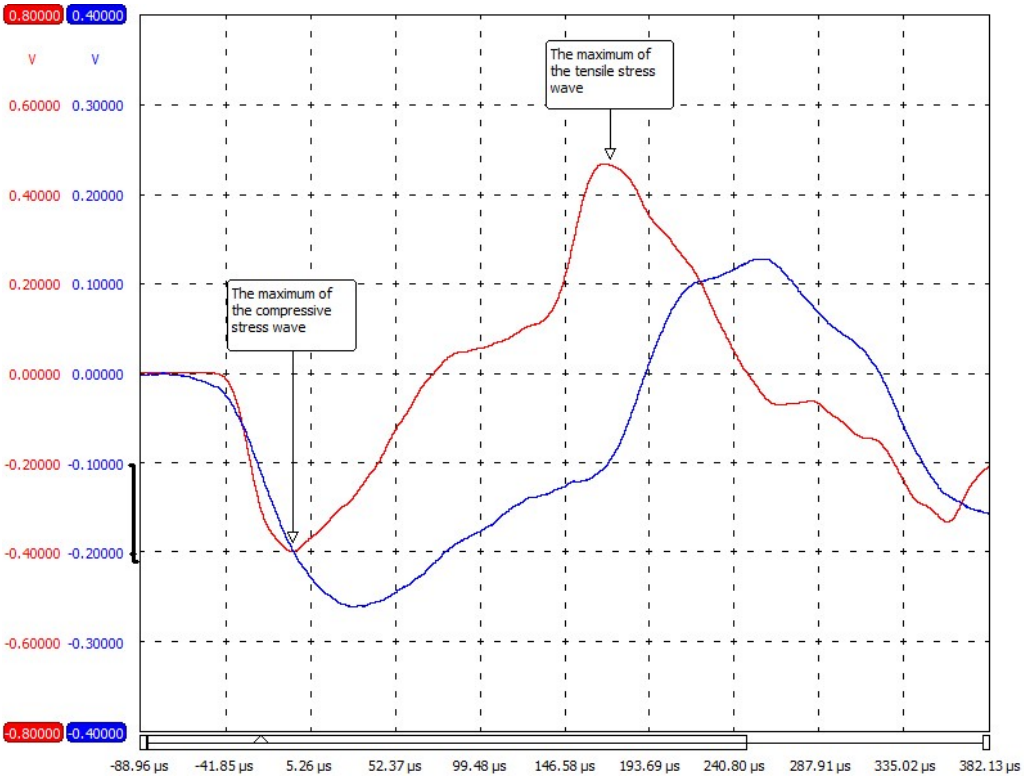

Figure 10.1 *Typical measurement result obtained from the impact tests when the magnetic field strength is 8 kA/m and impact generates a maximum stress of 8 MPa. One stress wave period is shown. Red curve indicates the search coil signal and blue curve indicates the strain gauge signal.*

The samples and measurements results were compared by comparing the standard deviation values of the results. The standard deviation s describes how widely values are dispersed from the average value according to Equation (10.1).

$$s = \sqrt{\frac{\sum(x-\bar{x})^2}{(n-1)}} \tag{10.1}$$

where x is the sample mean average and n is the sample size.

10.1.1 The impact induced voltage V_{rms} as a function of H

The sample T1 was measured in the initial state. The sample was not demagnetized. The objective of this experiment was to find out the magnetizing current by which the rms values of the voltage induced in the search coil reach the maximum as a function of applied magnetic field strength H. The magnetizing voltage was increased with 5 V intervals to the saturation magnetization at 100 V and it was then reduced back to zero with 5 V intervals. At each interval an impact was applied. The polarity of the magnetizing coil was changed and the measurements were repeated in order to get the minimum value of the rms value of the voltage induced in the search coil. The current fed to the magnetizing coil produces magnetic field strength H according to Equation (2.4).

The induced voltage V_{rms} values generated due to the impact loading are presented as a function of magnetic field strength H in Fig. 10.2 and in Fig. 10.3. It can be seen that when the magnetic field strength is zero the induced voltage V_{rms} is not zero. This is because the sample was not demagnetized and small amount of initial residual magnetism can be found.

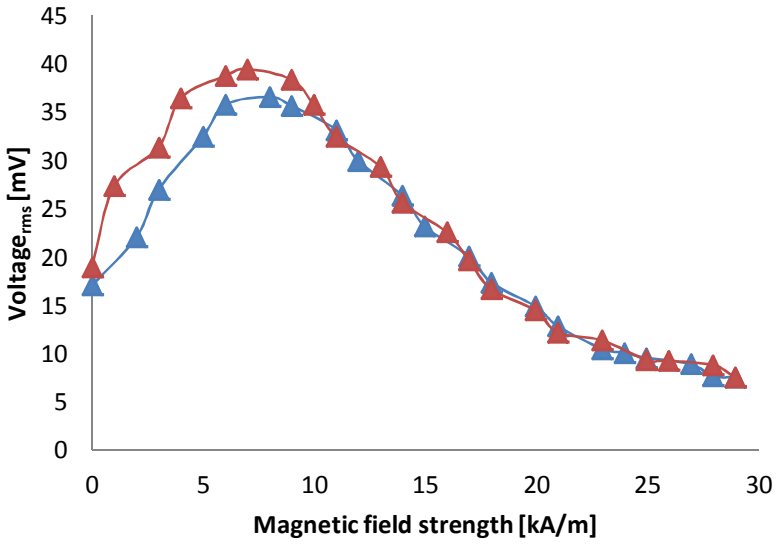

Figure 10.2 *The rms value of the induced voltage V during impact loading of the steel sample T1 as a function of positive magnetic field strength H. The critical magnetic field strength H_m 8 kA/m corresponds to the magnetizing current value 0,8 A. Blue curve: H was increased from 0 kA/m to 29,5 kA/m. Red curve: H was decreased from 29,5 kA/m to 0 kA/m.*

As the magnetic field strength H increases, the induced voltage V_{rms} increases until it reaches the maximum value at the critical magnetic field strength H_m. V_{rms} values start to decrease when the magnetic field strength exceeds the critical value H_m. Similar behavior has been reported for polycrystalline iron by Ruuskanen [20]. In the work of Ruuskanen the critical magnetic field strength H_m shows stress amplitude dependence; H_m increases as the stress amplitude increases.

The anhysteretic curve of the sample was not measured in this work but according to Ruuskanen [20] and Fig. 5.7 by Jiles [26] the maximum difference between the anhysteretic and hysteresis curves occurs at lower field strength than the observed critical magnetic field strength H_m.

In Fig. 10.2 two curves are presented. The lower curve (blue curve) indicates the changes in the induced voltage when the magnetic field strength was increased from the initial state to the positive magnetic saturation. The upper curve (red curve) indicates the changes in the induced voltage when the magnetic field strength was decreased from the positive magnetic saturation point to zero.

According to Jiles [26] the change in the magnetization is always towards to the anhysteretic state when stress is applied. The magnitude of the change in the magnetization due to applied stress depends on the distance between the working point and the anhysteretic curve.

In the high magnetic field region the material is in the magnetic saturation state and the anhysteretic and initial curves are close to each other. Therefore the stress-induced changes in the magnetization are small. Close to the saturation state at high magnetic field the upper curve follows the lower one and the change in the magnetization due to the applied impact is non-hysteretic. At high fields the material contains only one domain in which the saturation magnetization vector is aligned in the direction of easy magnetization. When the field is increased the magnetization vector rotates to the direction of applied field. This process is reversible.

In Fig. 10.2 the maximum of the V_{rms} value of the upper curve is higher than the maximum value of the lower curve. This can be explained in terms of the hysteresis behavior of steels. When increasing the magnetic field strength the changes in the magnetization lag behind.

The changes in the magnetization due to the applied stress depend on the domain structure and distribution in the material. It is known that the 90° walls are stress sensitive and the stress-induced change in the magnetization is due to the motion of the 90° walls. [1] Thus it can be suggested that at the critical magnetic field strength H_m the density of the 90° walls is at highest and the magnetic response of the material to the mechanical stress is at its maximum.

In Fig. 10.3 the induced voltage V_{rms} is plotted as a function of negative magnetic field strength H. When comparing the upper (red) and lower (blue) curve, it appears that the maximum of the induced voltage V_{rms} of the lower curve occurs at higher critical magnetic field strength H_m than for the upper curve. This again can be explained in terms of the hysteresis.

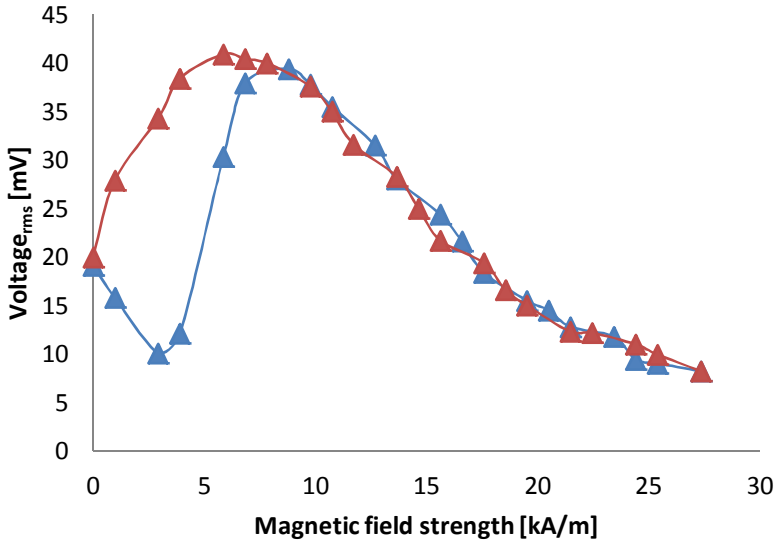

Figure 10.3 *The rms value of the induced voltage V during impact loading of the steel sample T1 as a function of negative magnetic field strength H. Blue curve: H was decreased from 0 kA/m to -29,5 kA/m. Red curve: H was increased from -29,5 kA/m to 0 kA/m.*

Figure 10.3 shows that the behavior of the curves at low magnetic field strength values is different. When the magnetic field is decreased towards to the negative saturation, the change in the induced voltage V_{rms} decreases in the beginning. The remanence in the material has to be overcome which occurs as a kink in the lower curve.

10.1.2 The influence of the impact on the remanence

The sample was magnetized to saturation state (100 V and 2,8 A) where magnetic field strength was 29,5 kA/m and the magnetizing current was then reduced to zero. Impact was applied five times and after each impact V_{rms} and $V_{p\text{-}p}$ values were measured. The experiment was repeated three times.

Figure 10.4 a) shows the magnetomechanical effect when the working point lies at the positive remanence. The induced voltage $V_{p\text{-}p}$ is plotted as a function of the impact number. The sample was initially magnetized to the positive saturation and the applied magnetic field strength was then decreased to zero. It can be seen that the second impact decreases the induced voltage $V_{p\text{-}p}$ but the next impacts do not drastically alter the induced voltage.

In Figure 10.4 a) the working point lies at the positive remanence $+B_r$ which is above the anhysteretic curve as illustrated in Fig. 10.5. The application of the impact causes the stress sensitive 90º domain walls to break away from the pinning sites and move towards the anhysteretic state. The results are in accordance with the theory by Jiles [26].

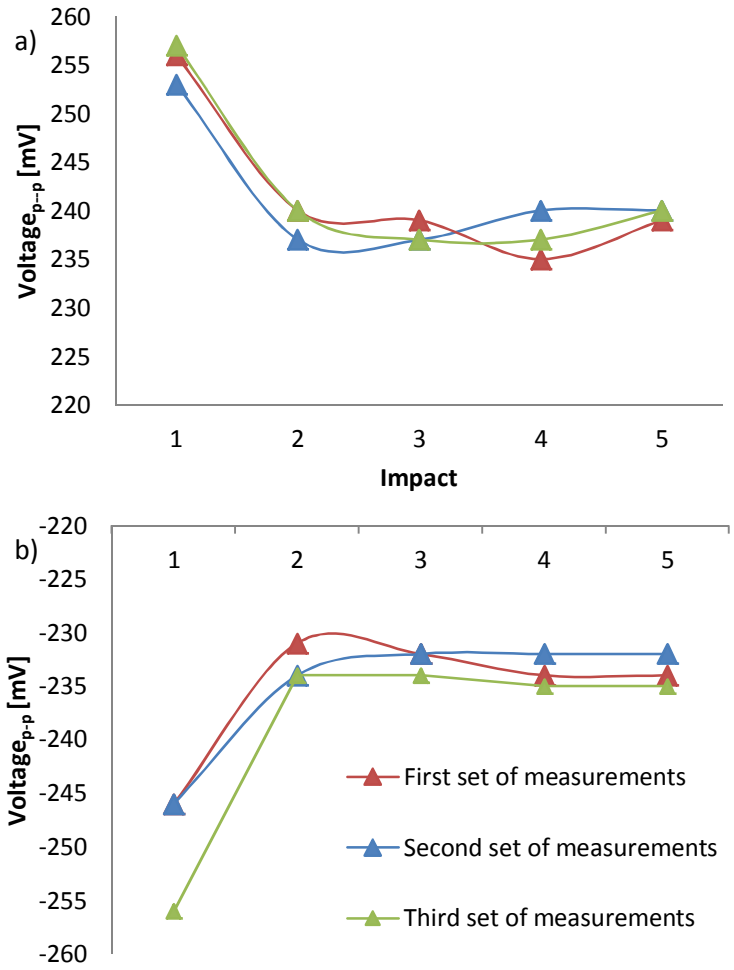

Figure 10.4 *The influence of repeated impacts on the induced voltage V_{p-p}. The working point lies a) above the anhysteretic curve at the positive remanence b) below the anhysteretic curve at the negative remanence.*

A decrease in the remanence was expected but the observed magnetomechanical effect is quite small. The change in the signal level between the first impact and the second one is roughly 20 mV. The small influence suggests that the impact is not strong enough to move the domain walls to the equilibrium position.

The magnetomechanical effect in the sample was studied also when the working point lies at the negative remanence, in other words below the anhysteretic curve. This curve is presented in Fig. 10.4 b). The change in the induced voltage is towards the anhysteretic as expected and the second impact decreases the induced voltage the most as in the previous case.

The length of the sample influences the results. The total length of the specimen bar T1 is 907 mm and the magnetizing coil covers only 100 mm of the length of the bar. When touching the bar end with a ferromagnetic tool, magnetic attraction between the tool and the bar was observed. Even if the magnetic field was removed, the ends of the bar remained magnetized. Consequently, the sample never reached the remanence point.

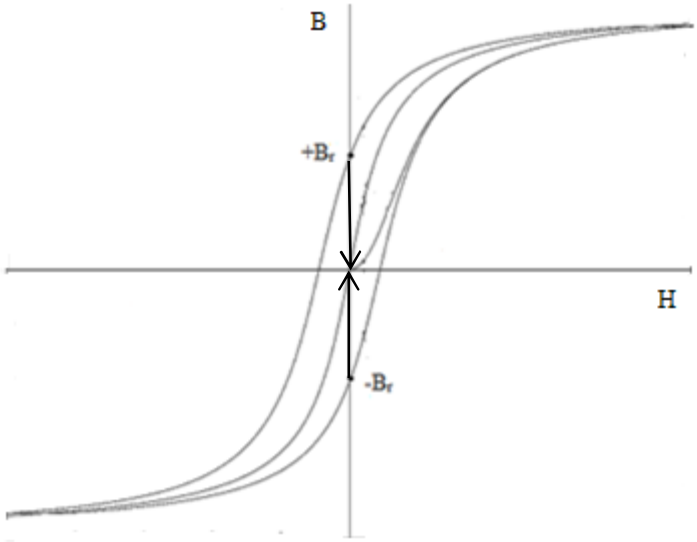

Figure 10.5 *Schematic illustration of the influence of stress on the magnetization when the working point lies at the positive remanence $+B_r$ and negative remanence $-B_r$. The arrows indicate the sign of the change in the magnetization due to the applied stress. (Figure after Pitman [48] and Dapino et al [25].)*

The measurements were repeated three times. All the curves have the same trend and the results are repeatable. The V_{rms} values were also plotted as a function of the number of the applied impact but the magnetomechanical effect did not manifest itself in these curves.

10.1.3 The influence of the impact on the magnetization at magnetic field strength of 8 kA/m

The bar was magnetized to the saturation state and the magnetizing current was then reduced to 0,8 A (8 kA/m). The impact was applied five times and after each impact the rms and Vp-p values were measured. The experiment was repeated three times. The polarity of the magnetizing was changed and the experiment was repeated.

Figure 10.6 shows the magnetomechanical effect in the steel sample when the working point lies a) on the upper hysteresis branch and b) on the lower hysteresis branch. In the case a) the sample was magnetized to the positive saturation state and the magnetic field was then reduced to 8 kA/m (0,8 A). In the case b) the sample was magnetized to the negative saturation and the magnetic field was then decreased to -8 kA/m (0,8 A). At this point the impact induced voltage reached its maximum.

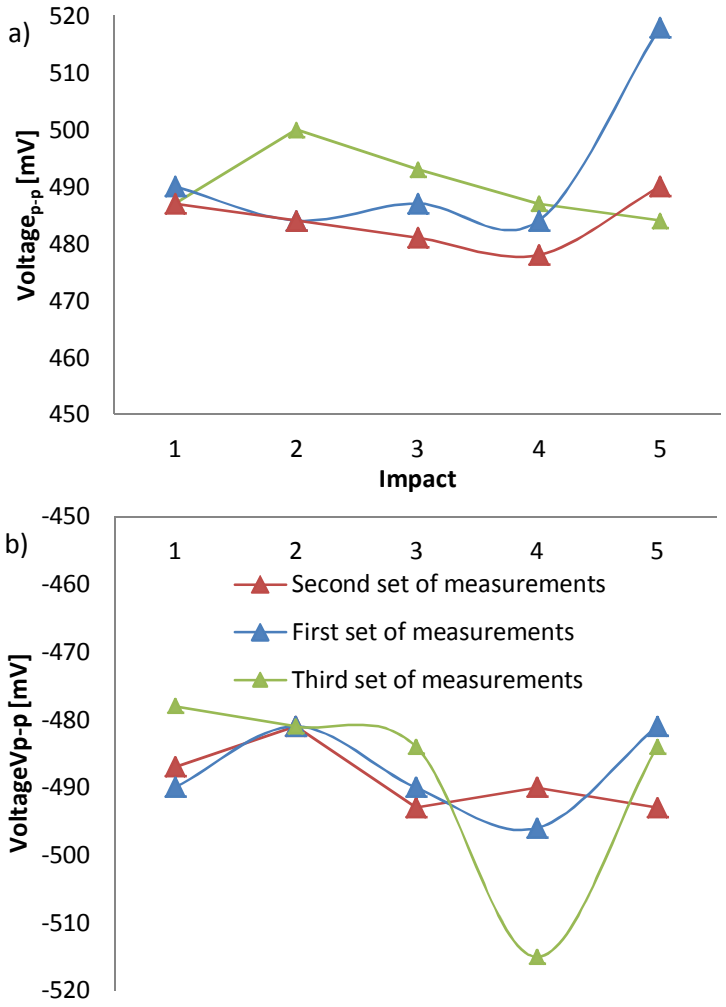

Figure 10.6 *The influence of repeated impacts on the induced voltage V_{p-p} when the working point lies a) on the upper hysteresis branch and b) on the lower hysteresis branch. The applied magnetic field is 8 kA/m.*

The signal level is higher in these measurements as compared with the signal levels obtained from the remanence point. There is scatter between the sets of measurements and no simple trend can be observed like in Fig. 10.4. The impact does not significantly influence the magnetization. As stated by Jiles [5] the displacement of the working point from the anhysteretic curve determines the magnitude of the change in the magnetization due to the applied stress. The results suggest that the working point lies very close to the anhysteretic curve and consequently the change in the magnetization towards anhysteretic state is low in amplitude. On the other hand the applied impact might be too small to have an influence on the magnetization.

10.1.4 Common point

The point where the curves in Fig. 10.2 begin to overlap was further studied in more detail. The objective was to study whether there is a common point in the hysteresis where the results are independent on the path. The sample was magnetized to the positive saturation and then the magnetizing current was reduced at 0,10 A intervals. At each interval the impact was applied. The obtained curve is called as the saturation curve.

Then the polarity of the magnetizing coil was reversed and the sample was magnetized to the saturation. The magnetizing current was increased at 0,10 A intervals and at each interval the impact was applied as previously. This curve is called as the remanence curve. The V_{rms} values of the curves are plotted in Fig. 10.7 a) and the V_{p-p} values are plotted in Fig. 10.7 b). The initial hysteresis curve is plotted in the same graph as a reference. It can be seen that the remanence curve and the saturation curve intersect in Fig. 10.7 a) when the magnetizing current is slightly over 0,8 A and in Fig. 10.7 b) when the magnetizing current is 0,8 A. The difference between the initial hysteresis curve and the intersection point is roughly 5 mV_{rms}.

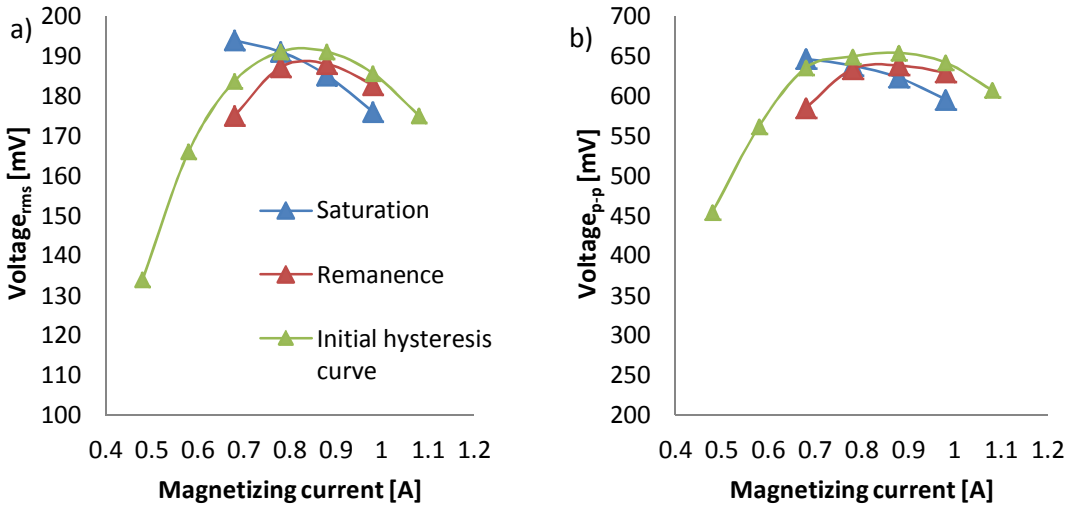

Figure 10.7 *The common point of the remanence curve and the saturation curve occurs a) at magnetizing current 0,85 A when comparing the V_{rms} values b) at magnetizing current 0,8 A when comparing V_{p-p} values.*

10.1.5 The influence of the magnetizing path on the induced voltage at the common point

Once the common point (magnetizing current 0,8 A and magnetic field strength 8 kA/m) was found, it was chosen as the working point of the measurements. The magnetizing path dependence of the results was investigated and the scatter of the results was compared between the studied two paths. In both cases impact was applied ten times and the measurement was repeated three times in order to check the repeatability of the results. Average $V_{p\text{-}p}$ and V_{rms} values were calculated over 30 signals.

Figure 10.8 shows an example of the results when the measurement point is approached from the saturation magnetization state. The standard deviation over 30 signals was calculated and the result is 9,1 mV. It can be seen that the measurement is repeatable because the scatter of the induced voltage values is small.

Path 1: The sample was magnetized to the positive saturation and the magnetizing current was then reduced to 0,8 A. The polarity of the magnetizing coil was reversed, the sample was magnetized to the negative saturation and the magnetizing current was then increased to -0,8 A. The difference between the average results in these cases was 9,80 $mV_{p\text{-}p}$ and 2,22 mV_{rms}.

Path 2: The sample was demagnetized and the magnetizing current was then increased to 0,8 A. The polarity of the magnetizing coil was reversed, the sample was demagnetized and the magnetizing current was then decreased to -0,8 A. The difference between the average results in these cases was 4,17 $mV_{p\text{-}p}$ and 2,25 mV_{rms}.

The standard deviation is in all cases in percent less than 1,7 %. Independent on whether the measurement point is approached from the demagnetized state or from the saturation state, the differences between the results are small. It can be concluded that it does not matter from which state, the saturation state or demagnetic state, the working point is approached.

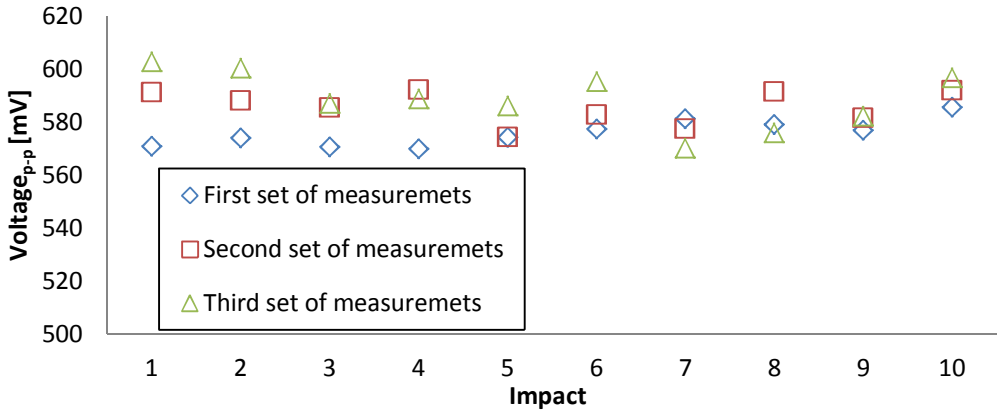

Figure 10.8 *An example of the measurement results when the sample was magnetized to the positive saturation sate and the magnetizing current was then reduced to 0,8 A. The Vp-p-values of the induced voltage were detected. The standard deviation over 30 signals is 9,1 mV which is in percent 1,6 %.*

10.1.6 The influence of magnetic history on the induced voltage V_{rms}

Figure 10.9 shows the influence of magnetic history of the sample on the measurement results. The initial curve forms when the sample is magnetized from the demagnetized state close to the positive saturation state. From the positive saturation state the magnetizing current was reduced to 0,5 A. This curve describes the upper branch on the hysteresis. The sample was magnetized to -0,5 A and -0,8 A and the influence of the magnetic history on the results was studied. The peak values of the induced voltage V_{rms} are achieved when the magnetizing current is 0,8 A except for the red curve.

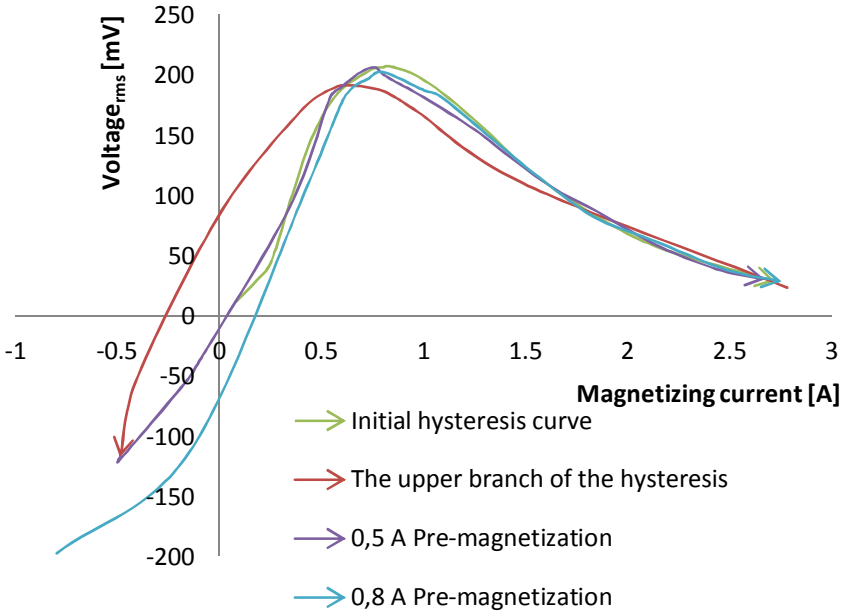

Figure 10.9 *The influence of the magnetic history on the results. The arrows describe the direction of the magnetizing current.*

10.2 Remarks on the measurements

Two different search coils were tested in order to find out if there is a difference in the induced signal between the studied search coils. Both of the studied search coils consisted of 200 turns of copper wire but the length of the coil was different in each coil. Figure 10.10 shows the difference between the search coil of 50 mm in length and the search coil of 20 mm in length. It was noticed that the search coil signal form of the 20 mm coil is sharper. The measurements were continued with the 20 mm coil.

During the measurements it was noticed that the mounting of the sample to the measurement device frame influences the results. If the sample is attached too tightly the surface stress wave is absorbed by the supports.

The magnetic field can be removed by keeping the magnetizing coil open or by short-circuiting the coil. It was noticed that opening the magnetizing coil gives higher signal amplitudes and consequently this method was chosen measurements.

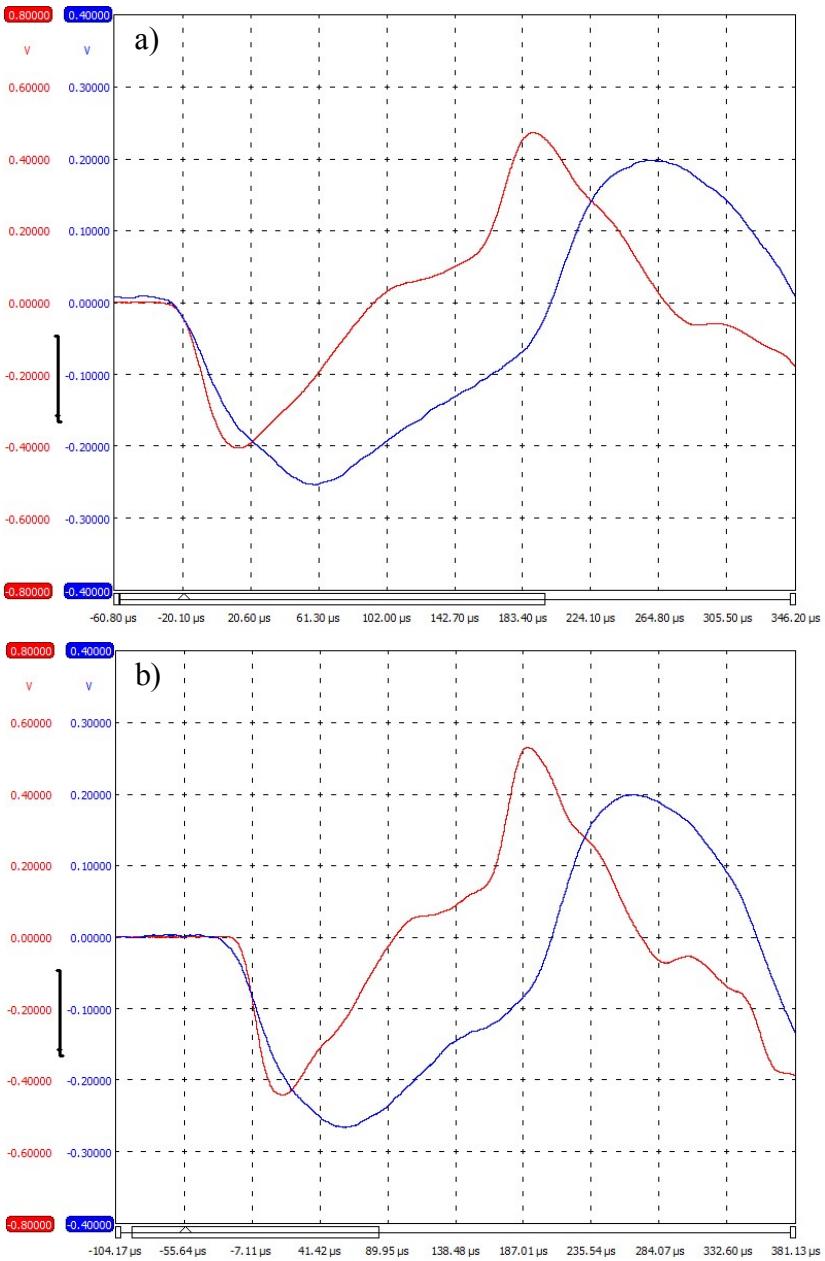

Figure 10.10 *Signal obtained a) on the search coil of 50 mm b) on the search coil of 20 mm. Red curve indicates the search coil signal and blue curve indicates the strain gauge signal.*

It was noticed that the temperature of the magnetizing coil influences the search coil signal amplitude as can be seen in Fig. 10.11 which shows the initial hysteresis curves measured with magnetizing coil at initial temperature and with magnetizing coil at elevated temperature. The magnetizing current increases the temperature of the magnetizing coil which has an influence on the temperature of the search coil and the sample.

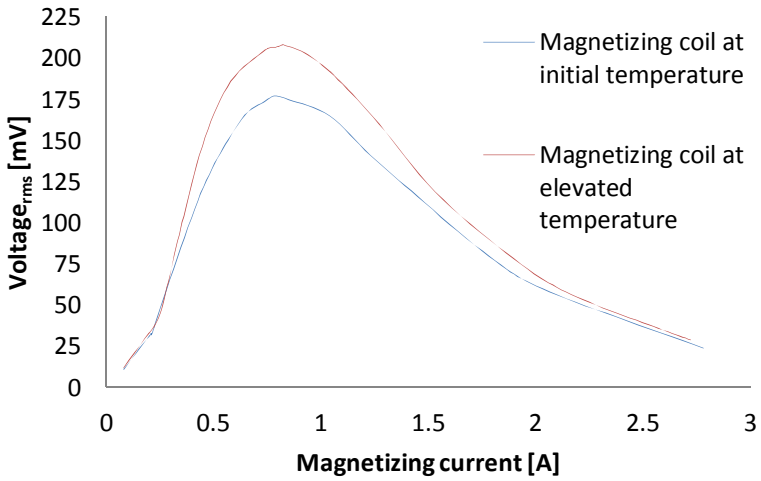

Figure 10.11 *The temperature dependence of the measurement results. The signal measured with magnetizing coil at a higher temperature has larger peak values of the induced voltage. The initial temperature was the room temperature.*

The increasing temperature increases the impedance of the search coil which results in higher signal amplitudes. A thermoelement was then installed to the search coil in order to monitor the temperature of the search coil and to control the influence of temperature on measurement results.

10.3 The scatter of the results on different samples

10.3.1 Parameters and measurements

The samples were measured in two series. The first series consisted of the samples T1-T4 and the second consisted of the samples T5-T9. The samples T1-T9 were measured with the following parameters:

- Filtering: 5600 pF capacitor
- Rubber mat under the sample
- Search coil of 200 turns in 20 mm length
- Measuring point: in the middle of the sample
- The temperature of the search coil was detected by a thermoelement placed in the frame of the search coil.
- Magnetization 8 kA/m (0,8 A constant current)
- Drop height of the impact piston: 25,3 mm

The measurement procedure consisted of the following steps:

1. The influence of the impact on the magnetic properties of the specimen in the initial state was measured. The aim of this experiment was to reveal whether there is remanence retained from the manufacturing process of the sample. The average over two

results was calculated. The sample T1 was demagnetized because it had been magnetized in the previous measurements.

2. The magnetic field strength of 8 kA/m (0,8 A) was applied and held constant when the impact was applied. The average value over six results was calculated.

3. The magnetic field was then removed and the influence of the impact on the induced voltage at positive remanence was obtained. The average value over three results was calculated.

10.3.2 The initial state of the samples T1-T4

Figure 10.12 shows the influence of the impact on the V_{p-p} values of the search coil signal at zero magnetic field strength. The assumption is that no signal is obtained because according to the studies by Rizzo et al. [24] ferromagnetic material cannot get magnetized in the demagnetized state by the means of applied stress only. Comparing the samples, it appears that the induced voltage V_{p-p} of the sample T1 is larger than the V_{p-p} values of the samples T2-T4.

The sample T1 was demagnetized, because it was exposed to various magnetic field strength values in the previous measurements. Despite the demagnetization, a small impact-induced voltage can be obtained. This means that the demagnetization process is not complete and remanence can be found in the sample T1. This can again be explained in terms of the length of the sample, which influences the level of the demagnetization. Due to the length of the bar, the ends of the bar are never fully demagnetized; consequently the magnetization of the ends influences the behavior of the measurement point in the middle of the bar. One possible explanation why the demagnetic state is not achieved is texture, which causes preferred domain orientation in the material. Even though the signal of the sample T1 is higher than the signal of the samples T2-T4 its significance can be considered as small. Figure 10.13 shows the search coil signal which implies that the magnetomechanical effect is small also in the sample T1.

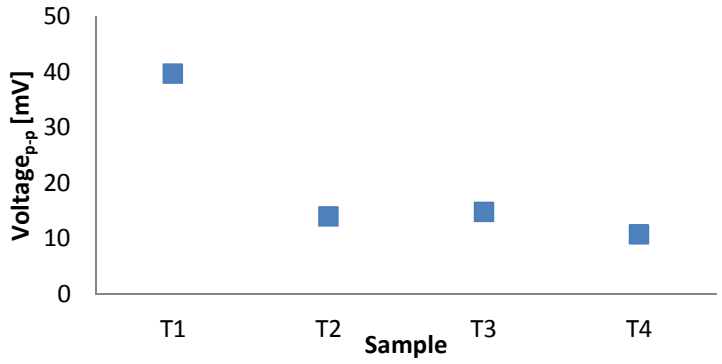

Figure 10.12 *The impact induced voltage V_{p-p} values of the search coil signal at zero magnetic field strength of the samples T1-T4. The V_{p-p} values are the average over two measurement results.*

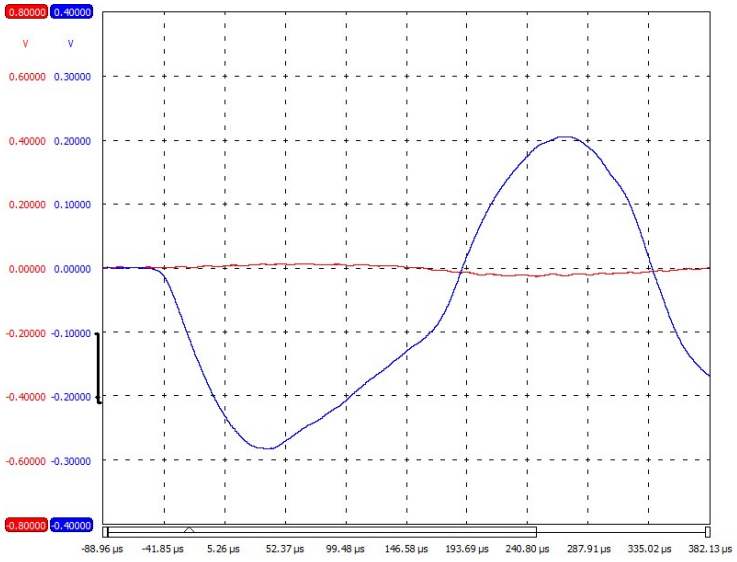

Figure 10.13 *The impact-induced search coil signal of sample T1 at zero magnetic field strength. The red curve indicates the search coil signal and the blue curve is the strain gauge signal.*

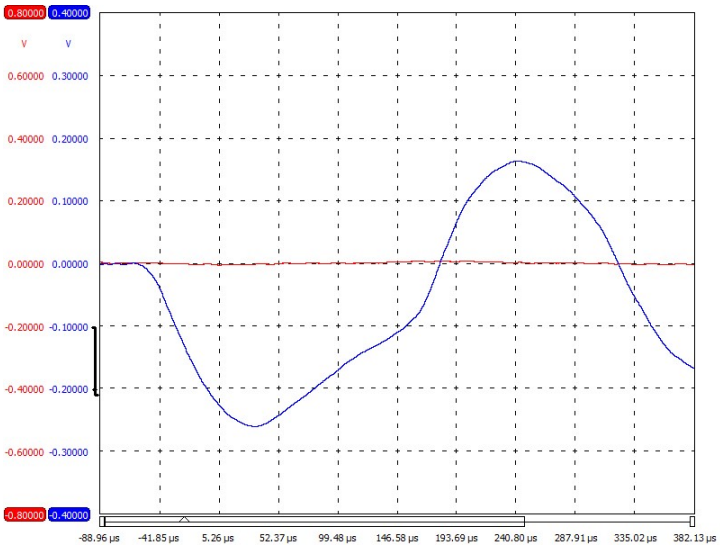

Figure 10.14 *The impact-induced search coil signal of the sample T3 at zero magnetic field strength. The red curve indicates the search coil signal and the blue curve is the strain gauge signal.*

Figure 10.14 shows typical measurement result of the initial sate on samples T2-T4. The result on sample T3 is presented as an example. Samples T2-T4 have not been exposed to the magnetic field during manufacturing process and no remanence can be detected. This measurement was repeated with the samples T5-T9 but the results are not presented here because the results were very similar to the results obtained on the samples T2-T4.

10.3.3 Samples T1-T4

The first sample group was measured in numerical order starting from the sample T1. Then the measurements were repeated in different order to see the repeatability of the results and to ensure that the order of the samples does not influence the results. When comparing two sets of measurements it can be seen that only the results of the sample T4 in the form of the search coil signal differ drastically from each other as shown in Fig. 10.15 and in Fig. 10.16. The scattering results of the samples T1-T3 are not so radical.

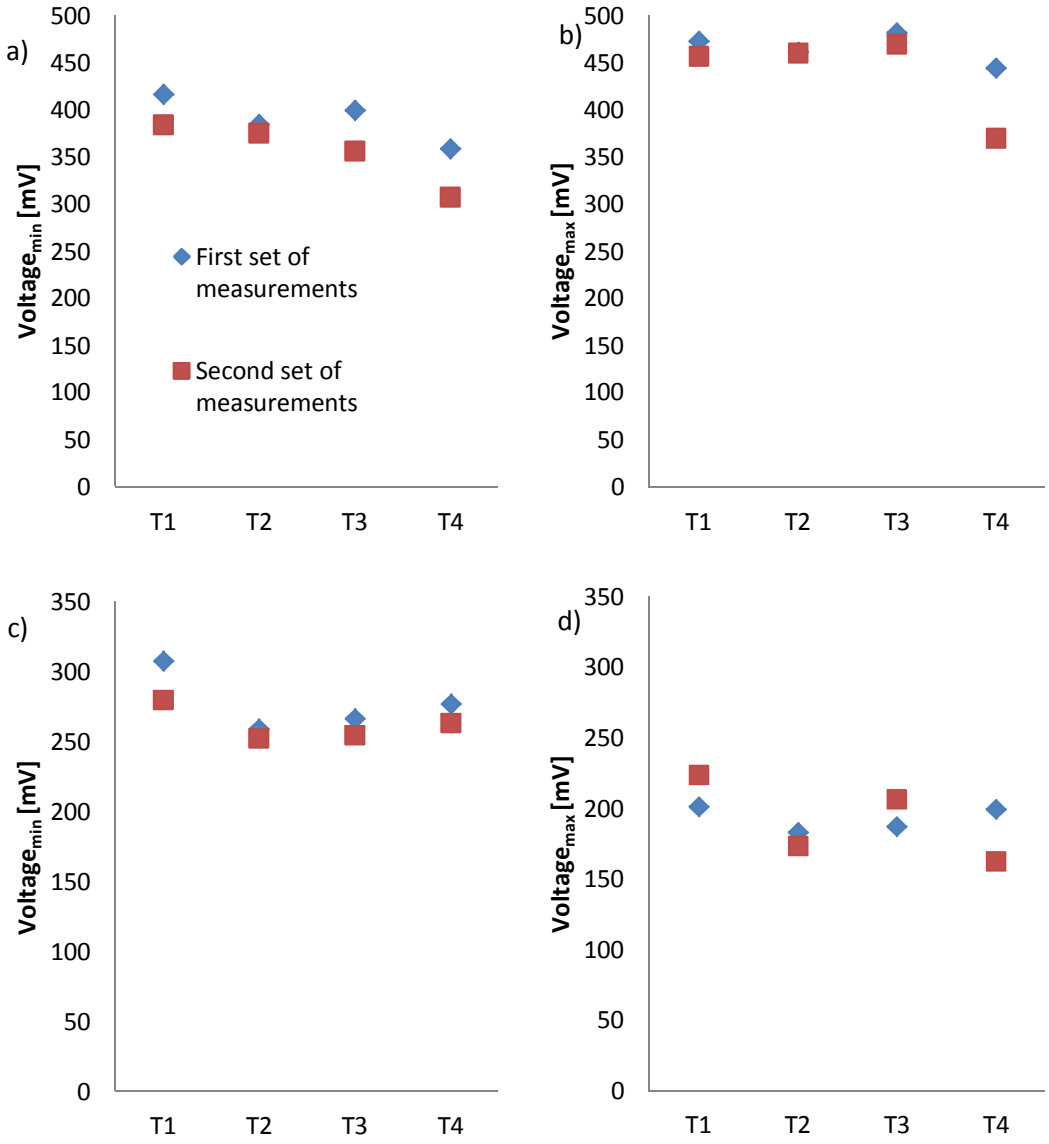

Figure 10.15 *The differences between two sets of measurements. The results describe the influence of the impact on the induced voltage at the magnetic field strength of 8 kA/m. Graphs a) and b) represent the search coil signal and c) and d) the strain gauge signal. Blue dots indicate the first set of measurements and red dots indicate the second set of measurements. V_{min} is the maximum of the compressive stress wave and V_{max} is the maximum of the tensile stress wave.*

It was noticed that the end of sample T4 was convex while the ends of the other samples were flat. This may explain the differences in the results obtained on sample T4. When the sample is placed in to the measurement device, removed and put back again, the position of the sample most probably changes. This happens because the samples are supported loosely. The position of the sample is critical only for the sample T4. If the position of the sample T4 changes the impact piston hits the bar at a different angle.

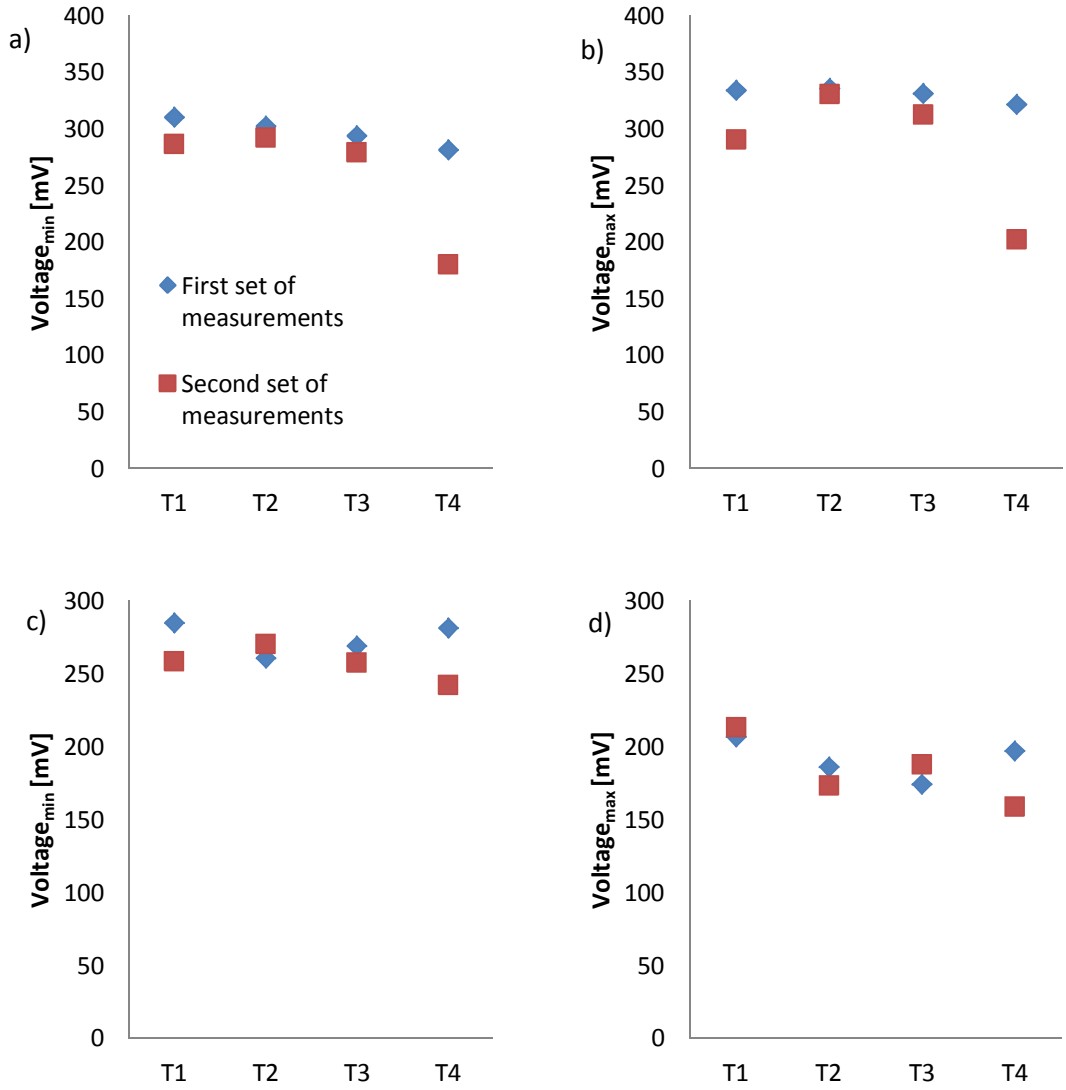

Figure 10.16 *The differences between two sets of measurements. The results describe the influence of the impact on the induced voltage when the working point lies at the positive remanence. Graphs a) and b) represent the search coil signal, whereas c) and d) show the strain gauge signal. Blue dots indicate the first set of measurements and red dots indicate the second set of measurements.* V_{min} *is the maximum of the compressive stress wave and* V_{max} *is the maximum of the tensile stress wave.*

Because the sample T4 differs from the samples T1-T3, the signal form of the sample T4 is studied in more detail. The differences in the signal form of samples T1 and T4 can be seen in Fig. 10.17. The signal form of the sample T4 is rounder. Figure 10.18 shows the difference in the signal form and amplitude obtained on sample T4 when measured on different days. The convex shape of the bar end alters the signal form but does not influence the amplitude.

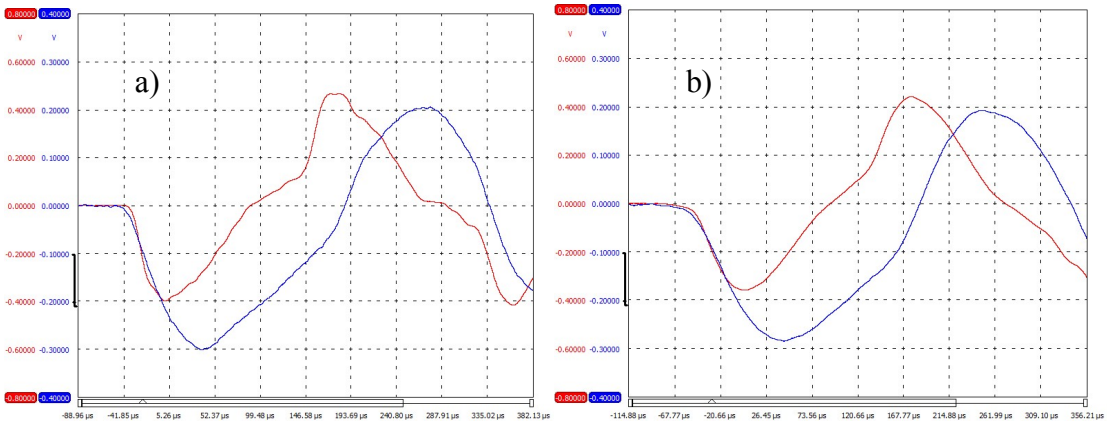

Figure 10.17 *The impact-induced voltage signals of the sample a) T1 b) T4 at the magnetic field strength of 8 kA/m. The red curve indicates the search coil signal and the blue curve is the strain gauge signal.*

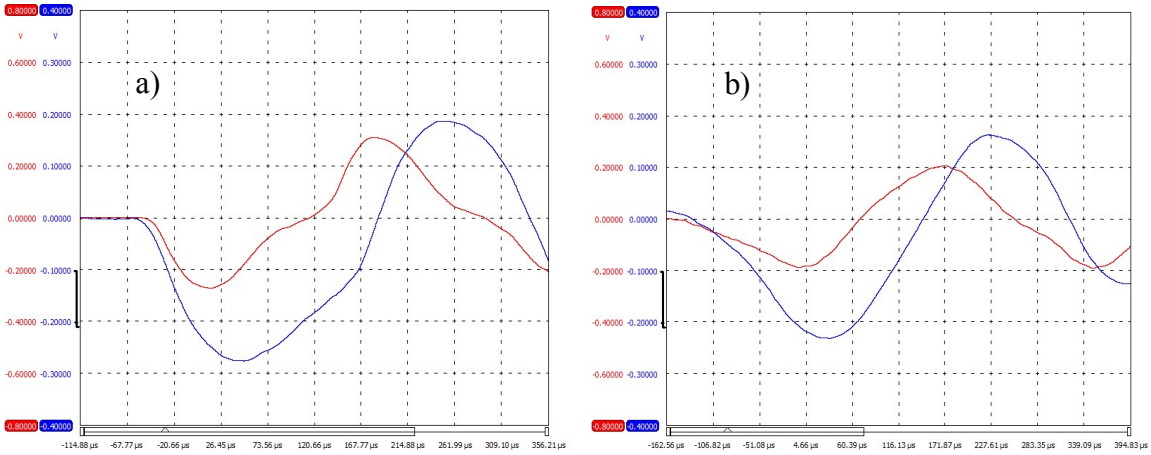

Figure 10.18 *The impact-induced voltage signals of the sample T4 when the working point lies at the positive remanence. a) The first set of measurements b) the second set of measurements. The measurements sets were taken on different days. The red curve indicates the search coil signal and the blue curve is the strain gauge signal.*

10.3.4 Samples T1-T9

The samples T5-T9 were measured according to the measurement procedure. The most important set of results of this work is presented in Fig. 10.19 which describes the scatter of the results on samples T1-T9. Both search coil and strain gauge values are presented. The first set of measurements on samples T1-T4 was also plotted in this graph.

It can be seen that the scatter of the strain gauge results is smaller than that of the search coil signal. The search coil signal shows higher amplitudes for tension stress wave (induced voltage V_{max}) than for compressive stress wave (induced voltage V_{min}) at magnetic field strength 8 kA/m and also when the magnetic field strength is zero. For strain gauge signal the situation is reversed. In addition the differences between the search coil signal values and strain gauge signal values are larger for tension stress wave.

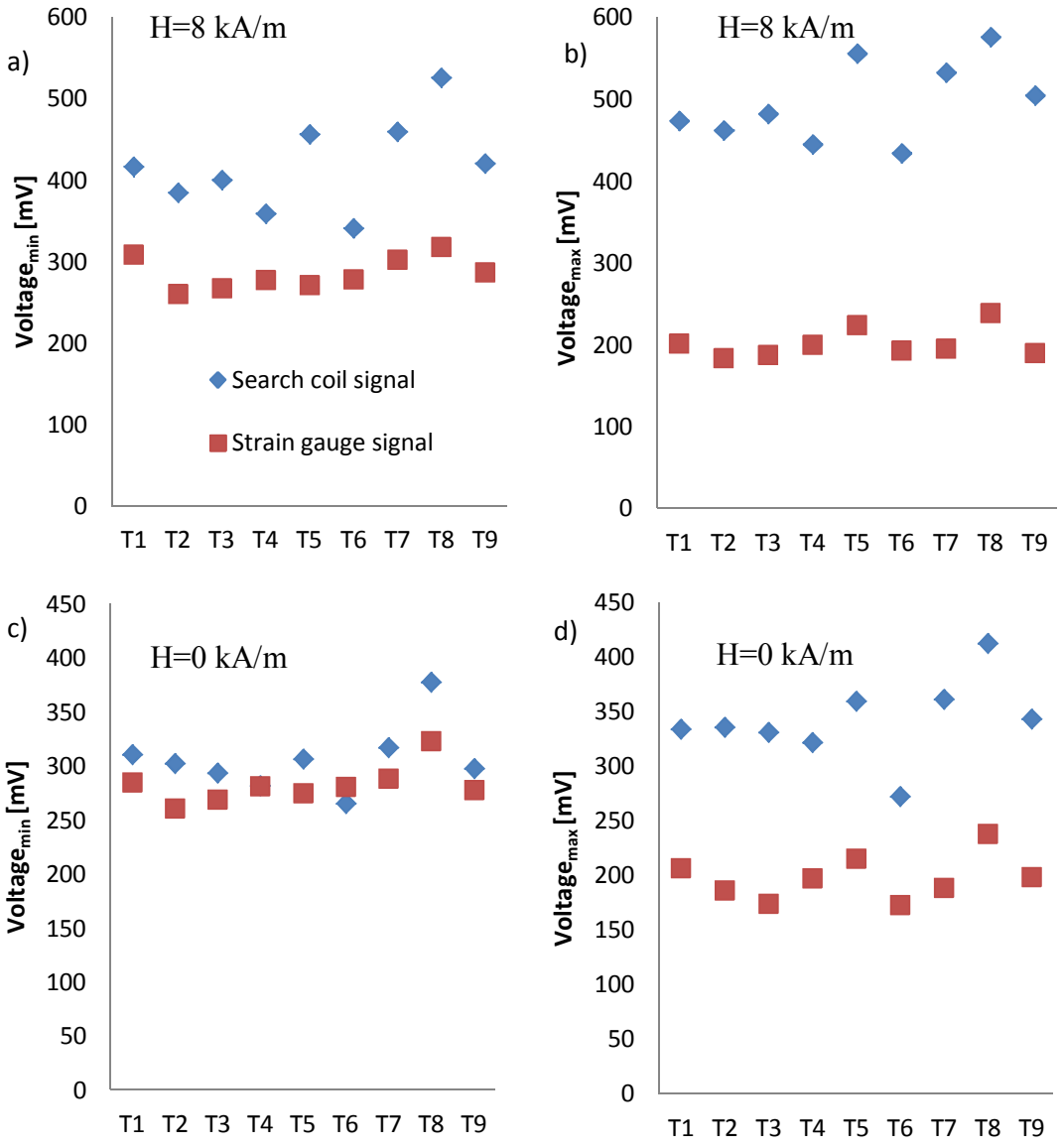

Figure 10.19 *The scatter of the results on samples T1-T9. Blue dots indicate the search coil signal and red dots indicate the strain gauge signal. V_{min} is the maximum of the compressive stress wave and V_{max} is the maximum of the tensile stress wave. The influence of the impact on the induced voltage signals at a) and b) the magnetic field strength of 8 kA/m, c) and d) when the magnetic field strength is zero.*

The scatter of the results on samples T5-T9 is significant as compared with the samples T1-T4. Samples T1-T4 and samples T5-T9 have different manufacturing dates. This might result in differences between the results of two sample groups. It should be mentioned that the samples T2-T9 have not been magnetized to the saturation value. Although scatter exists, the behavior of the samples is systematic in all cases.

When comparing the samples it can be seen that the sample T8 has the highest search coil signal values whereas the sample T6 has the lowest signal values. The signal forms of samples T6 and T8 are shown in Fig 10.20 when the magnetic field strength is 8 kA/m and in Fig 10.21 when the magnetic field strength is zero. It can be seen that the signal form and amplitude are different for magnetized sample and for the sample at remanence state. The output of the search coil signal is influenced by the magnetic history of the sample.

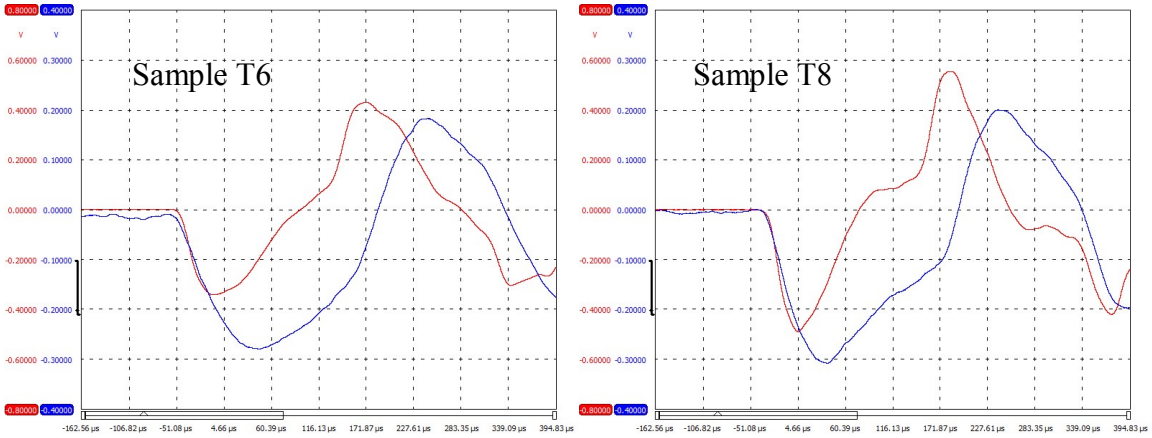

Figure 10.20 *Signal forms of the samples T6 and T8 when the magnetic field strength is 8 kA/m. The red curve is the search coil signal and the blue curve is the strain gauge signal.*

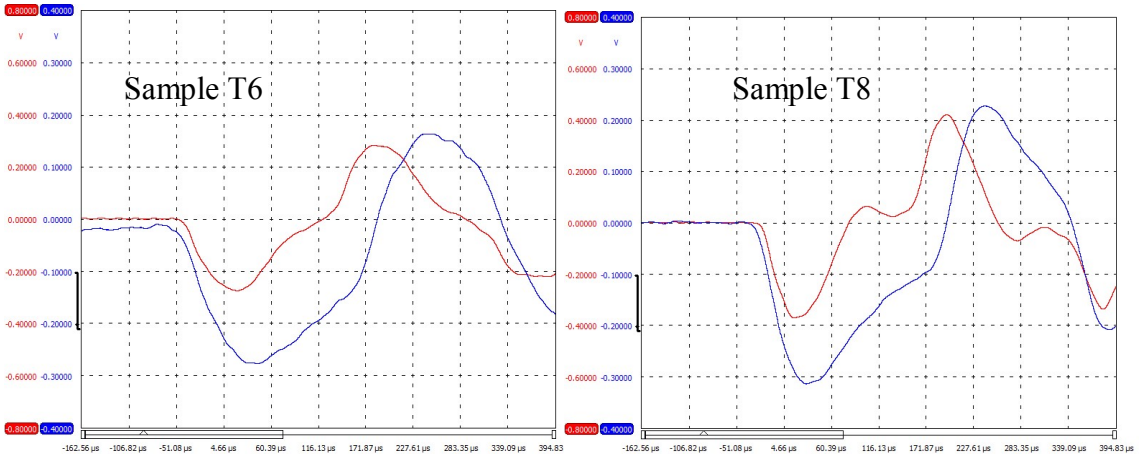

Figure 10.21 *Signal forms of the samples T6 and T8 when the magnetic field strength is 0 kA/m. The red curve is the search coil signal and the blue curve is the strain gauge signal.*

The standard deviations of the search coil values are presented in Table 10.1. The scatter of the results is the highest (14%) for compressive stress wave when the magnetic field strength is 8 kA/m and smallest (10%) at same field strength but for tensile stress wave.

Table 10.1 *The standard deviations of the search coil signal values.*

Condition	Compressive stress wave	Tensile stress wave
H=8 kA/m	14 %	10 %
H=0 kA/m	11 %	12 %

The optimal magnetic field strength was measured for sample T1 only. The optimal field strength may not be the same 8 kA/m for all the samples. As discovered in the elementary analysis of the sample TP 3.1, there may be slight differences in the carbon content of the samples due to the production tolerances. Even though the carbon content would vary only little, it may influence the magnetoelastic properties and consequently the induced voltage values. The scatter of the results on samples T1-T9 can also be explained in terms of the texture in the samples, which may vary from sample to sample. The differences in the texture cause different domain structures in the material, and consequently introduce differences in the magnetoelastic behavior of the samples.

10.4 Factors of uncertainty and challenges in magnetic measurements

There are several factors of uncertainty influencing the magnetic properties of the samples as well as the amplitude and form of the induced voltage signal. These parameters have to be taken into account when interpreting the results of the magnetic measurements. The parameters are summarized and divided into two groups: universal parameters and parameters which depend on the measurement device and set-up.

Measurement set up-dependent parameters:

- Impact loading (the plastic deformation limit was not exceeded in this work)
- Tensile stress and compressive stress
- The position of the sample in the impact test device
- Solenoid (impact piston) induced disturbances
- Temperature of the magnetizing coil
- Impact height
- Disturbances due to the mounting of the specimen to the impact test device
- The cross-sectional area of the impact piston
- The length of the search coil
- The method of decreasing the magnetizing current and voltage to zero
- Search coil location
- Macro and micro eddy currents

Universal parameters:

- Steel grade (composition)
- Microstructure of the sample
- Strain hardening (cold working)
- Heat treatment
- Texture and preferred domain orientation
- The initial magnetic state of the material
- Magnetic anisotropy (the direction of the magnetization and strain)
- The sign of the magnetostriction constant
- The critical magnetic field strength H_m
- Demagnetic state
- Magnetic hysteresis of the material
- Anhysteretic curve and the anhysteretic magnetization
- Domain structure and distribution in the material
- The length of the bar sample
- The shape of the bar end
- Demagnetizing field

Measurements were carried out under laboratory conditions. Tests in the industrial environment provide challenges. The samples measured in this work were in the as-received condition, i.e., they were not exposed to magnetic fields or prior service loading. A real component has complicated stress and magnetic histories. The change in the magnetization is difficult to predict when the initial magnetic state is unknown.

In real applications stress levels are higher than in the impact tests used in this study. If the impact height is increased, it may result in higher signal level and thus stronger magnetoelastic phenomena.

One of the major challenges is the interpretation of the results in the case of different materials and samples, since there is no known theoretical model taking takes into account all the factors influencing the magnetoelastic properties of the material. Interpretation of the signal form requires deep understanding of the phenomena related to magnetoelasticity. The output signal of the search coil is influenced by the design of the coil and sensor.

11 SUMMARY AND CONCLUSIONS

11.1 Literature survey

The aim of the work was to study the magnetic and magnetoelastic properties of steel bars. This thesis was divided into literature survey and experimental part. In the literature survey the basic magnetic properties of steels were reviewed. As an iron based metal alloy steel can be classified as a ferromagnetic material. Ferromagnetic materials contain magnetic domains and domain walls, which are responsible for the magnetization process. The key feature of the ferromagnetic materials is the hysteresis curve, which is formed due to the interaction between the domain walls and defects in the material. It was found that different microstructural features, such as grain size, composition and the presence of different phases influence the shape of the hysteresis curve, from which the magnetic properties of the material can be concluded.

Detailed study of the physical factors influencing the magnetoelasticity was presented in order to understand the results of the magnetic measurements. The interaction between stress and magnetization is complex especially in steels because there are several influencing factors. There are two mechanisms working simultaneously when stress and magnetic field are present: magnetostriction and magnetomechanical effect. Magnetostriction is the field-induced dimensional change in a ferromagnetic material. Magnetomechanical effect describes the change in the magnetization due to stress.

Magnetostriction in iron and steels is complicated because it depends on the magnetic field strength and mechanical stress. It was found that the magnetomechanical effect can be defined according to the law of approach. It implies that the working point (below or above the anhysteretic curve), the distance from the anhysteretic curve and the anhysteretic magnetization determine the sign and the magnitude of the magnetization due to the applied stress.

Recently magnetoelasticity has been studied widely because it can be exploited in condition monitoring of structural steel components. According to literature it seems that the basic phenomena behind the magnetostriction and magnetomechanical effect are well understood in general, but the details are still not fully agreed. The basic facts concerning the stress-induced change in magnetization can be found in the books by Cullity [1] and Bozorth [16] whose original editions were published decades ago. Despite the large amount of work, only little progress has been made. The change in magnetization under varying stress is difficult to model. This is due to the nonlinear and hysteretic character of the phenomenon.

11.2 Measurements

The experimental part of this thesis was divided into two parts. In the first part the hysteresis curves were measured and the basic magnetic properties of the samples were investigated. The materials studied in this work were low alloy steels, from which some were gas carburized. The results showed that the magnetic properties are influenced by the composition, microstructure and prior cold working.

The purpose of the second part of the experimental work was to build an impact loading device in order to measure the magnetoelastic properties of the steel bar samples. First the measurement parameters were studied and the most suitable were chosen. When the magnetic field strength H was increased the impact induced voltage V_{rms} increased and reached a maximum at a critical magnetic field strength H_m, which was 8 kA/m for the sample T1.

The magnetomechanical behaviour of the steel bars was studied at different points on the hysteresis curve. When the working point lies either at the positive or negative remanence, the change in the magnetization due to the impact (although very small) is towards the anhysteretic curve. However, when the sample was magnetized to the critical magnetic field strength H_m, the working point was located close to the anhysteretic state and consequently the influence of the impact on the induced voltage was small.

It was discovered that differences exist in the carbon content of the same steel grade due to the production tolerances. Elementary analysis of the samples is necessary in order to interpret the results with more accuracy. Small changes in the carbon content influence the magnetoelastic properties and consequently the measurement results.

The impact load measurements were carried out on nine steel bars of same steel grade. The main goal of these measurements was to find out how the search coil signal varies depending on the sample. The measurements revealed the scatter of the results within the studied sample range. Although scatter of the results occurred magnetoelasticity can be utilized in the stress evaluation of steel bars.

The identification of the factors of uncertainty related to the magnetic measurements was also an important goal of the work. The factors of uncertainty were identified in order to evaluate the reliability of the measurement results. In steel the influence of stress on magnetization is complicated because the magnetic behavior of steel depends on many factors. In general all the changes in the mechanical properties of the material influence also the magnetic behaviour and properties.

In order to further investigate the relationship between mechanical and magnetic properties in more detail, the microstructural analysis of the samples is essential. The microstructure of the steel is the key feature which determines the characteristic parameters of the hysteresis curve. The results obtained from the hysteresis curve measurements suggest that changes in the fundamental properties of the sample would also have an influence on the magnetoelastic properties. Hence different materials should be measured in order to find out the influence of the composition, heat treatment and cold working on the magnetoelastic properties.

REFERENCES

[1] Cullity, B.D. & Graham, C.D. Introduction to magnetic materials. Second edition. USA 2008, Wiley-IEEE Press, 832 p.

[2] Belahcen, A. Magnetoelasticity, magnetic forces and magnetostriction in the electrical machines. Doctoral dissertation, Helsinki University of Technology, Laboratory of Electromechanics, Report 72, Espoo 2004, 115 p.

[3] Jiles, D.C. Introduction to magnetism and magnetic materials. Second edition, USA, 1998, Chapman & Hall/CRC, 536 p.

[4] Joule, J.P. (1842) Ann. Electr. Magn. Chem., 8, 219.

[5] Hubert, O. & Rizzo, K.-J. Anhysteretic and dynamic piezomagnetic behaviour of a low carbon steel. Journal of Magnetism and Magnetic Materials 320(2008)20, pp. 979-982.

[6] Daniel, L. & Hubert, O. An equivalent stress for the influence of multiaxial stress on the magnetic behaviour. Journal of Applied Physics 105(2009)07A313.

[7] Daniel, L. & Hubert, O. Equivalent stress criteria for the effect of stress on magnetic behaviour. IEEE Transactions on magnetic materials 46(2010)8, pp. 3089-3092.

[8] Jiles, D.C. & Li, L. A new approach to modelling the magnetomechanical effect. Journal of Applied Physics 95(2004)11, pp. 7058-7060.

[9] Li, L. & Jiles, D.C. Modified Law of approach for the magnetomechanical model: Application of the Rayleigh law to stress. IEEE Transactions on magnetics 39(2003)5, pp. 3037-3039.

[10] Bulte, D.P & Langman, R.A. Origins of the magnetomechanical effect. Journal of Magnetism and Magnetic Materials 251(2002)2, pp. 229-243.

[11] Rizzo, K.J, Hubert, O., Daniel, L. A multiscale model for piezomagnetic behaviour-Coupled anhysteretic multiscale and hysteretic Jiles-Atherton approaches. European Journal of Electrical Engineering 12(2009)4, pp.525-540.

[12] Lollioz, L., Pattofatto, S. & Hubert, O. Application of piezomagnetism for the measurement of stress during an impact. Journal of Electrical Engineering 57(2006)8/S, pp. 15-20.

[13] Callister, William D. Jr. Materials Science and Engineering - an Introduction. 6th edition, USA 2003, John Wiley & Sons, 820p.

[14] Abrahams, E., Keffer, F. & Herbst, J.F. Ferromagnetism. AccessScience@McGraw-Hill, 2008, [WWW]. [Referred 27.4.2012].

[15] Yamasaki, T., Yamamoto, S. & Hirao, M. Effect of applied stresses on magneto-striction of low carbon steel. NDT&E International 29(1996)5, pp. 263-269.

[16] Bozorth, R.M. Ferromagnetism. Third edition, USA 1951, 669p.

[17] Rumiche, F., Indacochea, J.E. & Wang, M.L. Assessment of the effect of micro-structure on the magnetic behaviour of structural carbon steels using an electromagnetic sensor. Journal of Materials Engineering and Performance 17(2008)4, pp. 586-593.

[18] Jiles, D.C. & Atherton, D.L. Theory of the magnetization process in ferromagnets and its application to the magnetomechanical effect. Journal of Applied Physics 17(1984), pp. 1265-1281.

[19] Jiles, D.C. Development and characterization of the highly magnetostrictive alloy Tb-Dy-Fe for use in sensors and actuators. New Materials and Their Applications. Bristol: Institute of Physics Publishing, 1990.

[20] Ruuskanen, P. Magnetomechanical effect in polycrystalline iron and nickel during cyclic stressing. Doctoral dissertation, Tampere University of Technology, Publications 48. Tampere 1987, 97 p.

[21] Kalevo, N. Magnetomechanical behaviour of materials. Bachelor's thesis, Tampere University of Technology, 2010.

[22] Villari, E. Ann. Phys.Lpz 126(1865), pp. 87–122.

[23] Chikazumi, S. Physics of magnetism. USA 1964, John Wiley & Sons, 554p.

[24] Perevertov, O. Influence of the residual stress on the magnetization process in mild steel. Journal of Applied Physics 40(2007), pp. 949-954.

[25] Dapino, M.J., Smith, R.C., Faidley, L.E. & Flatau, A.B. A coupled structural-magnetic strain and stress model for magnetostrictive transducers. Journal of Intelligent Materials and Structures 11(2000)2, pp.135-152.

[26] Atherton, D.L. & Jiles, D.C. Effects of stress on the magnetization of steel. IEEE Transactions on magnetics 19(1983)5, pp. 2021-2023.

[27] Martensitic Structures, Metallography and Microstructures, Vol 9, ASM Handbook, ASM International, 2004, pp. 165–178

[28] Jiles, D.C. Theory of the magnetomechanical effect. Journal of Physics, D: Applied Physics 28 (1995), pp. 1537-1546.

[29] Jiles, D.C. & Devine, M.K. The law of approach as a means of modeling the magnetomechanical effect. Journal of Magnetism and Magnetic Materials 140-144(1995), pp. 1881-1882.

[30] Sablik, M.J. & Jiles, D.C. Coupled magnetoelastic theory of magnetic and magnetostrictive hysteresis. IEEE Transactions on magnetic materials 29(1993)3, pp. 2113-2122.

[31] Jiles, D.C. & Atherton, D.L. Theory of ferromagnetic hysteresis (invited). Journal of Applied Physics 55(1984)6, pp. 2115-2120.

[32] Krauss, G. Microstructures, Processing, and Properties of Steels, Properties and Selection: Irons, Steels, and High-Performance Alloys, Vol 1, ASM Handbook, ASM International, 1990.

[33] Kirkaldy, J.S. Thompson, B.A. & Baganis, E.A. Prediction of Multicomponent Equilibrium and Transformation Diagrams for Low Alloy Steels, in: Hardenability Concepts with Applications to Steel, D.V. Doane and J.S. Kirkaldy (eds.), The Metallurgical Society, 1978

[34] Devine, M.K. & Jiles, D.C. Composition dependence of the magnetomechanical effect and magnetostriction. IEEE Transactions on magnetics 32(1996)5, pp. 4740-4742.

[35] Tanner, B.K., Szpunar, S.N., Willcock, S.N., Morgan, L.L. & Mundel, P.A. Magnetic and metallurgical properties of high-tensile steels. Journal of Materials Science 23(1988)12, pp. 4534-4540.

[36] Metals Handbook. Metallography, Structures and Phase Diagrams, Vol 8. 8th edition. 1973, American Society for Metals.

[37] Anglada-Rivera, J., Padovese, L.R. & Capo-Sanchez, J. Magnetic Barkhausen Noise and hysteresis loop in commercial carbon steel: influence of applied tensile stress

and grain size. Journal of Magnetism and Magnetic Materials 231(2001)2-3, pp. 299-306.

[38] Ranjan, R., Jiles, D.C. & Rastogi, P.K. Magnetic properties of decarburized steels: An investigation of the effects of grain size and carbon content. IEEE Transactions on Magnetics 23(1987)3, pp. 1869-1876.

[39] Buttle, D & Scruby, C. Residual stresses: Measurement using magnetoelastic effects. Encyclopedia of materials: Science and Technology, 2001, pp. 8172-8180.

[40] Habermehl, S., Jiles, D.C. & Teller, C.M. Influence of heat treatment and chemical composition on the magnetic properties of ferromagnetic steels. IEEE Transactions on magnetics 21(1985)5, pp.1909-1911.

[41] Stanley, J.K. Electrical and magnetic properties. Crucible Steel Company of America. American Society for Metals, Metals Park, Ohio. USA, 1963

[42] Wun-Fogle, M., Restorff, J. B., Cuseo, J. M., Garshelish, I. J. & Bitar, S. Magnetostriction and magnetization of common high strength steels. IEEE Transactions on magnetics 45(2009)10, pp. 4112-4115.

[43] Pehlke, R.D. Steel Continuous Casting, Casting, Vol 15, ASM Handbook, ASM International, 2008, pp. 918–925.

[44] Guthrie, R.I.L. & Jonas, J.J. Steel Processing Technology, Properties and Selection: Irons, Steels, and High-Performance Alloys, Vol 1, ASM Handbook, ASM International, 1990, pp. 107–125.

[45] Lampman, S. Introduction to Surface Hardening of Steels, Heat Treating, Vol 4, ASM Handbook, ASM International, 1991, pp. 259–267.

[46] Kyowa electronic instruments Co., Ltd. What is a strain gage? Introduction to strain gages. http://www.straintech.fi/pdf/whats.pdf. [WWW]. [Referred 21.3.2012].

[47] ELEP-2610 Introduction to magnetic materials, Lecture notes 2011, Professor Pekka Ruuskanen, Tampere University of Technology.

[48] [53] Pitman, K.C. The influence of stress on ferromagnetic hysteresis. IEEE Transactions on Magnetics 26(1990)5, pp. 1978-1980.

APPENDIX 1
HYSTERESIS CURVES OF THE STUDIED STEEL GRADES

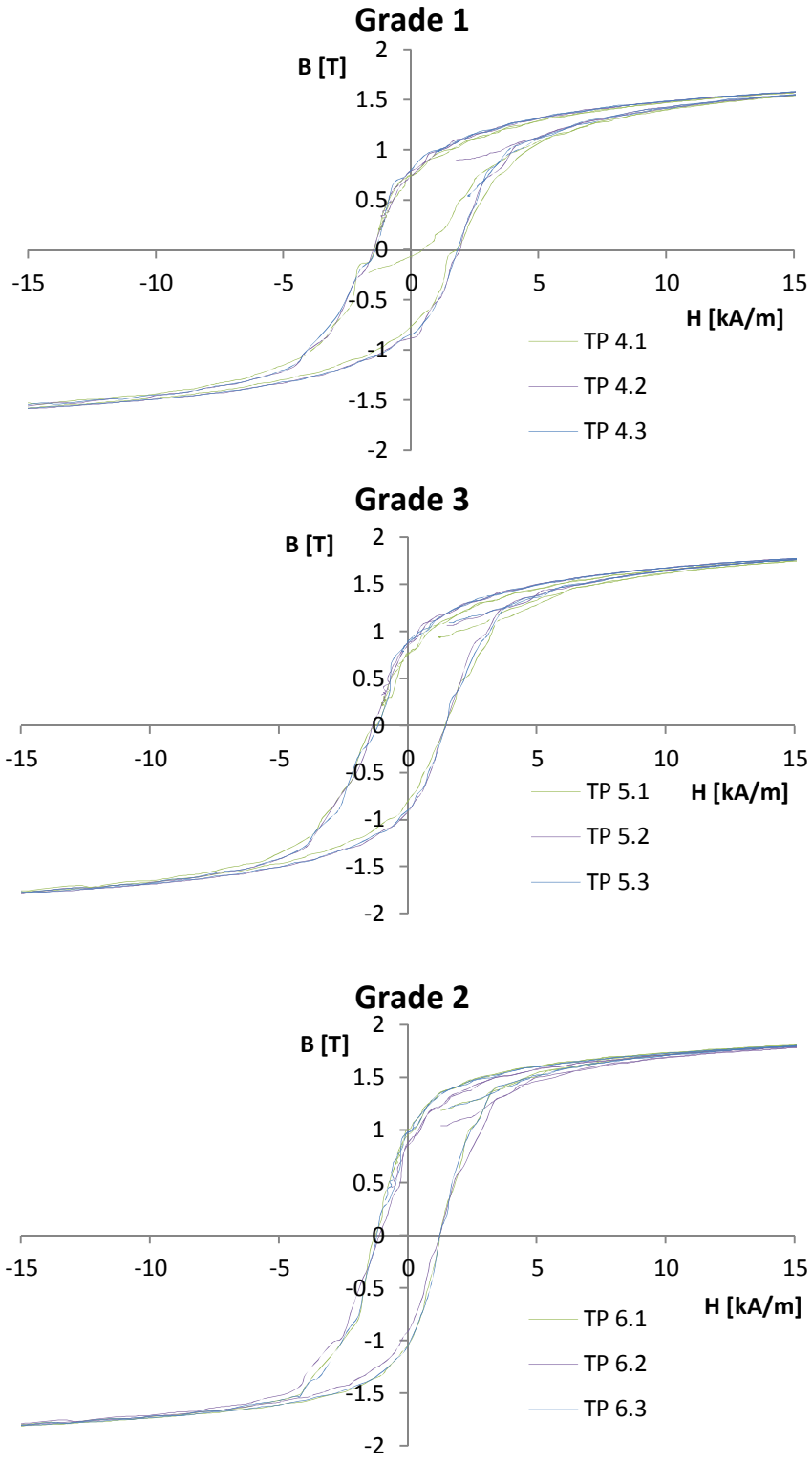

Figure 1 *The hysteresis curves of the steel grades 1, 2 and 3 in the sample group 2.*